Synaptic Senescence in Alzheimer's Disease

Joana Patrícia Sousa da Silva
Mestrado em Biologia Celular e Molecular
Faculdade de Ciências da Universidade do Porto
2020/2021

Orientador
Rodrigo Pinto dos Santos Antunes da Cunha, Faculdade de Medicina e Centro de Neurociências e Biologia Celular, Universidade de Coimbra

Coorientador
Paulo Jorge da Silva Correia de Sá, Instituto de Ciências Biomédicas Abel Salazar, Universidade do Porto

Todas as correções determinadas pelo júri, e só essas, foram efetuadas.

O Presidente do Júri,

Porto, _____/_____/_____

U.PORTO
FACULDADE DE CIÊNCIAS
UNIVERSIDADE DO PORTO

Agradecimentos

O trabalho que desenvolvi durante este ano de dissertação não teria sido possível sem a ajuda de várias pessoas. Assim, gostaria de agradecer ao professor Rodrigo Cunha pela oportunidade de poder realizar a minha dissertação no seu grupo de investigação e pela orientação do projeto; agradecer ao professor Paulo Correia de Sá pela sua orientação; e um agradecimento especial à doutora Paula Canas que me acompanhou neste ano de aprendizagem e que me auxiliou sempre que precisei.

Gostaria de agradecer aos meus colegas deste grupo de investigação que sempre se mostraram disponíveis para me ajudar. Obrigada, também à Cátia e ao João Pedro que me disponibilizaram as amostras corticais utilizadas neste trabalho.

Por fim, queria agradecer aos meus amigos e familiares pelo apoio e pela motivação indispensáveis durante este ano.

Resumo

A Doença de Alzheimer (AD) é a demência mais comum no mundo, afetando mais de 50 milhões de pessoas. O envelhecimento é o principal fator de risco para a AD, onde a senescência celular está presente na base quer do envelhecimento quer da neurodegeneração. Juntamente com a característica acumulação de péptidos de β-amilóide e tau hiperfosforilado, o dano sináptico e a disfunção mitocondrial também são encontrados na AD como características iniciais. Estas alterações podem ser a chave para a prevenção ou o atraso da progressão da doença.

Neste estudo, nós caracterizamos comportamentalmente e neuroquimicamente um modelo de início precoce da AD, os murganhos APP/PS1, e caracterizamos neuroquimicamente outro modelo de início precoce da AD, um modelo de injeção de $A\beta_{1-42}$, com enfoque em proteínas associadas com o metabolismo, autofagia e dinâmica mitocondrial e marcadores sinápticos.

Nós observamos que, aos 6 meses de idade, os murganhos APP/PS1 possuem uma deficiência cognitiva ligeira e parecem ser mais ansiosos do que os animais controlo. Além disso, através de avaliação por Western blot, eles têm níveis de LC3-I, um marcador autofágico, diminuídos, níveis de sintaxina diminuídos e níveis de PSD-95 aumentados, ambos marcadores sinápticos, em sinaptosomas corticais. Aos 9 meses de idade, este modelo mostrou possuir défices mnemónicos e de aprendizagem, bem como comportamentos do tipo-ansioso, tal como a tigmotaxia. Adicionalmente, através de avaliação por Western blot, nós observamos um decréscimo nos níveis de SIRT1 e pAMPK nos sinaptosomas corticais e um decréscimo nos níveis de SIRT1, MFN2 e SESN2 nos extratos totais corticais nesta idade. No modelo da AD de injeção de $A\beta_{1-42,}$ 14 dias após a injeção, nós observamos um aumento dos níveis de SNAP-25, PSD-95, sintaxina e sinaptofisina. Neste modelo, 20 dias após injeção, nós observamos um decréscimo nos níveis de MFN2 em sinaptosomas corticais, enquanto os níveis dos marcadores sinápticos voltaram aos níveis normais.

Em geral, estes resultados são indicativos de uma desregulação dos marcadores sinápticos em ambos os modelos da AD usados, e de uma potencial alteração: no metabolismo e dinâmica mitocondrial nos murganhos APP/PS1; numa alteração do metabolismo nas sinapses e também numa potencial alteração de dinâmica mitocondrial no modelo de injeção de $A\beta_{1-42}$.

Palavras-chave: Doença de Alzheimer, Senescência Sináptica, APP/PS1, Autofagia, Dinâmica Mitocondrial, Metabolismo, Morris Water Maze

Abstract

Alzheimer's disease (AD) is the most common dementia worldwide, affecting more than 50 million people. Aging is the major risk factor for AD, with cellular senescence being a key process underlying aging. Along with the characteristic accumulation of β-amyloid peptides and hyperphosphorylated tau, synaptic damage and mitochondria dysfunction are also found in AD, as early features. These alterations in the disease might be the key to prevent or delay disease progression.

In this study, we characterized behaviourally and neurochemically an early onset model of AD, the APP/PS1 mice, and characterized neurochemically another model of early AD, a $A\beta_{1-42}$-injected model, focusing on proteins associated with metabolism, autophagy and mitochondria dynamics and synaptic markers.

We found that, 6 months old APP/PS1 mice have a mild cognitive impairment and seem to be more anxious that control mice. Moreover, they have decreased levels of LC3-I, an autophagy marker, decreased levels of syntaxin and increased levels of PSD-95, both synaptic markers, in cortical synaptosomes. At 9 months of age, these mice showed memory and learning impairments, as well as anxiety-like behaviours such as thigmotaxis. Additionally, we found a decrease in the levels of SIRT1 and pAMPK in the cortical synaptosomes and a decrease in the levels of SIRT1, MFN2 and SESN2 in total cortical extracts at this age. In the $A\beta_{1-42}$-injected model of AD, 12 days after injection, we found an increase in SNAP-25, PSD-95, syntaxin and synaptophysin. In this model, 20 days after injection, we found a decrease in MFN2 levels in cortical synaptosomes while the synaptic markers returned to normal levels.

Overall, these results indicate that there is a dysregulation of synaptic markers in both early AD models tested, potential altered metabolism and mitochondria dynamics in APP/PS1 mice with a potential altered metabolism in the synapses and potential altered mitochondria dynamics in the $A\beta_{1-42}$-injected model.

Keywords: Alzheimer's Disease, Synaptic Senescence, APP/PS1, Autophagy, Mitochondria Dynamics, Metabolism, Morris Water Maze

Index

Index of Figures

Index of Tables

List of Abbreviations

2D – Two Dimensions

3D – Three Dimensions

aCSF – Artificial Cerebrospinal Fluid

AD – Alzheimer's Disease

ADP – Adenosine Di-Phosphate

AMP – Adenosine Mono-Phosphate

AMPK – 5' Adenosine Monophosphate-Activated Protein Kinase

ANOVA – Analysis of Variance

APOE – Apolipoprotein E

APP – Amyloid Precursor Protein

APS – Ammonium Persulphate

ATG – Autophagy Related Genes

ATP – Adenosine 5'-Triphosphate

Aβ – β-amyloid

BSA – Bovine Serum Albumin

CAPS – 3-(Cyclohexylamino)-1-Propane-Sulfonic Acid

CDK – Cyclin-Dependent Kinase

CNS – Central Nervous System

CR – Calorie Restriction

DDR – DNA Damage Response

Drp1 – Dynamin-Related Protein 1

DTT – Dithiothreitol

ECL – Enhanced Chemiluminescence

EPM – Elevated Plus Maze

ER – Endoplasmic Reticulum

ETC – Electron Transport Chain

Fis1 – Mitochondrial Fission 1 Protein

GAPDH – Glyceraldehyde 3-Phosphate Dehydrogenase

GFAP – Glial Fibrillary Acidic Protein

GMF – Glia Maturation Factor

IBA-1 – Ionized Calcium-Binding Adaptor Protein-1

Icv – Intracerebroventricular

IL – Interleukin

iPSCS – Induced Pluripotent Stem Cells

ITI – Inter-Trial Interval

KHR – Krebs HEPES Ringer

LC3 – Microtubule-Associated Protein 1A/1B-Light Chain 3B

LTP – Long-Term Potentiation

MCI – Mild Cognitive Impairment

MFN1 – Mitofusin 1

MFN2 – Mitofusin 2

MMP-3 – Matrix Metalloproteinase-3

mTOR – Mammalian Target Of Rapamycin

MWM – Morris Water Maze

NAD – Nicotinamide Adenine Dinucleotide

NAD^+ – Nicotinamide Adenine Dinucleotide

NFTs – Neurofibrillary Tangles

NOR – Novel Object Recognition

OMM – Outer Membrane of Mitochondria

OPA1 – Optic Atrophy-1

P38MAPK – p38MAP Kinase

pAMPK – Phosphorylated 5' Adenosine Monophosphate-Activated Protein Kinase

PBS – Phosphate-Buffered Saline

PE – Phosphatidylethanolamine

PGC-1α – Peroxisome Proliferator-Activated Receptor Gamma Coactivator 1-Alpha

PMSF – Phenylmethylsulfonyl Fluoride

pRb – Retinoblastoma Protein

Prp – Mouse Prion Protein

PS1 – Presenilin 1

PS2 – Presenilin 2

PSD-95 – Post Synaptic Density 95

RARβ – Retinoic Acid Receptor- β

RIPA Buffer – Radioimmunoprecipitation Assay Buffer

RNS – Reactive Nitrogen Species

ROS – Reactive Oxygen Species

SAHF – Senescence Associated Heterochromatin Foci

SASP – Senescence-Associated Secretory Phenotype

SA-β-Gal – Senescence-Associated β-Galactosidase

SEM – Standard Error of Mean

SIRT1 – Sirtuin 1

SIRT3 – Sirtuin 3

SIRTs – Sirtuins

SNAP-25 – Synaptosome-Associated Protein of 25 kDa

SNARE – N-Ethylmaleimide Sensitive Factor Attachment Receptors

WT – Wild-Type

ΔE9 – Exon 9 deletion

Introduction

1. Alzheimer's Disease

Currently, more than 50 million people worldwide live with dementia. This number is expected to triple by 2050, with low- and middle-income countries being the most affected (Alzheimer's Disease International *et al*., 2020). Alzheimer's disease (AD) is the most common dementia, positioning AD as a global health issue (Alzheimer's Disease International *et al*., 2020).

AD is a progressive neurodegenerative disease, clinically characterized by memory loss and cognitive deficits, involving cerebral cortical thinning and loss of hippocampal volume (Sabuncu, 2011; Serrano-Pozo *et al*., 2011).

Pathologically, AD is characterized by the accumulation of β-amyloid (Aβ) peptides in plaques extracellularly and hyperphosphorylation of tau in neurofibrillary tangles (NFTs) intracellularly, these being the two major hallmarks of this disease (Serrano-Pozo *et al*., 2011). Initially, before plaque accumulation, AD is characterized histologically by loss of neurons and synapses (Davies *et al*., 1987; Small, 2001) and neuroinflammation (Ransohoff, 2006).

Amyloid plaques are composed mainly by Aβ peptides with 40 ($A\beta_{1-40}$) or 42 ($A\beta_{1-42}$) amino acids (Citron *et al*., 1996). Aβ peptides are produced by sequential cleavage of the amyloid precursor protein (APP) by β-secretase and γ-secretase, the latter producing peptides with different lengths (from 37 to 42 amino acids) that are secreted extracellularly. This is known as the amyloidogenic pathway (Figure 1). On the other hand, in the non-amyloidogenic pathway, APP is cleaved by the α-secretase and γ-secretase to form p3, a secreted fragment (Haass *et al*., 2012)(Figure 1). Longer Aβ peptides are more insoluble and prone to self-aggregation than the shorter Aβ peptides (Jarrett *et al*., 1993). However, soluble Aβ peptides are responsible for the characteristic cognitive deficits in early AD before the formation of Aβ-containing plaques (Haass & Selkoe, 2007).

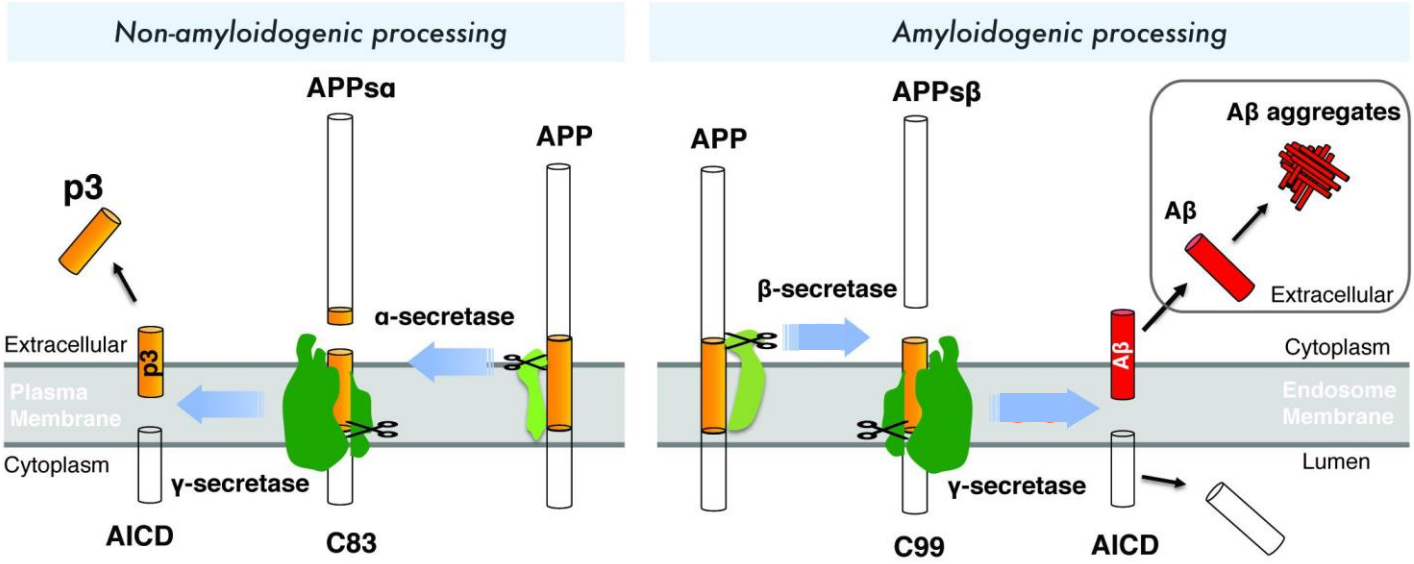

Figure 1 - Non-amyloidogenic and amyloidogenic processing of APP. During the non-amyloidogenic processing, APP is cleaved by α-secretase and γ-secretase sequentially, producing p3, a fragment that is secreted, and membrane-bound APP intracellular domain (AICD). During the amyloidogenic processing, APP is cleaved sequentially by β-secretase and γ-secretase, forming Aβ that is secreted and aggregates extracellularly, and AICD that is released intracellularly. Adapted from Zhao *et al.* (2020).

NFTs are composed, mainly, by hyperphosphorylated tau protein that aggregates into paired helical filaments (Bramblett *et al.*, 1993). Tau is present in the neurons and binds to microtubules to stabilize and maintain them. In AD, tau is hyperphosphorylated, which can lead to its separation from the microtubules (Castellani *et al.*, 2010). Hyperphosphorylated tau impairs axonal transport, which is essential for transport of organelles across the neurons (Reddy, 2011).

AD can be divided into two groups: a familial and a sporadic form. Familial AD is an early-onset form, autosomal and caused by mutations in 3 genes: APP, Presenilin 1 (PS1) and Presenilin 2 (PS2). Sporadic AD, a late-onset form, is usually present after the age of 65 (Alzheimer's Disease International *et al.*, 2020). This form of AD is caused by numerous factors that include genetic and environmental ones. The Alipoprotein E (APOE) gene is the biggest genetic risk factor for sporadic AD (Corder *et al.*, 1993). This gene has three allele variants: ε2, ε3 and ε4, each leading to different protein structures and functions. *APOE* ε4 provides a higher predisposition to AD than the other alleles and decreases the age of onset of the disease (Corder *et al.*, 1993; Yu *et al.*, 2014).

Age is the major risk factor for AD, as the prevalence of the disease increases with age. Furthermore, both AD and aging share various hallmarks (Armstrong, 2019). Nevertheless, numerous risk factors are responsible for AD, such as genetical and

demographic factors or lifestyle and environmental factors. Therefore, AD can be classified as a multi-factor disease (Armstrong, 2019).

2. Alzheimer's Disease Etiology

Alzheimer's etiology is still debatable, with various hypotheses being proposed by the research community.

One of the earliest hypotheses surged when Davies & Maloney (1976) found that choline acetyltransferase activity was reduced in the brains of AD patients compared to control brains. Choline acetyltransferase is responsible for the synthesis of acetylcholine, a neurotransmitter involved in cognitive processes. Thus, it was proposed that AD was a failure of the cholinergic system (Davies & Maloney, 1976; Ferreira-Vieira *et al*., 2016).

In 1991, Hardy and Allsop proposed that aggregates of amyloid peptides were responsible for the onset of AD and subsequent alterations found in the disease. Indeed, aggregation and accumulation of such peptides are a hallmark of the disease. This hypothesis is known as the amyloid cascade hypothesis (Hardy & Allsop, 1991; Hardy & Higgins, 1992).

However, plaques of β-amyloid do not correlate well with cognitive impairment (Arendt, 2009). Thus, soluble peptides were suggested as the main cause of AD as they cause neuronal damage even in the absence of amyloid plaques and can impair synaptic function by inhibiting long-term potentiation (LTP), impair synaptic structure by decreasing excitatory synaptic spines and impair memory of already acquired behaviours in rats (Hsia *et al*., 1999; Selkoe, 2008). Furthermore, amyloid plaques seem to act as a reservoir for these more toxic Aβ oligomers (Mucke & Selkoe, 2012)

The amyloid cascade hypothesis is the most accepted hypothesis currently, however, because cognitive deficit does not correlate well with plaque burden and healthy individuals have plaques at the time of death, different hypotheses for AD etiology were created (Liu *et al*., 2019).

Selkoe (2002) proposed AD as a synaptic failure. Interestingly, synaptic dysfunction appears prior to both amyloid plaques and neurofibrillary tangles and it is the best correlator with cognitive deficits (John & Reddy, 2021). In AD, there is a loss of synapses, mainly in the neocortex and hippocampus (Jeong, 2017) and a reduced spine density (John & Reddy, 2021; Kashyap *et al*., 2019). Furthermore, in the synapses of AD patients, there is a loss of pre- and postsynaptic proteins, such as synaptosome-

associated protein of 25 kDa (SNAP-25) and postsynaptic density protein 95 (PSD-95) respectively, as well as a loss of proteins present in the synaptic vesicles such as synaptophysin, associated with cognitive dysfunction (Arendt, 2009). It has been proposed that synaptic dysfunction is caused by soluble oligomers leading to cognitive deficits (Terry *et al*., 1991; Selkoe, 2008). Moreover, tau pathology found in AD, leads to an impairment in axonal transport that can compromise the transport of mitochondria and receptors to the synapses. This can lead to an inefficient adenosine 5'-triphosphate (ATP) production and calcium buffering, affecting synaptic transmission and potentially leading to synapse loss (John & Reddy, 2021). Interestingly, in the synapses, accumulation of Aβ occurs before tau hyperphosphorylation, however, tau is necessary for memory impairment (Bilousova *et al*., 2016; John & Reddy, 2021).

In 2004, Swerdlow and Khan proposed a new hypothesis for sporadic, late-onset AD's etiology: the mitochondrial cascade hypothesis, updated in 2014 (Swerdlow *et al*., 2014). Gene inheritance, especially mtDNA, defines electron transport chain (ETC) efficiency and basal reactive oxygen species (ROS) production, thus defining baseline mitochondrial function. ROS production correlates with mtDNA damage. Moreover, the rate of mitochondrial function changes is influenced by inherited and environment factors and these changes influence AD chronology (Swerdlow & Khan, 2004; Swerdlow *et al*., 2014). Furthermore, in late onset AD, APP expression is influenced by mitochondrial function (Swerdlow *et al*., 2014). Consistently, Aβ peptides were shown to entry mitochondria and disrupting the ETC and consequently decreasing ATP production and increasing ROS production leading to oxidative stress (Manczak *et al*., 2006).

Mitochondria are major producers of ROS and reactive nitrogen species (RNS), which can lead to oxidative stress when overproduced or when there are insufficient antioxidative defenses (Uttara *et al*., 2009). Indeed, oxidative stress is linked to neuronal dysfunction in AD, with neurons also having lower number of mitochondria (Hirai *et al*., 2001).

Interestingly, epigenetic dysregulation is also found in AD and aging brains. (Nativio *et al*., 2018), which could be partially explained by mitochondrial dysfunction, as mitochondrial metabolites are necessary for these epigenetic modifications (Matilainen *et al*., 2017) and mitochondria regulates nicotinamide adenine dinucleotide (NAD^+) levels, co-factor for sirtuins (SIRTs), which are histone deacyletases (Imai *et al*., 2000; Liu *et al*., 2019).

As hyperphosphorylated tau is present in AD, tau pathology has been studied as a promoter of AD (Frost *et al*., 2009). Tau pathology starts in the transentorhinal cortex and then spreads to other regions of the brain (Braak & Braak, 1991). This characteristic distribution allowed distinguishing 6 neuropathologic stages, widely used for assessment of the stage AD progression (Braak & Braak, 1991). Thus, tau pathology correlates with AD progression and symptoms (Kametani & Hasegawa, 2018). Furthermore, extracellular tau aggregates can enter cells and promote intracellular tau fibrillization, promoting protein misfolding (Frost *et al*., 2009). Moreover, tau pathology is also common in other neurodegenerative diseases (Spillantini & Goedert, 2013).

Currently, the search for drug therapies is focused on these four hypotheses (Liu *et al*., 2019). Nevertheless, other hypotheses have been proposed and involve altered calcium homeostasis, vascular dysregulation, inflammation, altered homeostasis of metal ions, among others (Liu *et al*., 2019).

3. Alzheimer's Disease Models

Research about AD has been performed in various systems, both *in vitro* and *in vivo*. *In vitro* models of AD include 2-dimensions (2D) and 3-dimensions (3D) cultures. 2D cultures can be based on induced pluripotent stem cells (iPSCs) derived neurons. As for 3D cultures, immortalized cell lines are used. Furthermore, 3D cultures of patient-derived iPSCs are also used. Finally, cerebral organoids or "mini-brains", have been, more recently used (Slanzi *et al*., 2020; Ranjan *et al*., 2018)

In vivo models of AD rely on transgenic and non-transgenic animals. Various animals can be used, such as invertebrate models, such as *Caenorhabditis elegans* and *Drosophila melanogaster* (Mhatre *et al*., 2012) and rodent models (Götz *et al*., 2018). Animal models try to mimic the disease allowing exploration of therapeutic options and further understanding of the disease pathology. Furthermore, animal models allow us to explore cognitive and behaviour performance, opposed to other models (Penney *et al*., 2019). Non-transgenic animal models rely on the injection of toxins such as soluble Aβ oligomers (Cleary *et al*., 2004) or streptozotocin (Chen *et al*., 2013) in the brains of the animals (Ranjan *et al*., 2018). Transgenic animal models are the most frequently used (Elder *et al*., 2010).

Various transgenic lines of mice have been created and described. Indeed, mice are often used as a rodent model of AD as they are evolutionary close with humans, both having similar brain regions and neurotransmitter systems (Perlman, 2016). These lines

focus mainly on mutations in APP, PS1 or PS2 genes, with some lines using tau and APOE human genes. While some models have mutations on the APP gene, others are bigenic and combine mutations in the APP and PS genes (Esquerda-Canals *et al.*, 2017).

One of the most widely used model is the double transgenic APP/PS1 mice. This model has a human PS1 with an Exon 9 deletion (ΔE9) and the APP transgene, which has the Swedish mutation, was humanized in the Aβ region (Jankowsky *et al*., 2001). The Swedish mutation favors the activity of β-secretase favoring the amyloidogenic pathway of the APP processing (Esquerda-Canals *et al.*, 2017). Since PS1 is present in the γ-secretase complex, ΔE9 favors production of $A\beta_{1-42}$ peptides (Esquerda-Canals *et al.*, 2017). *ps1* is under regulation of the mouse prion protein (PrP) promoter which directs its expression to the central nervous system (CNS) neurons (Jankowsky *et al*., 2001). APP/PS1 mice show an age-dependent amyloid plaque burden in the cortex and hippocampus, where plaques are easily detected starting at 6 months (Garcia-Alloza *et al*., 2006).

Other widely used models rely on Aβ injection in the brain of control mice to mimic the Aβ amyloid hypothesis. These models allow researchers to have more control of the experience. Here, the researcher can choose which isoform and species of Aβ to use, as well as the time point of injection and time point of analysis (Kim *et al*., 2016).

For example, Canas *et al.* (2009), showed that mice that received an intracerebroventricular administration of soluble $A\beta_{1-42}$ oligomers and were characterized behaviourally 15 days after the injection, show impairments of memory, evaluated by the Y-maze test and the object recognition (OR) test. As reference memory and synaptic function are impaired in this model, it is validated as an AD model (Canas *et al*., 2009; Gonçalves *et al*., 2019). Furthermore, Matos *et al.* (2012) performed a modified Y-Maze test with rats injected with soluble $A\beta_{1-42}$ oligomers 2 weeks after injection and observed a spatial memory impairment, as rats injected with $A\beta_{1-42}$ spent less time exploring the novel arm of the maze than control rats.

As we ought to find new therapeutics for AD, animal models allow us to perform different pharmacological analysis and study their impacts on memory, a major area affected by AD (Ranjan *et al*., 2018).

4. Senescence Markers & Potential Markers

Aging is the major risk factor for neurodegenerative diseases. In aging, alterations such as genomic instability, mitochondrial dysfunction, cellular senescence, altered intercellular communication, telomere attrition, loss of proteostasis, epigenetic alterations, deregulated nutrient-sensing and stem cell exhaustion, are present (Martínez-Cué & Rueda, 2020; López-Otín *et al*., 2013). As an organism ages, there is also an accumulation of senescent cells: this can limit regenerative capacities and favour age-related diseases (Muñoz-Espín & Serrano, 2014).

In keeping with aging as the major risk factor for AD, AD is also associated with these characteristic aging alterations (Hou *et al.,* 2019). For example, in AD, mitochondria dysfunction is an early feature of the disease, which leads to oxidative stress, a senescence trigger (Swerdlow, 2018). Furthermore, altered proteostasis is also found in AD, as protein aggregations are one of the disease's hallmarks (Serrano-Pozo *et al*., 2011).

Cellular senescence is a process in which cells achieve a permanent cell cycle arrest. Senescent cells have a distinct phenotype, designated senescence-associated secretory phenotype (SASP) in which they secrete interleukins, chemokines and other signalling molecules, thus promoting neuroinflammation (Lopes-Paciencia *et al*., 2019). These cells also have impaired mitochondrial function and changes in morphology, which promote ROS production that culminate in induction of oxidative stress. Mitochondrial changes also interfere with cellular metabolism by promoting a decrease in ATP production. Overall, senescent cells have altered morphology and metabolism and an increased genetic instability (Martínez-Cué & Rueda, 2020).

Senescence can be triggered by numerous stressors, almost all of them culminating in DNA damage, which activates the DNA damage response (DDR) mechanisms. Briefly, activated DNA damage response leads to activation of the p53 and/or the $p16^{INK4a}$ pathways. Activation of p53 activates *p21* transcription. p21 then blocks cyclin-dependent kinase 2 (CDK2). Upon activation, p16 binds CDK4 and CDK6. Blockage of CDK2, CDK4 and CDK4 block retinoblastoma protein (pRB) phosphorylation. The cell cycle arrest is mediated by the dephosphorylated Rb that indirectly inhibits the transcription of cell cycle genes (Kumari & Jat, 2021; Saez-Atienzar & Masliah, 2020). Induction of the $p53/p21^{WAF1/CIP1}$ pathway occurs in the initiation of senescence leading to a temporary cell cycle arrest while activation of the $p16^{INK4a}$ /pRB

pathway occurs later leading to a permanent cell cycle arrest (Kumari & Jat, 2021; Saez-Atienzar & Masliah, 2020).

4.1. Cell Cycle Markers

Given their involvement in the cell cycle, p53, $p21^{WAF1/CIP1}$, $p16^{INK4a}$ and pRB are often used to assess senescence. In fact, in senescent cells, there is an increase in the levels of these proteins (Kumari & Jat, 2021; Tan *et al*., 2014). $p16^{INK4a}$ is also a biomarker of aging, as its expression increases with age in various tissues (Krishnamurthy *et al*., 2004).

One of the morphological alterations present in senescent cells is nuclear rearrangement. Loss of Lamin B1, a filament present in the inner surface of the nuclear envelope, is a biomarker of senescence (Freund *et al*., 2012).

Senescence-associated β-galactosidase (SA-β-Gal) is a hydrolase that accumulates in the lysosomes of senescent cells. It is widely used as a senescence marker since its activity, in senescent cells, is detected by a colorimetric assay at pH 6.0, opposed to activity in normal cells at pH 4.0 (Dimri *et al.*, 1995).

Accumulation of lipofuscin, increased p38MAP kinase (p38MAPK), increased secreted SASP factors such as interleukin (IL) IL-1β, IL-6, IL-8 and matrix metalloproteinase-3 (MMP-3), and increased senescence-associated heterochromatin foci (SAHF) are other biomarkers used to assess senescence (Tan *et al*., 2014).

Senescent cells express a heterogeneous phenotype with alterations that are not specific to them (González-Gualda *et al*., 2020). For example, an increase in the $p16^{INK4a}$ can be found in different tumours (Romagosa *et al*., 2011) and β-galactosidase activity is detected in neurons of various ages (Piechota *et al*., 2016). Thus, a single biomarker is not sufficient for characterizing senescent cells. As there are not universal markers of senescence, for a correct assessment of senescent cells, a multimarker study is necessary (González-Gualda *et al*., 2020).

Furthermore, more detailed characterization of senescent cells in the CNS is needed. Since neurons are post-mitotic cells, senescence must be assessed through markers other than cell cycle arrest markers. Indeed, neurons and other brain cells show a senescence-like phenotype which includes SA-β-Gal activity, secretion of pro-inflammatory factors such as IL-6, increased ROS production and activation of p38MAPK (Dong *et al*., 2011; Jurk *et al*., 2012; Piechota *et al*., 2016; Wissler Gerdes *et al*., 2020).

4.2. Metabolism Markers

Mitochondria are double membrane organelles responsible for energy production in the form of ATP, which is essential for a cell's functions (Cai & Tammineni, 2017). In synapses, they are also responsible for calcium buffering and homeostasis, important for synaptic transmission, synaptic vesicle formation and synapse outgrowth (Reddy and Beal, 2008).

Neurons are highly energy demanding for their functions, especially neurotransmission, and thus, can be negatively affected by slight energy declines (Wallace & Chalkia, 2013). Therefore, neurons are prone to mitochondrial dysfunction while simultaneously having a low threshold for mitochondrial dysfunction tolerance (Wallace & Chalkia, 2013). Indeed, mitochondrial dysfunction and oxidative stress are associated with various neurodegenerative diseases (Johnson *et al*., 2021). Moreover, in AD, neuronal mitophagy is impaired (Fang *et al.,* 2019), and mitochondria have altered morphology and number (Reddy and Beal, 2008).

During oxidative phosphorylation in the mitochondria, ROS such as hydrogen peroxide, superoxide anion and hydroxyl radical, are produced. Excessive ROS production leads to oxidative stress (Ray *et al*., 2012). However, mitochondria have endogenous quality control systems that include mitochondrial fusion, fission, biogenesis and mitophagy (selective autophagy of mitochondria), to compensate functions and remove damaged mitochondria (Yoo & Jung, 2018).

4.2.1. Sirtuin1 and Sirtuin3

Calorie restriction (CR) is the best characterized non-genetic method that increases lifespan and slows down aging across various species (Bordone & Guarente, 2005). Sir2, a yeast sirtuin, is necessary for this increase and is up-regulated upon CR (Lin *et al*, 2002; Bordone & Guarente, 2005).

Sirtuins (SIRTs), the orthologs of Sir2 in yeast, are histone deacetylases whose activity require NAD^+, a coenzyme essential for energetic reactions (Imai *et al.*, 2000).

In mammals, there's 7 sirtuins (SIRT1-7) located in different organelles and with different functions. SIRT1 is a nuclear sirtuin that can also be found in the cytoplasm as it has two nuclear export signals (Vaquero *et al*., 2004; Michishita *et al*., 2005 Tanno *et al*., 2007). SIRT2 is cytoplasmic (North *et al*, 2003). SIRT3-5 are present in the

mitochondria (Michishita *et al*., 2005; Onyango *et al*., 2002). SIRT6 and SIRT7 are nuclear sirtuins with SIRT6 being associated with heterochromatic regions except nucleoli and SIRT7 being present in the nucleoli (Michishita *et al*., 2005). Of all the sirtuins, SIRT1 is the most studied, given its action on lifespan. SIRT1 and SIRT3 activity are present mostly in the brain, especially in the neurons (Anamika *et al*., 2019).

SIRT1 deacetylates the peroxisome proliferator-activated receptor gamma coactivator 1-alpha (PGC-1α), contributing to mitochondrial homeostasis (Chen *et al*., 2020; Figure 2a). SIRT1 also regulates 5' adenosine monophosphate-activated protein kinase (AMPK) and mechanistic target of rapamycin (mTOR) indirectly. Activation of SIRT1 by resveratrol at near-toxic concentrations, leads to mTOR inhibition and senescence suppression (Demidenko & Blagosklonny, 2009). Therefore, SIRT1 can indirectly regulate autophagy. SIRT1 is also fundamental for synaptic plasticity, cognition and learning (Michan *et al*., 2010).

SIRT3 seems to be the main sirtuin in the mitochondria and, as mitochondria dysfunction is present in neurodegenerative diseases, SIRT3 is hypothesized to be relevant for these diseases (Anamika *et al*., 2019). Indeed, SIRT3 is involved in mitochondrial homeostasis, regulating processes such as antioxidant defences and ATP production (Anamika *et al*., 2019; Figure 2a). SIRT3 is also responsible for mitochondria integrity, regulating proteins involved in fission and fusion of the mitochondria and preventing excessive fission that leads to fragmentation and dysfunction (Meng *et al*., 2019). An increase in ROS leds to an increase in SIRT3 in primary hippocampal cultures, with this protein having a neuroprotective effect (Weir *et al*., 2012). Furthermore, SIRT3 can promote mitochondria biogenesis by activating PGC-1α (Meng *et al*., 2019).

4.2.2. AMP-Activated Protein Kinase

AMPK is a cellular energy sensor. This enzyme senses ratios of ADP/ATP (ADP, adenosine di-phosphate) and AMP/ATP (AMP, adenosine mono-phosphate). When a cell is stressed, there are increased levels of cellular AMP and/or ADP and Ca^{2+} and decreased levels of cellular ATP. These alterations represent the canonical mechanisms that activate AMPK (Hardie *et al*., 2012).

Therefore, AMPK can be activated by two mechanisms: binding of AMP/ATP or phosphorylation of the residue 172, a threonine. Both phosphorylation and binding of AMP increase the activity of AMPK while binding of ATP decreases its activity. Thus, the

ratio of cellular AMP/ATP, which defines the cells' energy state, regulates AMPK activity (Yang *et al*., 2020).

Once activated, AMPK promotes catabolic pathways, such as autophagy and glucose uptake, to produce ATP, and inhibits anabolic pathways, such as biosynthesis of macromolecules (Hardie *et al*., 2012; Figure 2b). Activated AMPK upregulates PGC-1α, a transcription coactivator that initiates mitochondrial biogenesis and has antioxidant properties (Jager *et al*., 2007; Yang *et al*., 2020; Figure 2c). Activated AMPK also activates ULK1, necessary for initiation of the phagophores, therefore, promoting autophagy (specially mitophagy) (Egan *et al*., 2010). Furthermore, activated AMPK can directly and indirectly inhibit mTOR, a negative regulator of autophagy (Garza-Lombó *et al*., 2018; Gwinn *et al*., 2008; Inoki *et al*., 2003). The mTOR signalling pathway is responsible for regulation of numerous processes, such as transcription and translation of proteins, autophagy, cytoskeleton dynamics, metabolism and neurodevelopment (Switon *et al*., 2017).

Activation of AMPK lowers Aβ deposits and inhibits β-secretase expression, which reduces the production of Aβ peptides by interfering with the amyloidogenic pathway of the APP metabolism (Lu *et al*., 2010). Furthermore, suppression of the mTOR signalling pathway in a transgenic mice model of AD, led to an increase in autophagy, reducing Aβ levels and ameliorating cognitive deficits (Caccamo *et al*., 2014). Activation of AMPK is, thus, a promising therapeutic target for neurodegenerative diseases.

4.2.3. Sestrin2

Sestrins are stress-response proteins with 3 main functions: inhibition of ROS production, leucine-sensor and inhibition of mTOR (Chen *et al*., 2019).

Sestrins activate Nfr2, a transcription factor involved in antioxidant mechanisms, and indirectly regenerate overoxidized peroxiredoxins thus, inhibiting oxidative stress (Bae *et al*., 2013). Furthermore, Sestrin2 (SESN2) activates AMPK which inhibits mTOR signaling pathway, promoting autophagy and inhibiting cell proliferation (Budanov & Karin, 2008; Chen *et al*., 2019; Figure 2b).

Increased oxidative stress is common in neurodegenerative diseases and aging, as a result of an imbalance in ROS and RNS production and antioxidant defences (Liguori *et al*., 2018). In AD brains, SESN2 co-locates with phosphorylated tau in neurofibrillary lesions (Soontornniyomkij *et al*., 2012).

As SESN2 has antioxidant properties and promotes autophagy that can eliminate protein aggregates, SESN2 is a promising therapeutic target for neurodegenerative diseases (Chen *et al*., 2019).

4.3. Autophagy

Autophagy is a process where degradation of organelles occurs to maintain homeostasis. Autophagy is kept at baseline levels, however it can be induced in stress conditions, such as nutrient deprivation, to promote cell survival and energy production (Glick *et al*., 2010). Autophagy is also essential for removing protein aggregates, which characterize many neurodegenerative diseases. Thus, as expected, autophagy is impaired in these diseases. Furthermore, autophagy activity declines with age (Park *et al*., 2020).

In a mouse model of AD, with mutations in the APP gene, Manczak *et al*. (2018) found impaired autophagy and mitophagy, resulting from the accumulation of mutant APP and Aβ peptides. Furthermore, inhibition of mTOR, which led to promotion of autophagy, reduced Aβ levels in a mouse model of AD (Spilman *et al*., 2010). Therefore, promotion of autophagy could be a promising target for potential therapeutics for neurodegenerative diseases.

There are 3 forms of autophagy: macroautophagy, microautophagy and chaperone-mediated autophagy (Glick *et al*., 2010). Macro-autophagy involves *de novo* formation of autophagosomes, double-membrane vesicles that sequester the cargo for degradation (Parzych & Klionsky, 2014). The phagophore is formed at specific sites in mammals. After elongation of the phagophore, it begins to curve as, then, the double-membranes close forming the autophagosome. Several autophagy related genes (ATGs) homologs are involved in this process. The autophagosome then fuses with lysosomes, forming autolysosomes, and the cargo is degraded (Parzych & Klionsky, 2014).

Microtubule-associated protein 1A/1B-light chain 3B (LC3) is a protein involved in the formation of the autophagosomes (Kirisako *et al*., 1999). LC3 has two isoforms: LC3-I, the cytoplasmic form; and LC3-II, the autophagosome membrane-bound form (Kabeya *et al*., 2000). LC3-I is cleaved by ATG4, exposing a glycine residue which allows LC3-I to be conjugated to phosphatidylethanolamine (PE) to form LC3-II (Kabeya *et al*., 2004; Figure 2d).

LC3 binds to both outer and inner autophagosome membranes. Upon degradation of autolysosomes cargo, LC3-II bound to the outer membrane is released while LC3-II bound in the inner membrane is degraded (Parzych & Klionsky, 2014). Thus, LC3 can be used as an indicator of autophagy, as the amount of LC3-II correlates with the number of autophagosomes (Mizushima & Yoshimori, 2007).

4.4. Mitochondria Dynamics

Mitochondria are dynamic organelles that can fuse or fission according to the cell's needs. These dynamics are controlled by mitofusin 1 (MFN1), mitofusin 2 (MFN2) and the optic atrophy-1 (OPA1) protein, which are GTPases that regulate mitochondrial fusion while dynamin-related protein 1 (Drp1) and the mitochondrial fission 1 protein (Fis1) control mitochondrial fission (Sita *et al*., 2020)

MFN2, a transmembrane protein, is found predominantly in the contact sites between mitochondria and the endoplasmic reticulum (ER), therefore having an important role in mitochondrial calcium uptake from the ER and ER morphology (de Brito & Scorrano, 2008). MFN2 is located in the outer membrane of mitochondria (OMM) and in the mitochondria-associated ER membranes (MAM) (de Brito & Scorrano, 2008; Sita *et al*., 2020).

Mitochondria fusion allows mitochondria to share cytosolic elements while mitochondria fission aids in the process of eliminating impaired mitochondria (Yan *et al*., 2013). A balance between mitochondria fusion and fission is essential for maintenance of mitochondria's homeostasis and integrity (Yan *et al*., 2013; Sita *et al*., 2020). Indeed, disruption of this balance contributes to mitochondria dysfunction and neurodegeneration (Knott *et al*., 2008) and promotion of mitophagy (Reddy & Oliver, 2019). Furthermore, increased levels of MFN2 are associated with elongated mitochondria that cause senescence-associated changes, such as increased ROS and DNA damage (Lee *et al*., 2007).

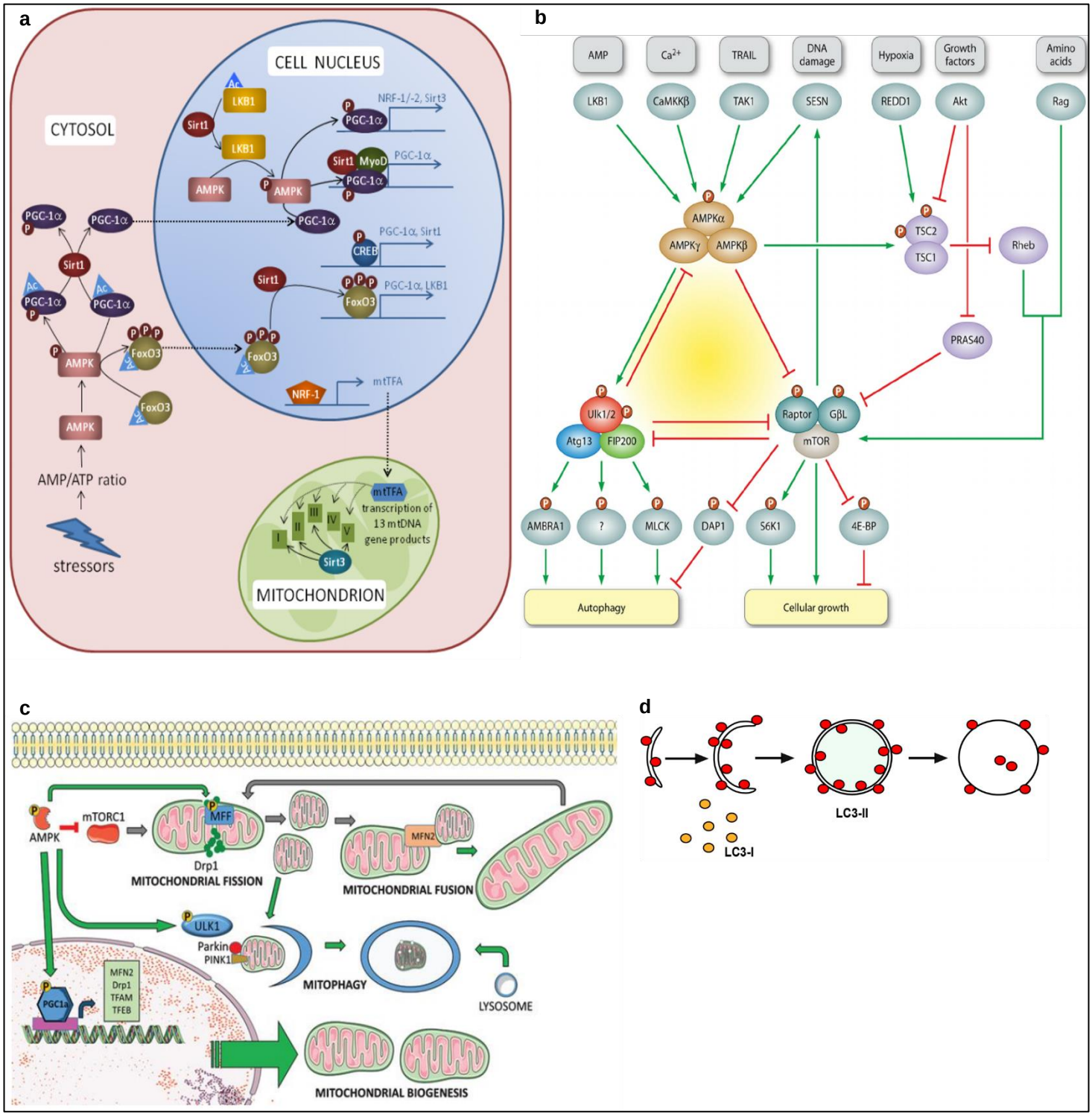

Figure 2 – Pathways in which SIRT1, SIRT3, SESN2, AMPK, pAMPK, LC3 and MFN2 are involved**. a.** AMPK when activated, activates PGC-1α by phosphorylation. SIRT1 deacetylates PGC-1α, activating it. PGC-1α, then regulates the expression of the proteins involved in the subunits of the ETC. SIRT3 deacetylates the subunits of the ETC in the mitochondria, activating them. Retrieved from Brenmoehl & Hoeflich (2013); **b.** AMPK is a key player in autophagy and cellular growth via its interaction with the Ulk1/2 and TOR complexes. AMPK and mTOR oppositely regulate Ulk1/2-Atg13-FIP200, which regulates autophagy, with AMPK promoting autophagy and mTOR inhibiting autophagy. SESN2 is a stress sensor that activates AMPK, thus indirectly inhibiting mTOR. Moreover, activation of mTOR leads to accumulation of SESN. Retrieved from Alers *et al.* (2012); **c.** activated AMPK regulates mitochondria quality control processes. It phosphorylates ULK1 promoting mitophagy, inhibits mTOR and activates PGC-1α which facilitates expression of mitochondria fission (*Drp1*) and fusion (*Mfn2*) genes; Retrieved from Curry *et al*. (2018)**; d.** In autophagy, LC3-I is cleaved and lipidated to form LC3-II which binds to the autophagosomes; Retrieved from Grasso *et al*. (2015).

Overall, aging is the major risk factor for AD, and both aging and AD share common cellular alterations (Hou *et al.,* 2019). Cellular senescence is one of the alterations found in both aging and AD, with senescence being a contributor to the pathology in neurodegenerative diseases (Martínez-Cué & Rueda, 2020). Inefficient mitophagy, impaired mitochondria dynamics and quality control mechanisms and altered metabolism can lead to neurodegeneration (Cai & Jeong, 2020; Reddy, 2009). It is known that mitochondria dysfunction is an early AD feature, just like synaptic dysfunction (Selkoe, 2002; Swerdlow, 2018). However, it is unknown if these key markers of senescence are present in synapses causing the early synaptic dysfunction characteristic of AD. Attempting to target these early modifications of AD in synapses could allow us to develop new therapeutics that can prevent or delay disease progression.

5. Aims

We aim to perform a behavioural and neurochemical characterization of APP/PS1 mice at two time points. Thus, starting at 6 months old which is at the onset of disease-like phenotype, we aim to perform a behavioural characterization of motor, mood and memory of APP/PS1 mice.

This is complemented by neurochemical characterization of APP/PS1 mice focusing on purified synapse (synaptosomes) of cortical regions. We aim to characterize alterations in synaptic markers by Western blot, assessing synapse loss and perform a quantification by Western blot of proteins that are involved in metabolism, autophagy, mitochondrial dynamics and associated with aging and senescence.

Furthermore, to explore if these potential alterations are consistent in other validated models of AD, we aim to neurochemically characterize, as described before, a Aβ soluble peptides icv-injected model of AD at two different time-points.

Overall, we aim to understand if there are alterations in synaptic markers and senescence-related proteins, in the synapses of a mice model of AD at the onset of the AD-like phenotype, which is evaluated by behaviour analysis and if these alterations are present in a different validated model of AD.

Methods and Materials

1. Animals

Female APPswe/PSEN1dE9 (henceforward APP/PS1) transgenic mice with 5-9 months were initially purchased from The Jackson Laboratory (MMRRC stock #34832; donated by Dr. David R Borchelt, University of Florida). To maintain the colonies, male hemizygous APP/PS1 mice were crossed with female WT littermate mice. In this study, 5-7 months old mice were obtained by crossing hemizygous APP/PS1 female and male mice or crossing of female WT littermate mice with male hemizygous APP/PS1 mice. Moreover, 8-9 months old mice were obtained by crossing female WT (B6C3F1/J) mice with male hemizygous APP/PS1 mice.

Male C57Bl/6 (WT, Wild-Type) mice were obtained from Charles River Laboratories (Barcelona, Spain). Synthetic amyloid-β peptide fragment 1-42 ($A\beta_{1-42}$, 0.5 mM, Bachem) was dissolved in water. At 9-11 weeks, mice were intracerebroventricular (icv) injected with 4 µL of the $A\beta_{1-42}$ solution (corresponding to a final concentration of 2 nmol) in the lateral ventricle (Canas *et al.*, 2009). Age-matched vehicle animals were icv-injected with 4 µL of filtered water. Mice were sacrificed 14 or 20 days after $A\beta_{1-42}$ injection (Canas *et al.*, 2009; Matos *et al*., 2012). Cortices of these mice were kindly provided by teammates for this study.

All mice were kept in cages with 1-3 littermates and with *ad libitum* food and water. The cages were kept at 21-23ºC with 50-60% humidity. The room was kept in a 12 hours dark/light cycle with light from 7h00 to 19h00.

All procedures were made in accordance with the "Three Rs" european legislation, ORBEA n° 243_2020/1210—72020.

2. Behaviour Analysis

Behavioural analysis was performed in a sound-attenuated room maintained at 21-23ºC and 50-60% humidity with red lighting (10 lux, light intensity).

Between trials, the apparatus and objects used were cleaned with a 10% ethanol solution. Animals from the same cage were kept in transport cages between trials to avoid contact between animals that had already completed the test and animals that had not.

Prior to behaviour testing, mice were picked up and placed in a flat surface while still in hold and allowed to move freely (handling). This procedure was done 2 times a week for 4 minutes. The experimental design is represented in Figure 3 and Figure 4.

The tests were video-recorded and analysed with the ANY-maze Video Tracking Software (Stoelting Europe, Dublin, Ireland).

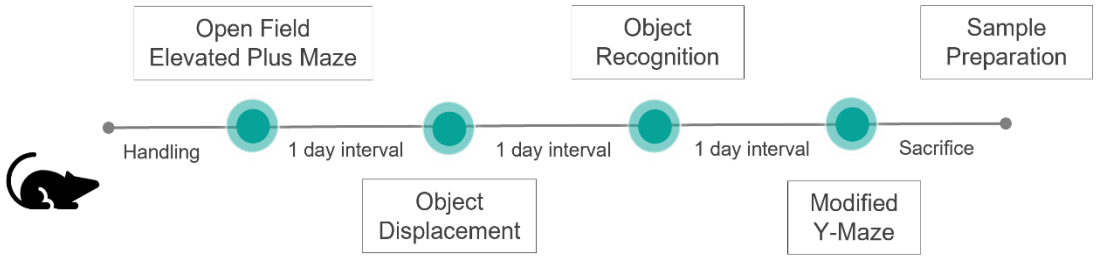

Figure 3 – Timeline of the experimental design for the tests performed with the 6 months old APP/PS1 female mice.

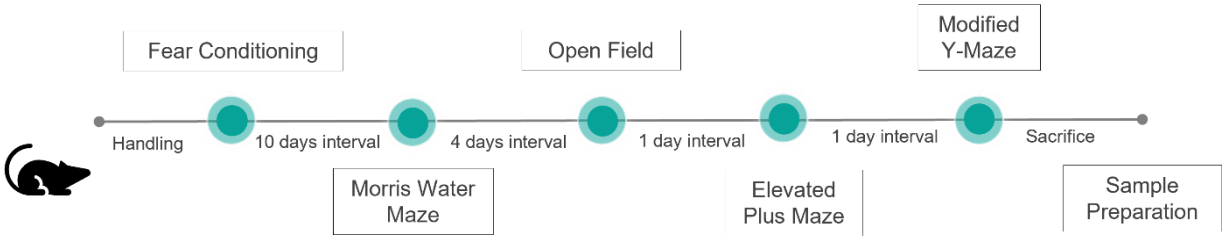

Figure 4 - Timeline of the experimental design for the tests performed with the 9 months old APP/PS1 female mice.

2.1. Open Field

The open field test was first described in 1934 by Hall and is useful to assess locomotor activity and anxiety-like behaviour in mice. Imaginary "center" and "periphery" zones were defined in the AnyMaze software for assessing anxiety-like behaviour (Fig. 5b).

Mice were loaded on the center of a 38x38 cm grey acrylic box and allowed to explore the arena for 5 minutes (Fig. 5a). Parameters such distance travelled (in meters), maximum speed reached, time spent in the center and number of entries in the center were evaluated.

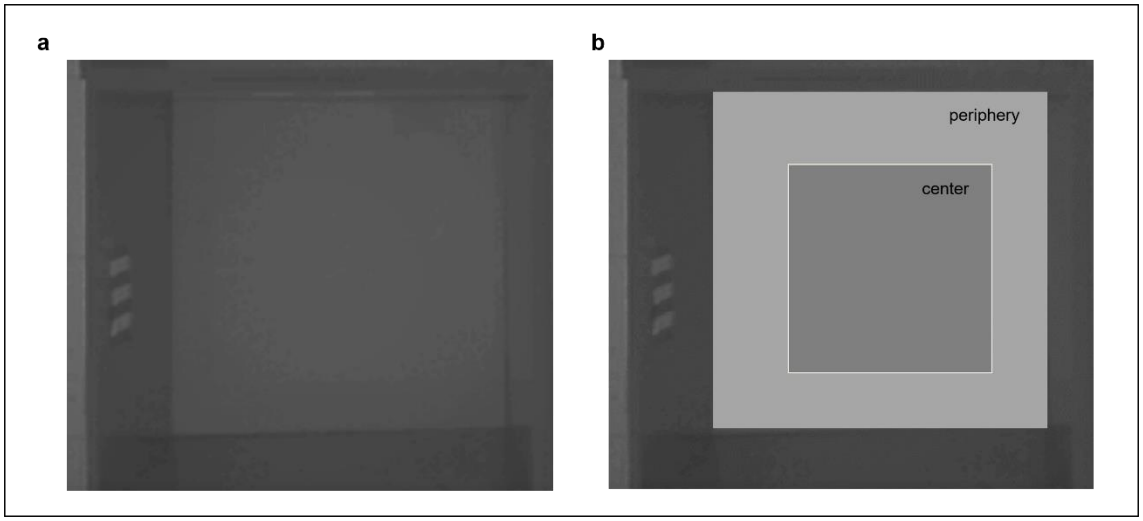

Figure 5 – Representative images of the Open Field apparatus used for the behaviour characterization of the 6 months old APP/PS1 female mice. **a.** The Open Field test apparatus; **b.** The imaginary center and periphery zones of the apparatus defined in the AnyMaze software.

2.2. Object Displacement

The object displacement (OD) test is useful for assessing hippocampal-dependent spatial memory (Assini *et al.,* 2009). This method was adapted from Viana da Silva *et al.* (2016).

In the habituation phase of the test, animals were placed in the open field arena for 5 minutes and allowed to explore, being then retrieved to their cages and the apparatus cleaned.

An inter-trial interval (ITI) of 1 hour was applied between the habituation phase and the acquisition phase. In the acquisition phase of the test, two identical bottles were placed equidistant from one another in one side of the apparatus. Mice were allowed to explore for 10 minutes.

At the end of the acquisition phase, an ITI of 90 minutes was applied before the test phase. In this phase, one of the bottles was moved to the other side of the apparatus (Fig. 6). To avoid bias, the displaced bottle was on the right side of the apparatus 50% of the tests and on the left side of the apparatus 50% of the remaining tests. If the animals showed a clear preference for one of the bottles, then, the bottle displaced was the one less explored. The animals were placed in the center of the apparatus and allowed to explore the objects for 5 minutes. In this test, "exploring" is considered when the animal is in the zone of the object, defined in the ANYmaze software and interacting with the bottle, *e.g.* sniffing.

Spatial memory is expressed by the following Displacement Index:

$$\frac{Time\ spent\ exploring\ the\ displaced\ object}{Time\ spent\ exploring\ the\ displcaed\ object + Time\ spent\ exploring\ the\ nondisplaced\ object} \times 100$$

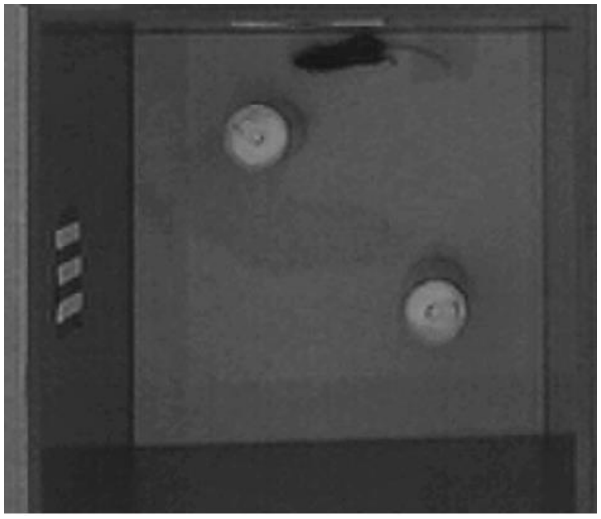

Figure 6 - Representative images of the Open Field apparatus with the objects used in the Object Displacement test for the behaviour characterization of the 6 months old APP/PS1 female mice

2.3. Object Recognition

This test was adapted from Ennaceur and Delacour (1988), who first described it, and assesses the declarative memory of rodents.

In the habituation phase, animals were placed in the open field arena for 5 minutes and allowed to explore freely. Then, the animals were returned to their cages and the apparatus was cleaned.

Two identical bottles were placed in opposite corners of the arena, 5 cm away from the wall. After an ITI of 1h, the mice were loaded into the apparatus again and were allowed to explore the objects for 10 minutes (acquisition phase). The time the mice spent exploring each object was recorded. We considered "exploring" when the mice were interacting with the objects. The animals were returned to their cages and the apparatus was cleaned.

One of the bottles was replaced by a different one in the same place, meaning the apparatus had one familiar object (from the acquisition phase) and one novel object (Fig. 7). If the animal did not show any bias towards one of the objects in the acquisition phase, the object replaced was the one in the left upper corner in 50% of the trials, and

the one in the right lower corner 50% of the times. If the animal had a bias, the object replaced was the one they spent more time exploring. The mice were loaded again in the arena, after an ITI of 90 minutes, and allowed to explore the objects for 5 minutes.

The Recognition Index, by which declarative memory is expressed, was calculated as follows:

$$\frac{Time\ spent\ exploring\ the\ novel\ object}{Time\ spent\ exploring\ the\ novel\ object + Time\ spent\ exploring\ the\ familiar\ object} \times 100$$

Figure 7 - Representative images of the Open Field apparatus with the objects used in the Object Recognition test for the behaviour characterization of the 6 months old APP/PS1 female mice.

2.4. Modified Y-Maze

The modified Y-Maze test is used for assessing spatial reference memory, a form of memory that involves the hippocampus (Negrón-Oyarzo *et al.* 2018). This method was adapted from Viana da Silva *et al*. (2016). In this test, a Y-shaped apparatus was used (Fig. 8). The arms of the apparatus were designed: start arm, other arm and novel arm.

During the acquisition phase, the novel arm of the apparatus was inaccessible. Mice were placed in the start arm, facing the wall and allowed to explore the two arms for 5 minutes.

The test phase began after an ITI of 2 hours and the novel arm was made accessible. The animals were placed in the start arm, facing the wall and allowed to explore for 5 minutes. Time spent in the novel arm was evaluated to estimated spatial memory.

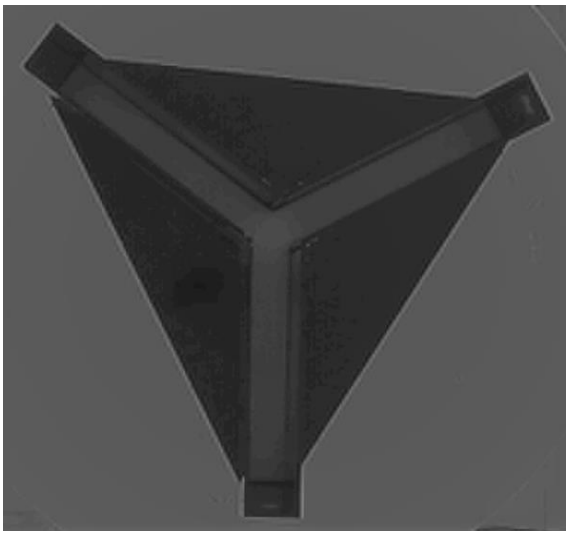

Figure 8 - Representative images of the modified Y-Maze apparatus used for the behaviour characterization of the 6 months old APP/PS1 female mice

2.5. Elevated Plus Maze

The elevated plus maze test is used to measure anxiety-like behaviour in mice (Lister, 1987). Rodents show a natural preference for the closed arms (more protected) of the maze but have some natural curiosity to explore the open arms (more exposed). However, the use of anxiolytic agents can decrease the preference for the closed arms whereas the use of anxiogenic agents can increase this preference for the closed arms (Lister, 1987). Therefore, the lower the ratio of time spent in the closed versus the open arms, the more anxious the mice are. This method was adapted from Dias *et al*. (2021)

In this test, the apparatus used had two open arms (*i.e.* without lateral walls) and two closed arms and was supported 50 cm above the table (Fig. 9). The mice were placed in the center of the apparatus facing an open arm and allowed to explore for 5 minutes. An entry in the open arms was recorded when the mouse had its four paws in the open arms. Parameters such as number of entries in the open arms and time spent in the open arms are evaluated.

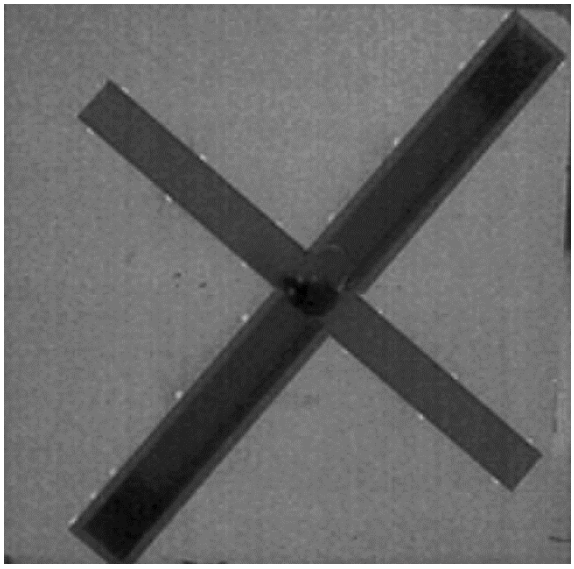

Figure 9 - Representative images of the Elevated Plus Maze apparatus used for the behaviour characterization of the 6 months old APP/PS1 female mice

2.6. Morris Water Maze

The Morris Water Maze test was first described in 1981 by Richard Morris and later adapted (Morris, 1981; Morris, 1984). This test can be used to assess spatial learning and reference memory (Vorhees & Williams, 2006). Reference memory is a form of long-term memory in which the hippocampus and cortex are the most involved. Besides, performance in this test correlates with LTP, a form of hippocampal synaptic plasticity (Vorhees & Williams, 2006).

This method was adapted from Moreira-de-Sá *et al.* (2020). A circular pool was filled half-way with water at 21ºC. The maze was divided into four imaginary and equal quadrants by four points: north, south, west, east.

To allow mice to escape the maze, a circular and transparent platform was submerged 1 cm below the surface, in the middle of one of the quadrants. The water of the pool is colored white, thus rendered opaque, with white paint (Faber Castell Tempera Fun Paint). In these conditions, the animals cannot see the platform, and there are no auditory or olfactory cues. However, distal cues (extra-maze) are used to aid mice in spatial localization of the platform.

The test is composed of 4 trials per day. In each trial a semi-random start position is used, hence all positions are chosen but only one time (*e.g.* N, W, S, E). Visual cues are placed equidistantly in the walls in the room in which the test was performed. Mice were habituated in the room of the test, for 1 hour before beginning the procedures, with red light (10 lx).

After each trial, mice were placed in a cage with a heating pad before being retrieved to their home cages, to minimize the animal's suffering.

The test is recorded and analyzed by the AnyMaze software, recording the number of crossings in each quadrant, the swimming pattern of the animals and their ability to find the hidden platform.

2.6.1. Spatial Acquisition

During spatial acquisition, mice learn how to reach the platform in a direct path from different start positions using distal cues.

The mice were placed in the pool in the start position. The trial ended when mice reached the platform and stayed on it for ten seconds. If this did not occur, then the test was finished after one minute. In this case, after the test mice were guided to the platform and placed on it for ten seconds.

Latency to reach the platform is evaluated and used to create a learning curve. The acquisition phase is finished when average control latency to reach the platform is less than the predefined time of 20 seconds. This occurred after 6 days of testing.

2.6.2. Probe Trial

In this phase, the reference memory is evaluated thus, this phase was performed 24 hours after the last day of acquisition.

In the probe trial or transfer test, the platform was removed. Mice were loaded in the position in which they had a faster latency to reach the platform the day before and allowed to explore for 1 minute.

Reference memory is evaluated by assessing the number of crossings in the site where the platform was and the time mice spent in each quadrant, which reflect mice's "spatial bias".

2.6.3. Reversal Learning And Probe Trial

For this phase, all conditions mentioned in the acquisition phase (2.6.1.) were kept, except that the platform was placed in the opposite quadrant. Therefore, mice had to re-learn how to find the platform in its new location using the strategies they had already learned.

To assess reference memory, a probe trial was performed in the same conditions described in section 2.6.2.

2.6.4. Cued Learning

This phase is a control for the MWM test, as visual, motor and motivation to escape impairment can affect the mice performance on the test (Morris, 1984).

In this test, the platform is decorated with adornments and is placed 1 cm above the water surface, in order to help mice locate it. Therefore, mice, if not visually impaired, can see the platform and are expected to navigate towards it in a direct path. Latency to reach the platform was assessed.

2.6.5. Search Strategies

Mice search strategies were evaluated by the AnyMaze Software. Videos of the probe trial were analysed, and a path was created from the start of the trial till the mice crossed the site where the platform was for the first time. Based on the path created, hippocampal-dependent or non-hippocampal-dependent strategies were assigned to each mice (Garthe & Kempermann, 2013; Janus, 2004, Moreira-de-Sá *et al*., 2020).

2.7. Fear Conditioning

The Fear Conditioning test is a form of Pavlovian conditioning first described by Pavlov (1927). In this test an association between a neutral conditioned stimulus and a noxious unconditional stimulus is created. Mice, then exhibit a conditioned response which is often freezing, a defence behaviour. This process involves both the hippocampus for processing the context and the amygdala (more specifically the basolateral amygdala) for creation and storage of the association (Maren, 2001). This addresses both memory and emotion, as mice learn that some stimuli lead to unpleasant results.

After each trial, the chambers were cleaned with 10% ethanol and the mice were returned to the transport cage to avoid having mice that completed the test and mice that had not in the same cage. After all animals from the same home cage completed the test, they were returned to their home cages.

This method here described was adapted from Aguiar *et al.* (2010).

2.7.1. Acquisition

In the acquisition phase, animals were placed in a sound-attenuated chamber and habituated for 140 seconds. The chamber had transparent PVC walls, was covered at the top and the floor was composed of grid metal (context A). The chamber was illuminated by white light (450-650nm) and near-infrared light (940 nm).

After the habituation, an auditory tone of 4 KHz, 80-dB was delivered for 20 seconds. In the last 2 seconds of the auditory tone, a 0.5-mA foot-shock was delivered. The auditory tone and foot-shock were repeated 4 times with a 120 seconds interval, totaling 4 auditory tones and 4 foot-shocks.

The time mice spent in freezing behaviour was evaluated, in the habituation before the shock and then between shocks thus, for 128 seconds. Freezing is a species-specific defense mechanism and has been defined as "suppression of all movement except that required for respiration" (Anagnostaras, 2010).

2.7.2. Contextual Fear Conditioning

To evaluate contextual fear conditioning, 24 hours after the acquisition phase, the animals were placed again in the same chambers in context A, except that no auditory tone or foot-shock was delivered. Time spent in freezing behaviour was evaluated in every minute of the test.

2.7.3. Cued Fear Conditioning

To evaluate the cued fear conditioning, animals were placed in the sound-attenuated chambers in context B to avoid spatial recognition. Context B differs from context A in three dimensions: first, the walls of the chamber had a different pattern; second, the floor was covered with white PVC; third, the chamber was illuminated only by near-infrared light (940 nm).

After the 140 seconds habituation, a 4 KHz, 80-db auditory tone was delivered for 20 seconds. No foot-shock was delivered. Another auditory tone was delivered 120 seconds after, and the process was repeated totaling 4 delivered auditory tones. Time spent in freezing behaviour was evaluated right after each auditory tone.

3. Sample Preparation

Mice were sacrificed by one of two methods: cervical dislocation followed by decapitation; or intraperitoneal injection of avertin (2.2.2-tribromoethanol 70.7 mM, 2-

methyl-2-butanol 113.4 mM, NaCl 138 mM, pure ethanol 12.5% in Phosphate-buffered saline (PBS), Sigma), an anesthetic, followed by perfusion in the heart with a sucrose solution (KCl 2 mM, sucrose 180 mM, glucose 20 mM, L-acid ascorbic 1.3 mM, sodium pyruvate 0.4 mM, $CaCl_2$ 0.4 mM, $MgCl_2$ 8 mM and NaH_2PO_4 1.3 mM and $NaHCO_3$ 26 mM in H_2O)

The brains were then dissected on an ice-cold oxygenated artificial cerebrospinal fluid solution (aCSF; NaCl 124 mM, KCl 3 mM, $NaHCO_3$ 26 mM, NaH_2PO_4 1.25 mM, D-Glucose 10 mM, $MgSO_4$ 1mM, $CaCl_2$ 2 mM) or a 10% sucrose solution (sucrose 0.32 M, EDTA-Na 1 mM, HEPES 10 mM and bovine serum albumin (BSA) 1 mg/mL, pH 7.4). The cortex was collected and used for further analysis or stored at -20ºC.

4. Synaptosomal Preparation

Synaptosomes are an enriched preparation of the synaptic compartment which has extensively been characterized and explored in our research group (Canas *et al*., 2009; Moreira-de-Sá *et al*., 2021; Rebola *et al.*, 2005). Synaptosomal preparation was done as described in Rebola *et al.* (2005). The cortex was homogenised in 10 mL of a 10% sucrose solution (sucrose 0.32 M, EDTA-Na 1 mM, HEPES 10 mM and BSA 1 mg/mL, pH 7.4) at 4ºC. The mixture was then centrifuged at 3000 × *g* for 10 minutes at 4ºC.

The supernatant was collected and centrifuged again at 14000 × *g* for 12 minutes at 4ºC. The pellet was resuspended in 1 mL of a 45% (v/v) Percoll solution (45% v/v Percoll and NaCl 0.067 M, pH 7.4, volume set with KHR)

The sample was then centrifuged at 16400 × *g* for 2 minutes at 4ºC. The top layer, which contains the synaptosomes, was collected and resuspended in 2 mL of a Krebs HEPES Ringer (KHR) solution (NaCl 140 mM, EDTA-Na 1 mM, HEPES 10 mM, KCl 5 mM and glucose 5 mM, pH 7.4). The sample was then centrifuged at 16400 × *g* for 2 minutes at 4ºC. The pellet was resuspended in 250 µL of the same KHR solution.

5. Total Protein Extracts of Brain Tissue

Fresh cortex tissue was weighted and 10 mg were used for preparation of total protein extracts. The tissue was homogenised in radioimmunoprecipitation assay buffer (RIPA buffer; Tris-HCl 50 mM pH 7.4, NaCl 150 mM, IGEPAL (NP-40) 1%, sodium

deoxycholate 0.5%, EDTA 1mM and SDS 0.1%) with phenylmethylsulfonyl fluoride (PMSF) 1 mM and dithiothreitol (DTT) 1 mM.

The homogenate was placed at 4ºC with agitation for 2 hours, followed by a centrifugation at 13000 × *g* for 20 minutes at 4ºC. The supernatant was collected and stored at -20ºC.

6. Protein Quantitation

The determination of protein concentration was assessed with the Pierce™ BCA Protein Assay Kit (Pierce™, Thermo Scientific™). The BCA method is a colorimetric method where BSA is used as a standard.

A standard curve with several dilutions of BSA in water was prepared with 2, 1, 0.5, 0.25, 0.125, 0.0625 and 0 µg/µL of BSA. Synaptosomes samples and KHR were diluted 1:20 in H_2O and total protein extracts samples and RIPA buffer were diluted 1:10 in H_2O.

Protein quantitation was prepared in a 96 well dish in which was added 25 µL of water in each well and in triplicate. Then, 25 µL of the standard curve dilution, sample or buffers were added. BCA reagent was prepared according to kit instructions and 200 µL of the reagent were added to each used well.

The plate was incubated for 30 minutes at 37ºC in obscurity. Following incubation, the plate was read in a Microplate Reader (Spectra Max Plus) at 570 nm. Obtained values were used to calculate the standard curve and with it, calculate the protein concentration in the samples in µg/µL.

7. Western Blot Analysis

7.1. Preparation of Samples For Western Blot

After synaptosomal preparation, the sample was collected and centrifuged at 16400 x *g* for 2 minutes at 4ºC. The pellet was then resuspended in RIPA buffer with PMSF 1mM and DTT 1mM and stored at -20ºC. DTT is a reductant which aids in protein denaturation and PMSF is a serine and cysteine protease inhibitor.

Synaptosomal and total protein extracts samples were normalized with sample buffer 6x (Tris 500 mM, DTT 600 mM, SDS 10%, glycerol 30% and bromophenol 0.012%) and H_2O and heated for 20 minutes at 70ºC for denaturation.

7.2. SDS-PAGE

Samples (15, 30 or 60 µg of protein) were loaded on a 10% or 15% SDS-PAGE gel, with a 4% stacking gel (Table 1). The system was filled with running buffer (Table 2) and electrophoresis was performed at 80V for 15-20 minutes in the initial phase. In the final phase, electrophoresis was performed at 110V for 40-60 minutes. NZYColour Protein Marker II (NZYtech, Portugal) was used as a molecular marker.

Table 1 – Composition of the resolving and stacking gel used in the Western blot analysis

Resolving gel		**Stacking gel**
10%	**4%**	**15%**
4.1 mL H_2O	6.1 mL H_2O	2.4 mL H_2O
3.3 mL Acrilamide 30%	1.3 mL Acrilamide 30%	5 mL Acrilamide 30%
2.5 mL Tris-HCl 1.5 M	2.5 mL Tris-HCl 0.5 M	2.5 mL Tris-HCl 1.5 M
0.1 mL SDS 10%	0.1 mL SDS 10%	0.1 mL SDS 10%
50 µL of APS 10%	50 µL of APS 10%	50 µL of APS 10%
5 µL of TEMED	10 µL of TEMED	5 µL of TEMED

Table 2 - Composition of the running buffer used in the Western blot analysis

Running buffer 5x	**Running Buffer 1x**
15 g Tris-HCl	100 mL Running Buffer 5x
156.67 g Bicine	900 mL H_2O
5 g SDS	
1000 mL H_2O, pH 8.3	

7.3. Electrotransfering

After SDS-PAGE, the contents of the gel were electro transferred to a nitrocellulose membrane. A wet transfer method is used where gel and nitrocellulose membrane were sandwiched between filter paper wetted in 3-(cyclohexylamino)-1-propane-sulfonic acid (CAPS)(Table 3) and submerged in a cassette filled with CAPS (Table 3).

Table 3 – Composition of the CAPS buffer used in the Western blot analysis

CAPS 10x	**CAPS 1x**
22.1 g CAPS	100 mL CAPS 10x
1000 mL H_2O, pH 11	100 mL methanol
	800 mL H_2O

Electrotransfering was performed with 1A of constant current at 4ºC with agitation, for 2 hours. Membranes were then stained with a solution of Ponceau S to verify if electrotransfer was successfully done.

7.4. Immunodetection

The membranes were incubated for 1 hour at room temperature (RT) with agitation with 5% skim milk in TBS-T or 5% BSA in TBS-T (Table 4 and Table 5). Following blocking, the membranes were incubated with the primary antibodies diluted in TBS-T with 1% skim milk or 5% BSA (Table 6). This incubation was done overnight at 4ºC and with agitation. The next day, membranes were washed, at RT with agitation, with TBS-T 3 times for 10 minutes and incubated with the secondary antibodies diluted in 1% skim milk in TBS-T or 5% BSA in TBS-T for 2 hours, at RT, with agitation (Table 7). The secondary antibodies used were conjugated with peroxidase for detection.

Table 4 – Composition of the TBS solution used for immunodetection in the Western blot analysis

TBS 10x	**TBS-T 1x**
24.2 g Tris-HCl (20 mM)	100 mL TBS 10x
80.0 g NaCl sodium chloride (137 mM), pH 7.6	900 mL H_2O
	1 mL Tween 20

Table 5 - Composition of the skim milk and BSA solutions used for immunodetection in the Western blot analysis

5%Skim Milk / BSA	**1% Skim Milk / BSA**
100 mL TBS-T 1x	100 mL TBS-T 1x
5 g dry skim milk or BSA	1 g dry skim milk or BSA

Table 6 – Primary antibodies used for Western blotting analysis and information about its supplier, reference and host, as well as blocking agent used for immunodetection and dilution of the antibody.

Target	Supplier	Reference	Host	Dilution	Blocking agent used
Sestrin 2	ProteinTech	21346-1-AP	Rabbit	1:2000	Skim milk
AMPK	Santa Cruz	sc-25792	Rabbit	1:2000	Skim milk
pAMPK	Santa Cruz	sc-33524-R	Rabbit	1:2000	BSA
Sirtuin 1	Cell Signaling	2028	Rabbit	1:1000	BSA
Sirtuin 3	Cell Signaling	2627	Rabbit	1:1000	BSA
Mitofusin 2	Abcam	AB50838	Rabbit	1:5000	BSA
LC3	Sigma	L7543	Rabbit	1:5000	BSA
GAPDH	Abcam	ab9485	Rabbit	1:5000 (for analysis of 6 months of age APP/PS1 female mice) 1:10000 (for analysis of 9 months of age APP/PS1 female mice and $A\beta_{1-42}$-injected mice)	BSA or Skim milk
PSD-95	Cell Signaling	3450	Mouse	1:10000	Skim milk
SNAP-25	Sigma	S5187	Mouse	1:10000	Skim milk
Syntaxin	Sigma	S0664	Mouse	1:10000	Skim milk
Synaptophysin	Sigma	S5768	Mouse	1:10000	Skim milk

Table 7 – Secondary antibodies used for Western Blotting analysis and information about its supplier, reference and host, as well as blocking agent used for immunodetection and dilution of the antibody.

Target	Supplier	Reference	Host	Dilution	Blocking agent used
Goat anti-mouse - peroxidase conjugated	Thermo Fisher	31432	Mouse	1:5000	Skim milk
Goat anti-rabbit - peroxidase conjugated	Thermo Fisher	31462	Rabbit	1:5000	Skim milk

Membranes were then washed with TBS-T 3 times for 10 minutes. Membranes were incubated with an enhanced chemiluminescence (ECL) kit (Pierce™ Thermo Scientific), a West Pico kit (SuperSignal™ Thermo Scientific) or a Immobilon® Forte (Millipore) solution, that are substrates of peroxidase. Detection was analysed using a ChemiDoc (BioRad) and quantification was performed in the ImageLab software.

7.5. Membrane Stripping And Re-Probing

After immunodetection, membranes were washed with TBS-T 2 times for 10 minutes, followed by 2 washes with a stripping solution for 15 minutes (Table 8). This solution allows removal of the primary and secondary antibodies, thus, being useful for re-probing of the same membrane for a normalization protein and/or other proteins of interest. Then, membranes were again washed with TBS-T for 10 minutes and immunodetection was performed as described in Section 7.4.

Table 8 – Composition of the stripping solution used for membrane stripping in Western blot analysis

Stripping Solution
15 g Glicine
1 g SDS
10 mL Tween 20, pH 2.2

Density levels of the protein of interest were obtained by applying a ratio between the density of the protein of interest and the density of glyceraldehyde 3-phosphate

dehydrogenase (GAPDH). GAPDH is considered a housekeeping protein, as its density is not altered between samples of control and samples of interest, which makes it a reliable loading control and normalization protein (Wu *et a*l., 2012).

8. Statistical Analysis

Statistical analysis was performed using GraphPad Prism Software version 8.1.1. (GraphPad Software, La Jolla California USA). Results are presented as mean ± standard error of mean (SEM). Significance level was set for p value < 0.05 in all tests.

Unpaired Student's *t*-test was used for comparisons between two independent groups. For comparisons between two or more groups a two-way analysis of variance (ANOVA) was used followed by a *post hoc* Sidak's multiple comparison test. A chi-square test was used for analysis of search strategies in the MWM test. Each result was analysed for outlier values, by a ROUT method with a Q = 1%, and any outlier detected was excluded from the results.

Results

1. Behaviour Characterization of 6 Months Old Female APP/PS1 Mice

APP/PS1 mice were first characterized by behaviour analysis for a phenotype confirmation of AD-like pathology. Thus, at 6 months of age, female APP/PS1 and WT littermates mice were submitted to various tests that assess memory and mood.

In the open field test, locomotion and anxiety-like behaviour are evaluated (Hall, 1934). No alterations in total distance travelled (WT: 17.2 ± 2.0 m; APP/PS1: 18.9 ± 1.2 m; p=0.5824; n=6-34; Fig. 10a), and maximum speed (WT: 0.25 ± 0.01 m/s; APP/PS1: 0.30 ± 0.01 m/s; p=0.0591; n=6-34; Fig. 10b), were observed between genotypes, indicating that mice's locomotion is not compromised. APP/PS1 mice spent less time in the center of the apparatus than WT mice (WT: 33.4 ± 12.4%; APP/PS1: 13.5 ± 1.7%; p=0.0036; n=6-34; Fig. 10b), which could be an indicator of anxiety, while no alterations were found in the number of entries in the center of the arena between genotypes (WT: 52.6 ± 1.5; APP/PS1: 34.8 ± 3.6; p=0.0664, n=5-34, Fig. 10d).

Anxiety-like behaviour is further assessed in the EPM test, in which APP/PS1 mice spent less time in the open arms of the apparatus than WT mice (WT: 25.1 ± 5.3%; APP/PS1: 11.9 ± 2.1%; p=0.0214, n=6-34; Fig. 10f). Furthermore, APP/PS1 mice also entered less times in the open arms compared to control mice (WT: 12.3 ± 3.8; APP/PS1: 5.3 ± 0.9; p=0.0100; n=6-34; Fig. 10g), thus supporting the idea that APP/PS1 seem to be more anxious than WT mice.

To assess memory and learning, modified Y-Maze, OD test and OR test were used. Both modified Y-Maze and OD test are used to assess spatial memory. The OR test assesses declarative memory.

In the modified Y-Maze, APP/PS1 mice spent less time in the novel arm than WT mice (WT: 37.0 ± 5.2%; APP/PS1: 26.2 ± 1.5%; p=0.0121; n=6-33; Fig. 10e).

In the OD and OR tests, a preference index is used to identify mice's potential preference for one of the objects. Since two objects are displayed, a baseline of 50% is applied for results interpretation. Thus, a preference index of 50% means there is no preference for any object; below 50%, the mice prefer the familiar object; and above 50% mice prefer the novel object (Antunes & Biala, 2011). Mice have a natural preference for novelty as they can remember the familiar object (Antunes & Biala, 2011).

No alterations were found between APP/PS1 and WT mice in the preference indexes of the OD (WT: 47.9 ± 6.7%; APP/PS1: 41.2 ± 4.6%; p=0.5513; n=6-32; Fig. 10h) and OR tests (WT: 58.2 ± 6.8%; APP/PS1: 50.2 ± 3.3%; p=0.3325; n=6-32; Fig. 10i).

Overall, these results show that APP/PS1 display anxiety-like behaviours and their spatial memory is mildly impaired.

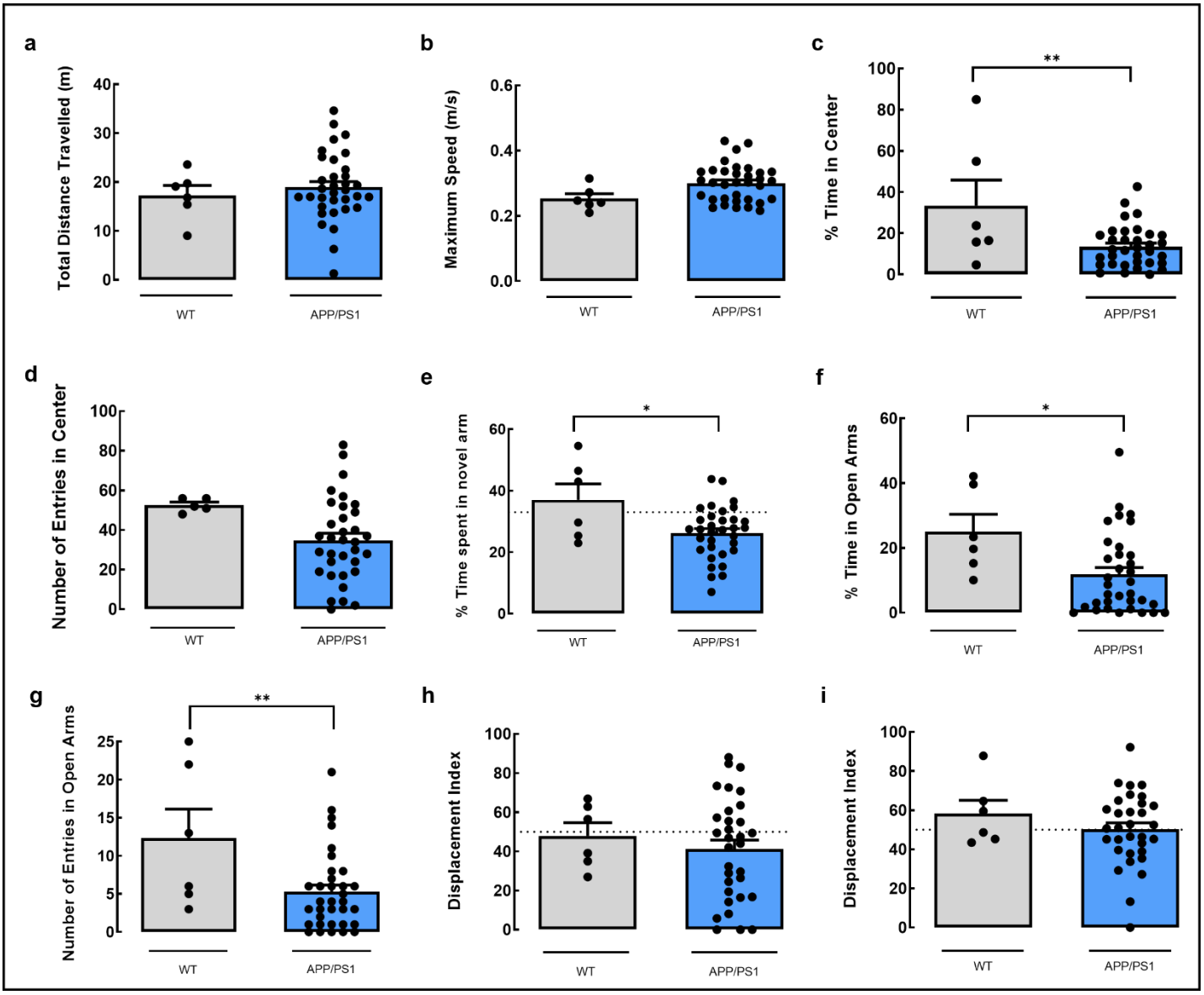

Figure 10 - Behaviour analysis of 6 months old female APP/PS1 mice. In the open field test, total distance travelled in meters (**a.**) the maximum speed reached in meters by seconds (**b.**) percentage of time spent in the center of the open field arena (**c.**) and number of entries in the center of the arena (**d.**) were evaluated. In the Modified Y-Maze, we evaluated the percentage of time spent in the novel arm of the maze (**e.**). In the Elevated Plus Maze, we registered the percentage of time spent in the open arms of the maze (**f.**) and the number of entries in the open arms (**g.**). The displacement index is calculated in the Object Displacement test (**h.**) and the recognition index is assessed in the Object Recognition Test (**i.**). * p< 0.05; ** p< 0.005, using a Student's unpaired *t*-test. Values are mean ± SEM of 5-6 WT and 32-34 APP/PS1 mice. A significant decrease in the percentage of time spent in the center of the open field arena in the OF test, the percentage of time spent in the novel arm of the maze in the Modified Y-Maze test, the percentage of time spent in the open arms and number of entries in the open arms of the maze in the EPM test was found in APP/PS1 mice compared to control WT mice.

2. Neurochemical Characterization of 6 Months Old Female APP/PS1 Mice

After behaviour characterization, female APP/PS1 and wild-type C57BL/6 littermates with 6 months were sacrificed and their cortices were used for preparation of synaptosomes.

Synaptosomes are isolated nerve terminals that reseal after separation from the axon. These structures retain the post-synaptic density, a protein specialization. The synaptosomes prepared are viable and are composed by cytoplasm, synaptic vesicles, few mitochondria and cytoskeleton (Dunkley, 2008; Evans, 2015).

Synaptosomal extracts were then used for estimating the densities of various protein involved in the cell's metabolism, autophagy and mitochondria dynamics, by Western blotting.

Sirtuins are involved in the cell's metabolism, their activity being influenced by NAD^+ levels in the cell (Rizzi & Roriz-Cruz, 2018). We analysed SIRT1, a nuclear sirtuin, and SIRT3, a mitochondrial sirtuin. No alterations were observed in SIRT1 levels in APP/PS1 mice compared to WT mice (WT: 100.0 ± 3.0%; APP/PS1: 85.8 ± 7.2%; p=0.0617; n=4-8; Fig. 11a) nor in SIRT3 (WT: 100.0 ± 2.4%; APP/PS1: 85.8 ± 12.5%; p=0.4271; n=4-7; Fig. 11b).

AMPK is a sensor and regulator of cell's energy. AMPK levels are not altered in APP/PS1 mice compared to WT mice (WT: 100.0 ± 6.0%; APP/PS1: 134.9 ± 16.9%; p=0.2547; n=3-8; Fig. 11c). Furthermore, there is no alteration in phosphorylated AMPK levels between genotypes (WT: 100.0 ± 15.4%; APP/PS1: 74.3 ± 24.5%; p=0.4337; n=4-5; Fig. 11d), indicating that in APP/PS1 there are no changes in activation of AMPK through phosphorylation.

As for SESN2, a stress-response protein, no changes were observed between genotypes (WT: 100.0 ± 14.2%; APP/PS1: 66.9 ± 15.0%; p=0.1740; n=5-9; Fig. 11e)

To evaluate autophagy in AD, we determined LC3-I and LC3-II levels in synaptosomes. Interestingly, LC3-I is increased in APP/PS1 mice compared to WT mice (WT: 100.0 ± 5.4%; APP/PS1: 142.1 ± 12.7%; p=0.0355; n=5-9; Fig. 11f), while no alterations in LC3-II levels were found (WT: 100.0 ± 5.6%; APP/PS1: 144.0 ± 34.4%; p=0.2750; n=3; Fig. 11g). However, for a reliable indication of autophagic flux, the LC3-II/LC3-I ratio must be calculated. We found no alterations in the LC3-II/LC3-I ratio

between APP/PS1 and WT mice (WT: 1.02 ± 0.04; APP/PS1: 0.91 ± 0.15; p=0.5029; n=3; Fig. 11h).

To explore potential alterations in the mitochondria dynamics, we assessed MFN2 density in synaptosomes. We found that mitochondrial fusion is presumably not altered in APP/PS1 mice compared to WT mice, as no alteration in MFN2 levels are observed (WT: 100.0 ± 5.5%; APP/PS1: 78.1 ± 7.3%; p=0.0782; n=4-8; Fig. 11i).

Overall, these results indicate that, cortical synapses of 6 months old APP/PS1 mice do not show an apparent impairment in the metabolism, autophagy and mitochondrial fusion.

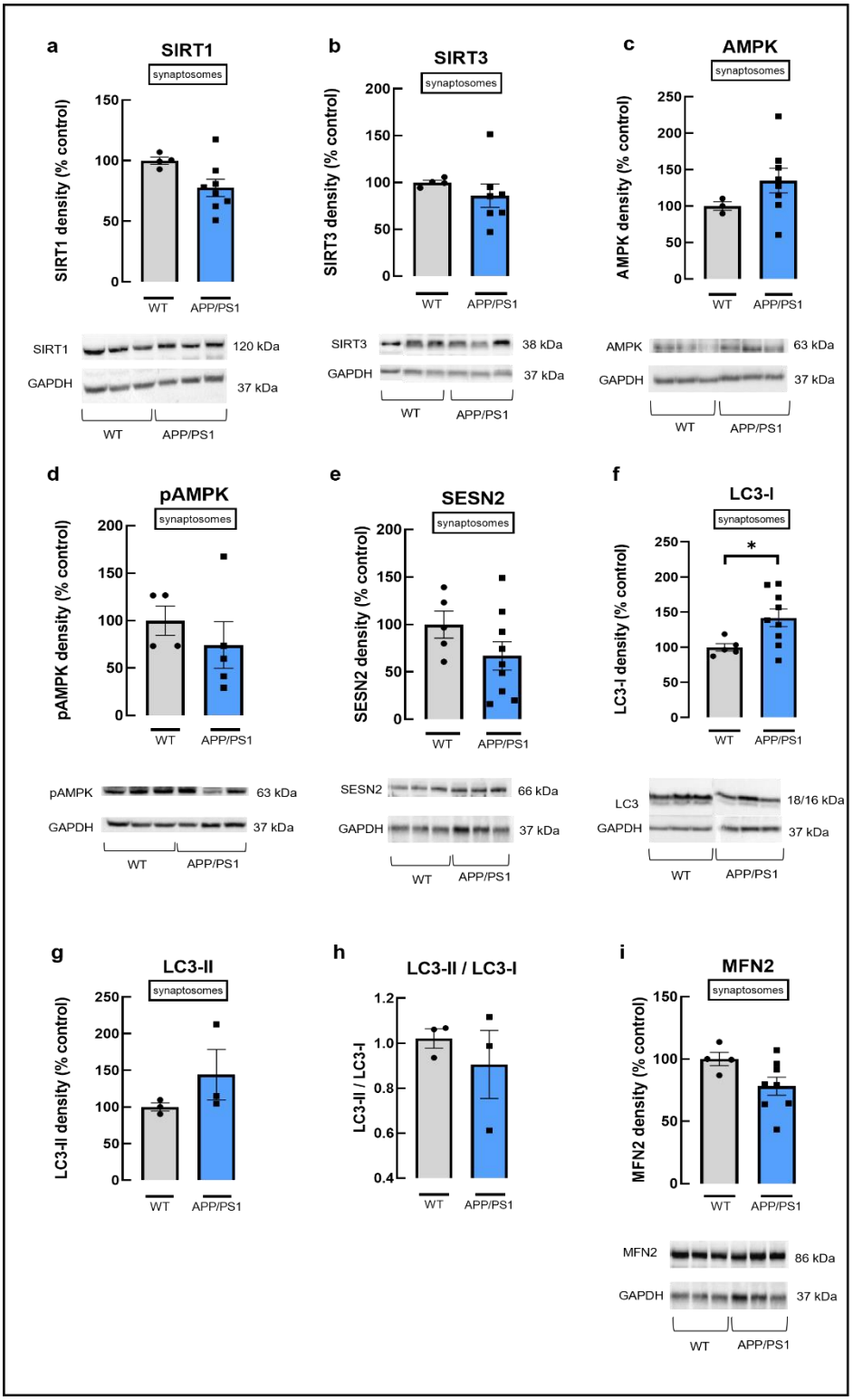

Figure 11 - Relative density of proteins **a.** SIRT1, **b.** SIRT3, **c.** AMPK, **d.** pAMPK, **e.** SESN2, **f.** LC3-I, **g.** LC3-II, **h.** LC3-II/LC3-I, **i.** MFN2 in cortical synaptosomes of 6 months old female APP/PS1. GAPDH was used as a loading control, thus results as presented as a ratio between the density of the protein of interest and GAPDH. Results are presented as a percentage of values of control mice (WT), which was designated 100%. * $p<0.05$, using a Student's unpaired *t*-test. Values are mean ± SEM of 3-5 WT and 3-9 APP/PS1 mice. No significant alterations were found in the levels of these proteins, except for LC3-I, where a significant increase was observed in APP/PS1 mice compared to control WT mice.

We evaluated synaptic protein markers as, in AD, loss of these markers is correlated with cognitive decline (Arendt, 2009). Therefore, levels of pre-synaptic membrane proteins SNAP-25 and syntaxin, synaptic vesicles membranes and extra-synaptic protein synaptophysin and post-synaptic membrane protein PSD-95, were estimated by Western blotting. Nor SNAP-25 (WT: 100.0 ± 50.2%; APP/PS1: 80.5 ± 17.8%; p=0.7001, n=4-5, Fig. 12a) nor synaptophysin (WT: 100.0 ± 8.2%; APP/PS1: 110.1 ± 13.2%; p=0.6209, n=4-8; Fig. 12c) levels were altered in APP/PS1 mice. On the other hand, syntaxin levels were decreased in APP/PS1 mice in comparison with WT (WT: 100.0 ± 0.4%; APP/PS1: 66.4 ± 5.2%; p=0.0030, n=3-5; Fig. 12b) and PSD-95 levels were increased in APP/PS1 mice (WT: 100.0 ± 4.4%; APP/PS1: 151.5 ± 14.9%; p=0.0401, n=4-8; Fig. 12d).

A summary of the alterations found in cortical synapses of 6 months old APP/PS1 female mice is presented in Table 9.

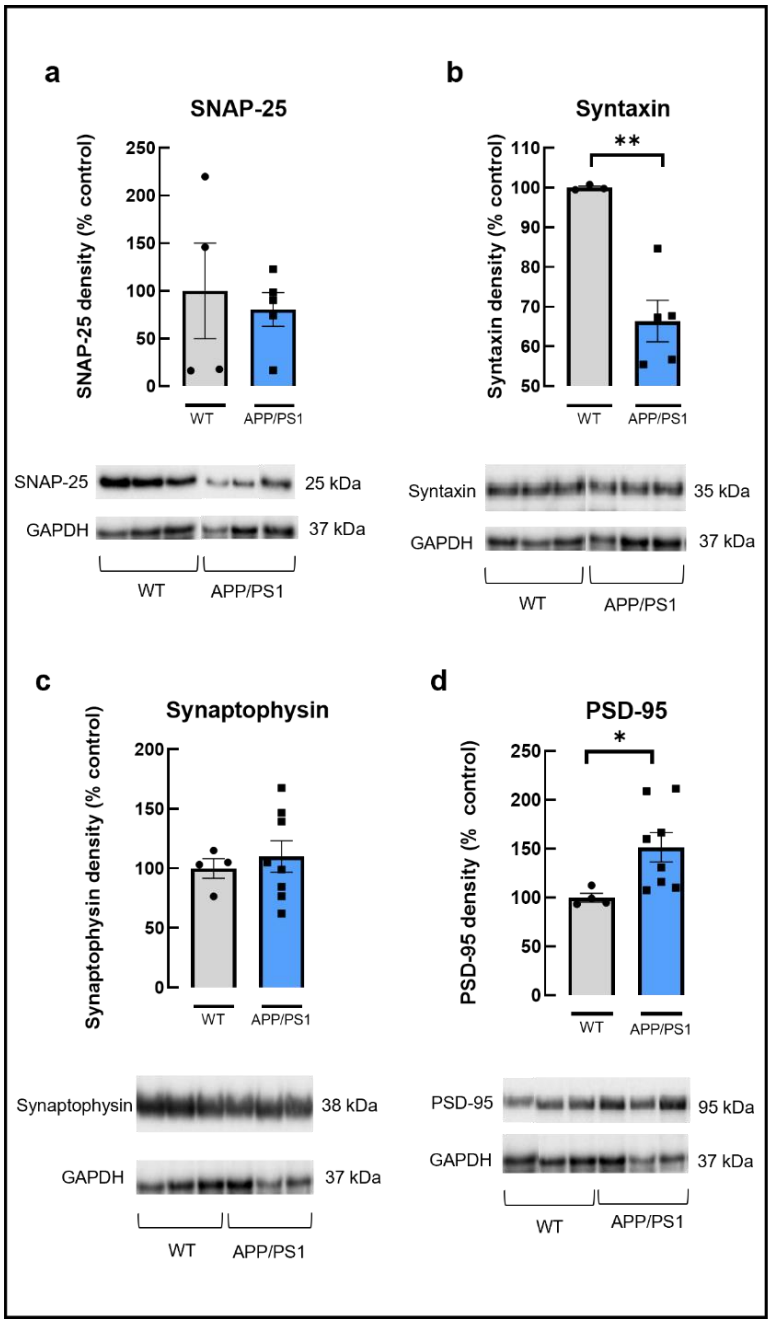

Figure 12 - Relative density of synaptic markers in cortical synaptosomes of 6 months old female APP/PS1 mice. Immunocontent of **a.** SNAP-25, **b.** syntaxin, **c.** synaptophysin and **d.** PSD-95. GAPDH was used as a loading control, thus results as presented as a ratio between the density of the protein of interest and GAPDH. Results are presented as a percentage of values of control mice (WT), which was designated 100%; * $p<0.05$; ** $p<0.005$, using a Student's unpaired *t*-test. Values are mean ± SEM of 3-4 WT and 5-8 APP/PS1 mice. A significant decrease in the levels of syntaxin, and a significant increase in the levels of PSD-95 was found in APP/PS1 mice compared to control WT mice. No significant alterations were found in the levels of SNAP-25 and synaptophysin in APP/PS1 mice.

Table 9 - Summary of the alterations of levels of SIRT1, SIRT3, SESN2, AMPK, pAMPK, MFN2, LC3 and synaptic proteins SNAP-25, syntaxin, synaptophysin and PSD-95 in cortical synaptosomes of 6 months old female APP/PS1 mice compared to control WT mice; = represents no alterations found, ↑ represents an increase and ↓ represents a decrease.

		Cortical synaptosomes of 6 months old mice
Protein	Process involved or localization	ΔAPP/PS1 vs. WT
SIRT1	Metabolism	=
SIRT3	Metabolism	=
SESN2	Stress response	=
AMPK	Sensor of energy	=
pAMPK	Sensor of energy	=
MFN2	Mitochondria fusion	=
LC3-I LC3-II LC3-II/LC3-I	Autophagy	↑ = =
SNAP-25	Pre-synaptic	=
Syntaxin	Pre-synaptic	↓
Synaptophysin	Pre-synaptic vesicle and extra-synaptic	=
PSD-95	Post-synaptic	↑

3. Behaviour Characterization of 9 Months Old Female APP/PS1 Mice

Behaviour analysis were conducted in 9 months old female APP/PS1 mice and WT littermates, with tests assessing spatial memory, anxiety-like behaviour and fear being performed.

In the OF test, no differences between APP/PS1 and WT were observed in total distance travelled in the apparatus (WT: 20.3 ± 2.4 m; APP/PS1: 15.2 ± 2.2 m; p=0.2160, n=5-13; Fig. 13a) nor in the maximum speed reached (WT: 0.30 ± 0.01 m/s; APP/PS1: 0.26 ± 0.02 m/s; p=0.1899, n=5-13; Fig. 13b), which means APP/PS1 mice do not have overt motor impairments. APP/PS1 mice show anxiety-like behaviour when compared with WT mice as they spent less time in the center area of the OF arena (WT: 27.9 ± 6.2%; APP/PS1: 4.9 ± 1.4%; p=0.0003, n=5-10; Fig. 13c) and entered the center area less number of times (WT: 71.2 ± 8.0; APP/PS1: 24.3 ± 4.4; p<0.0001, n=5-13; Fig. 13d). However, in the EPM test, no differences were observed in the time spent in the open arm of the apparatus (WT: 8.0 ± 3.3%; APP/PS1: 3.0 ± 1.1%; p=0.0824; n=5-11; Fig. 13f) nor in the number of entries in said arm (WT: 2.4 ± 1.2; APP/PS1: 1.4 ± 0.3; p=0.2733; n=5-13; Fig. 13g) between APP/PS1 and WT mice.

For assessment of spatial memory, the modified Y-Maze test was performed, and no differences were observed in the time spent in the novel arm of the maze between APP/PS1 and WT mice (WT: 31.4 ± 6.8%; APP/PS1: 30.3 ± 4.7%; p=0.9023; n=5-13; Fig. 13e).

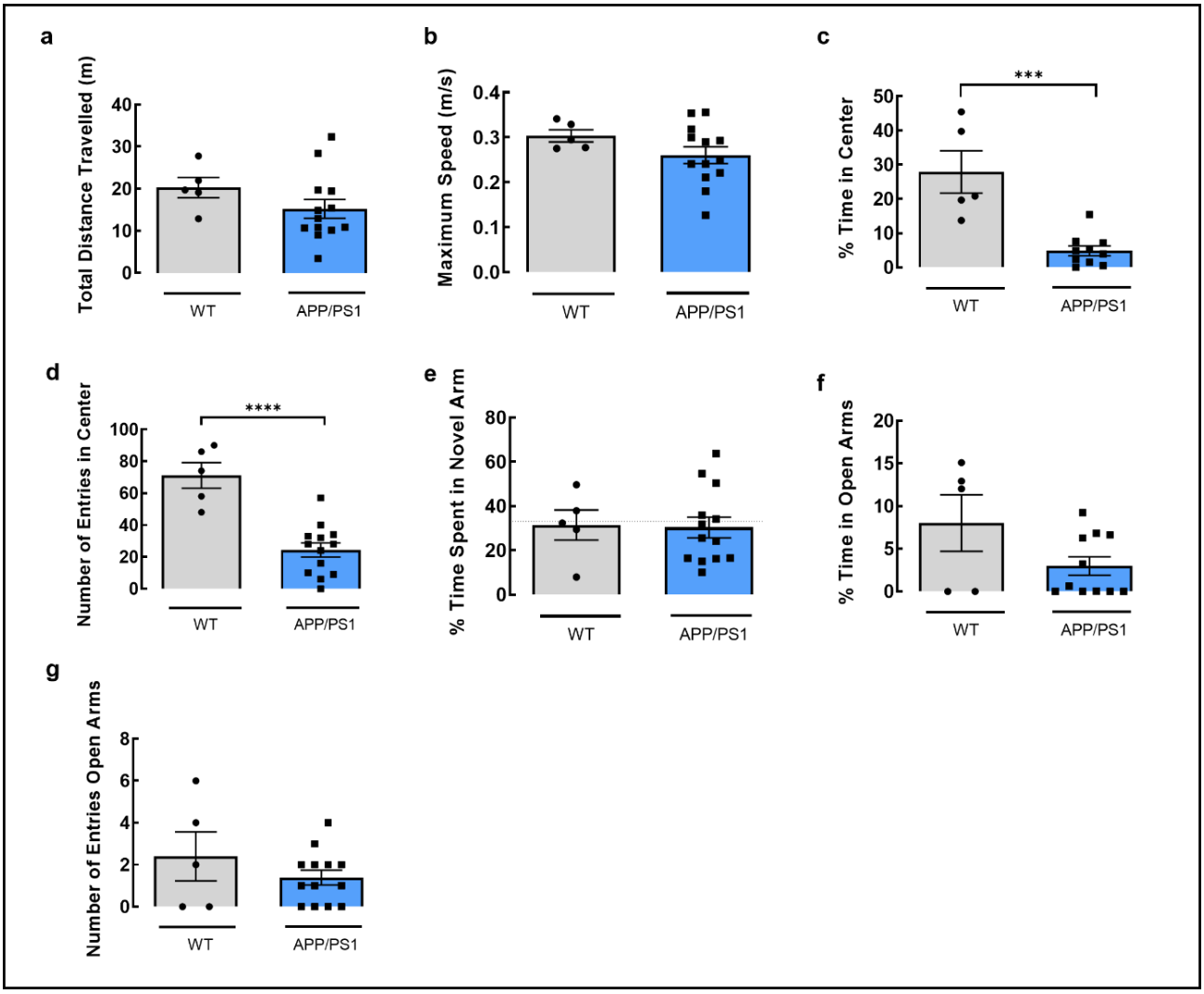

Figure 13 - Behaviour analysis of 9 months old female APP/PS1 mice. In the open field test, total distance travelled in meters (**a.**), the maximum speed reached in meters by seconds (**b.**), percentage of time spent in the center (**c.**) and number of entries in the center of the open field arena (**d.**) were evaluated. In the Modified Y-Maze, we evaluated the percentage of time spent in the novel arm of the maze (**e.**). In the Elevated Plus Maze, we registered the percentage of time spent in the open arms of the maze (**f.**) and the number of entries in the open arms (**g.**). *** p< 0.0005; **** p< 0.0001 using a Student's unpaired *t*-test. Values are mean ± SEM of 5 WT and 10-13 APP/PS1 mice. A significant decrease in the percentage of time spent in the center of the open field arena and number of entries in the center of the open field arena in the OF test, was found in APP/PS1 mice compared to control WT mice.

For a further memory characterization, to assess spatial reference memory and learning, the Morris Water Maze test was used (n=4-8). A visual acuity test was performed in the MWM as control for the test. The platform was made visible and latency to reach the platform was evaluated. Two criteria were defined: first, 4 trials were performed but only the last 2 were analysed; second, mice that took longer than 20 seconds to reach the platform were excluded from further analysis.

During the spatial acquisition, latency to reach the platform was evaluated. Over the days of this phase, latency to reach the platform decreased in both APP/PS1 (day 1: 60.0 ± 0.0 s; day 6: 44.3 ± 6.0 s; p=0.0061; n=8; Fig. 15a) and control mice (day 1: 60.0 ± 0.0 s; day 6: 11.0 ± 3.3 s; p<0.0001; n=4; Fig. 14a). Furthermore, after 6 days of training, control mice reached in platform in less than 20 seconds, which was the pre-defined latency used for considering learning. However, APP/PS1 mice, on the same day, take double the time to reach the platform (p=0.0006, n=4-8, Fig. 14a).

On the probe day, 24 hours after the last spatial acquisition day, the platform was removed to assess mice's memory retention. Firstly, to detect spatial bias the time spent in each quadrant was evaluated. Mice would spend more time in the quadrant where the platform in the acquisition phase was than in the other quadrants. However, no preference for one of the quadrants was detected (Fig. 14b). Secondly, the number of crossings in the site where the platform was in the acquisition phase were evaluated. Mice that cross the platform's site numerous times are mice that learned its position even if no sensory cue, as touching the platform, are present. APP/PS1 mice crossed the site of the platform less times than control mice (WT: 4.5 ± 1.2; APP/PS1: 1.4 ± 0.5; p=0.0183, n=4-8, Fig. 14c). All together, these results suggest that APP/PS1 mice have a spatial memory and learning impairment, as they showed slower learning of the platform localization, and affected spatial memory of its position.

In this test, thigmotaxic behaviour could also be evaluated and used for assessing anxiety. Thus, time spent swimming close to the maze walls was evaluated. APP/PS1 mice spent significantly more time swimming close to walls than control mice (WT: 11.4 ± 2.4 s; APP/PS1: 29.0 ± 3.8 s; p=0.0121, n=4-8, Fig. 14d), indicating that APP/PS1 mice are more anxious than WT mice.

On the probe day, search strategies used to find the site of the platform were also evaluated to determine if each mice's capacity to locate the platform was done by using a hippocampal or non-hippocampal dependent strategy.

Here, we observed that control mice use mostly hippocampus-dependent strategies (75%) while APP/PS1 mice use non hippocampus-dependent and hippocampus-dependent strategies equally (50%) (p=0.0003, n=4-8, Fig. 14e). Representative figures of the search strategies observed are present in Figure 15.

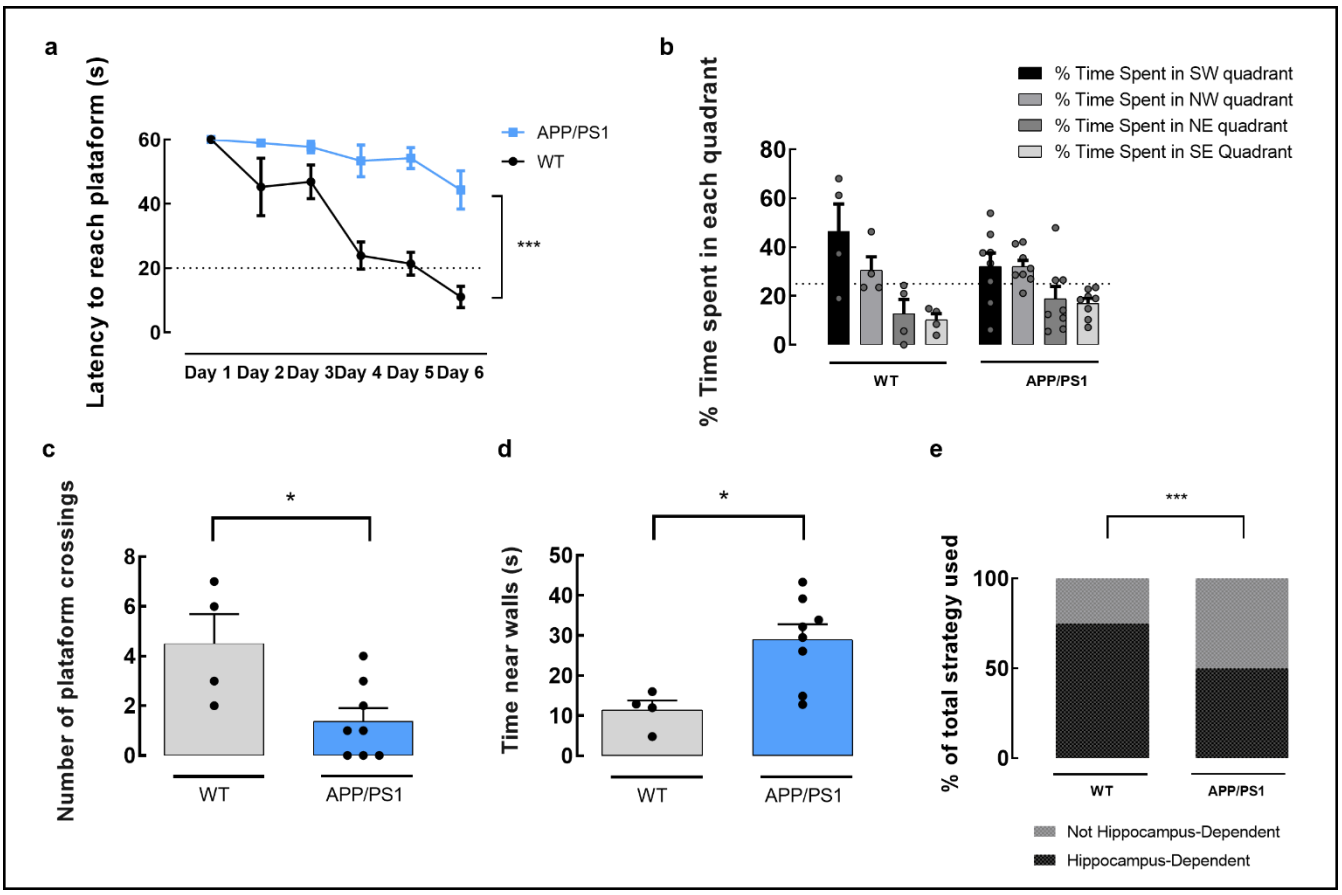

Figure 14 - Morris Water Maze test, performed with 9 months old female APP/PS1 mice. **a.** Latency to reach the platform during the 6 days of the test. **b.** Percentage of time spent in each quadrant during the probe day. During acquisition, the platform was in the SW quadrant. **c.** Number of crossings in the platform site in the probe day. **d.** Time spent swimming close to the walls. **e.** Percentage of animals that used a hippocampus-dependent of non hippocampus-dependent search strategy for the platform during the probe trial. * $p<0.05$, by a Student's unpaired *t*-test; *** $p<0.001$, by a Two-way ANOVA test, followed by a *post hoc* Sidak's multiple comparison test or a Chi-square test; A Two-Way ANOVA followed by a multiple comparisons test was used to analyse the percentage of time spent in each quadrant during the probe day; a Student's unpaired *t*-test was used to analyse the number of crossings in the platform site in the probe day and the time spent swimming close to the walls and a Chi-square test was used to analyse the percentage of animals that used a hippocampus-dependent of non-hippocampus dependent search strategy for the platform during the probe trial. Values are mean ± SEM of 4 WT and 8 APP/PS1 mice

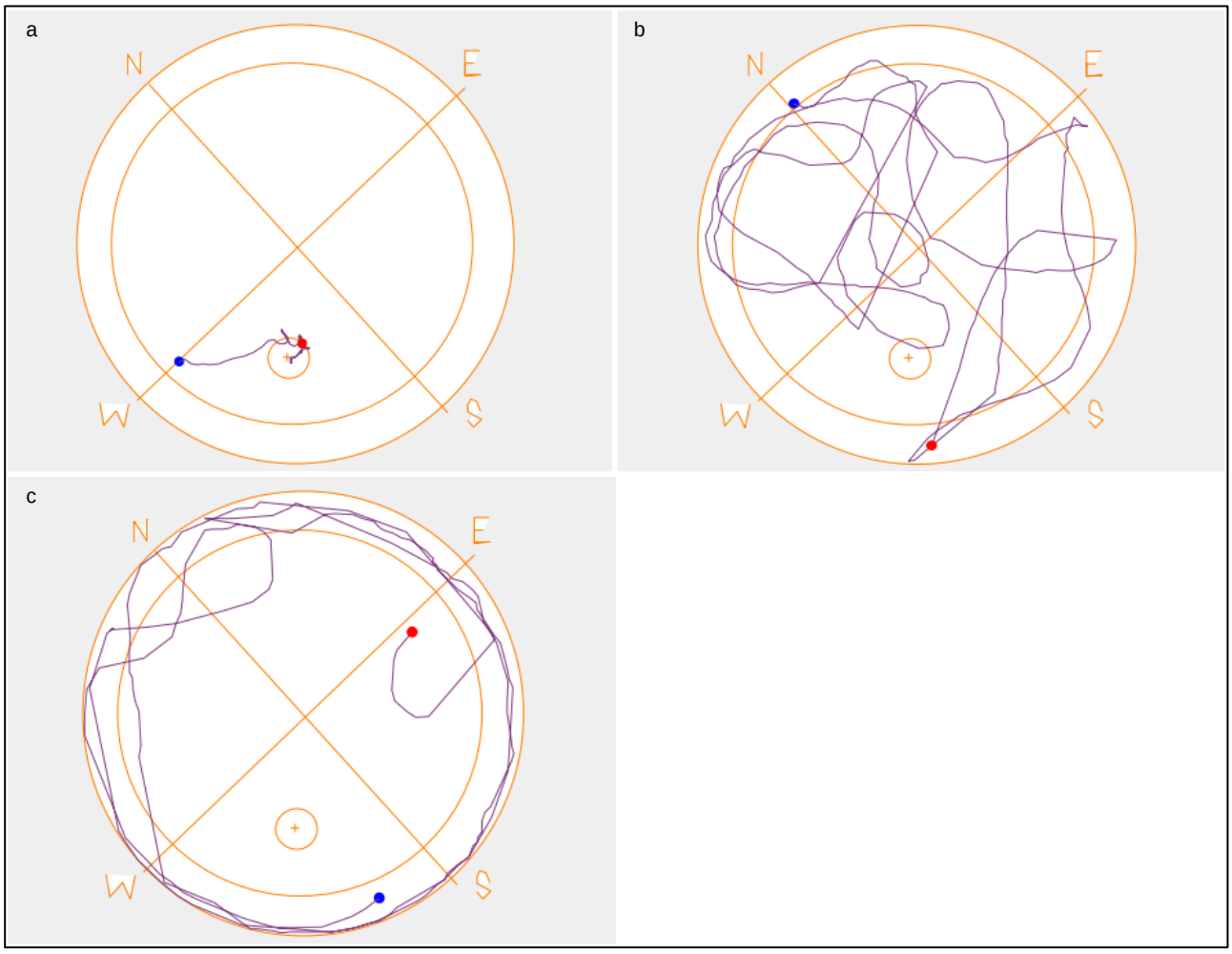

Figure 15 – Representative examples of the search strategies obtained in the MWM test using the AnyMaze software. **a.** A hippocampus-dependent strategy, defined as focal search. **b.** A non hippocampus-dependent strategy, defined as random search. **c.** Thigmotaxis, which is considered a non-hippocampus dependent strategy. The blue dot represents the mice's location at the beginning of the trial and the red dot represents mice's location at the end of the trial. The blue line is mice's path during the trial.

A reversal test was performed after the probe trial. In this test, the platform is moved to the opposite quadrant, and mice's ability to re-learn the platform's position is assessed. Latency to reach the platform decreases from day 1 to day 2 in both control (day 1: 23.6 ± 6.9 s; day 2: 11.4 ± 2.0 s; n=4) and APP/PS1 mice (day 1: 53.9 ± 4.6 s; day 2: 50.0 ± 3.3 s; n=8) (Figure 16), with WT mice finding the platform in less than 20 seconds right in the second day of test. On this last day, APP/PS1 mice latency to reach the platform is higher than WT mice ($p<0.0001$).

Overall, APP/PS1 mice seem to have a learning impairment compared to control mice.

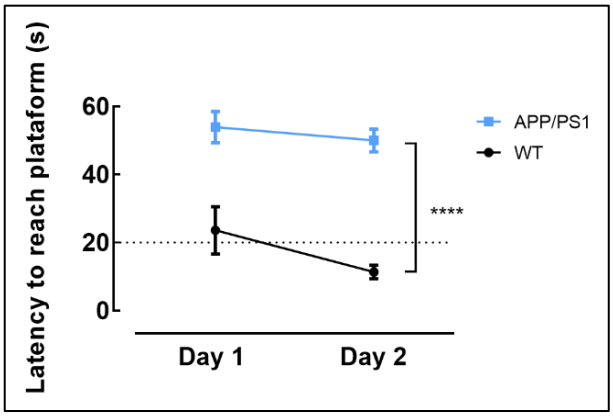

Figure 16 - Latency to reach the platform during the 2 days of the reversal trials of the Morris Water Maze test, performed with 9 months old female APP/PS1 mice. **** $p < 0.0001$, by a Two-way ANOVA test, followed by a *post hoc* Sidak's multiple comparison test. Values are mean ± SEM of 4 WT and 8 APP/PS1 mice.

A fear conditioning test was used to assess the connection between emotion, memory and learning. This test is based on the creation of an association between a neutral and a noxious stimulus, that involved the basolateral amygdala and the hippocampus (LeDoux, 2000).

During the acquisition phase, the percentage of time spent in freezing behaviour is analysed. No differences were found between APP/PS1 and control mice (Figure 17a).

In the next day, context conditioning was evaluated. For that, the same conditions for the acquisition phase were kept, except that no tone or shock was delivered. APP/PS1 mice spent more time freezing in minute 4 of the test than control mice (WT: 27.7 ± 6.8%; APP/PS1: 66.2 ± 9.0%; p=0.0292; n=4-12; Figure 17b).

In the final day of testing, a cue test was performed. The same conditions of the acquisition phase were kept, except that the context of the chamber was altered. APP/PS1 mice have a higher percentage of time spent freezing than control mice in the habituation phase of the test (WT: 5.2 ± 2.1%; APP/PS1: 22.2 ± 4.9%; p=0.0345, n=4-12; Fig. 17c). This could be an indicator that APP/PS1 generalize fear to other contexts. During the test, no differences were found between control and APP/PS1 in the percentage of time spent in freezing behaviour.

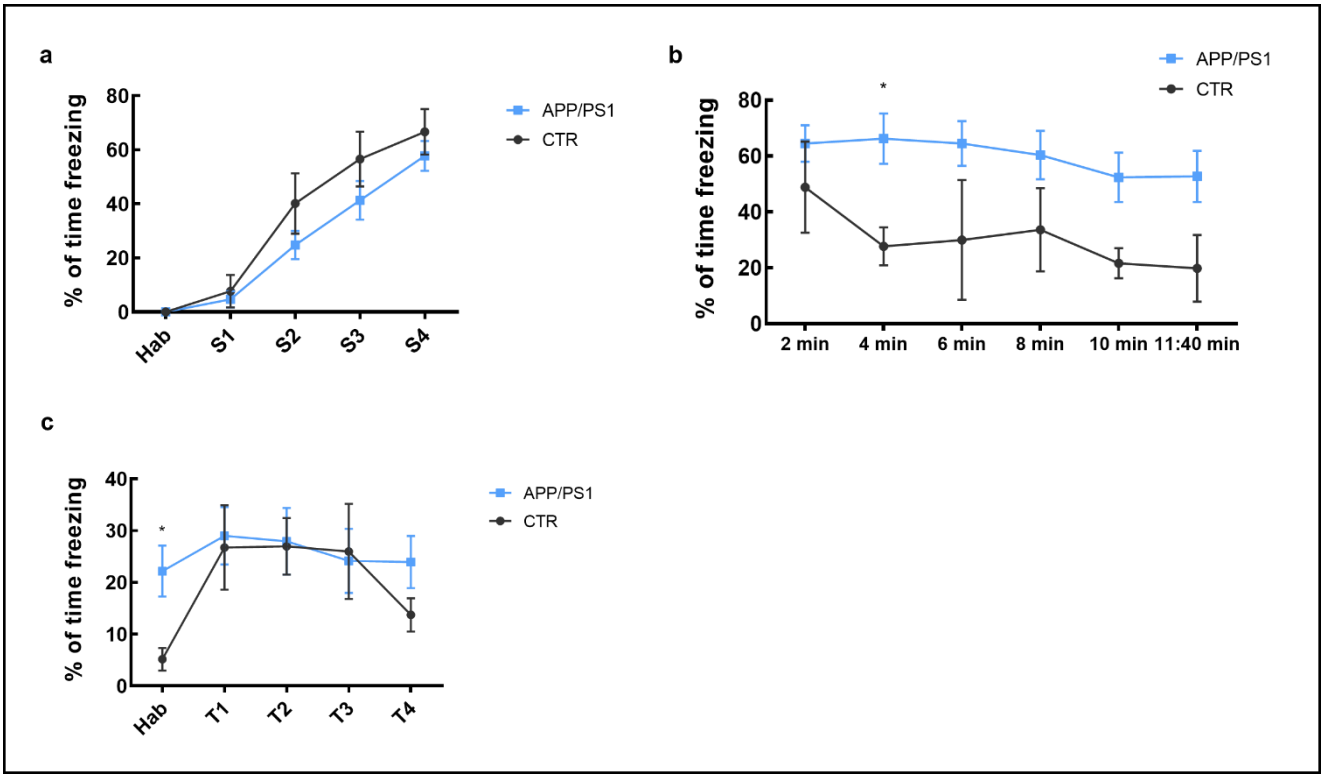

Figure 17 - Fear Conditioning Test with 9 months old female APP/PS1 mice. **a.** Percentage of time spent in freezing in the acquisition phase. **b.** Percentage of time spent in freezing in the Context Fear Conditioning. **c.** Percentage of time spent in freezing in the Cued Fear Conditioning. * $p < 0.05$, by a Two-Way ANOVA followed by a *post hoc* Sidak's multiple comparisons test. Values are mean ± SEM of 4 WT and 12 APP/PS1 mice. Hab – Habituation phase of the test; S1-4 and T1-4 – Time-points of freezing evaluation.

4. Neurochemical Characterization of 9 Months Old Female APP/PS1 Mice

Given the results of Western blotting of APP/PS1 mice with 6 months old, a new analysis was performed with APP/PS1 mice with 9 months old. The cortices of APP/PS1 female mice and WT littermates were used for preparation of synaptosomes and total protein extracts. As the latter englobe proteins from different cortical cells, the comparison of these extracts allows concluding on enrichment of the tested proteins.

SIRT1 is decreased in both the synaptosomes (WT: 100.0 ± 15.5%; APP/PS1: 66.1 ± 6.1%; p=0.0466; n=4-6; Fig. 18a) and total protein extracts (WT: 100.0 ± 4.6%; APP/PS1: 69.3 ± 5.6%; p=0.0026; n=5-7; Fig. 19a) of APP/PS1 mice compared to WT mice. As for SIRT3, no alterations were found in its levels in either synaptosomes (WT: 100.0 ± 12.5%; APP/PS1: 120.7 ± 12.0%; p=0.2699; n=5-7; Fig. 18b) or total protein extracts (WT: 100.0 ± 2.9%; APP/PS1: 110.3 ± 6.4%; p=0.2284; n=5-7; Fig. 19b).

Density levels of AMPK were found to be unaltered in synaptosomes of APP/PS1 mice compared to WT mice (WT: 100.0 ± 13.6%; APP/PS1: 95.8 ± 3.7%; p=0.7354; n=5-7; Fig. 18c) as well as in total extracts (WT: 100.0 ± 2.4%; APP/PS1: 67.7 ± 13.0%; p=0.0673; n=5-7; Fig. 19c). However, phosphorylated AMPK levels were decreased in synaptosomes of APP/PS1 mice compared to WT mice (WT: 100.0 ± 17.8%; APP/PS1: 57.7 ± 4.0%; p=0.0212; n=5-7; Fig. 18d), but no alterations were found in total protein extracts between genotypes (WT: 100.0 ± 13.5%; APP/PS1: 165.1 ± 36.3%; p=0.1783; n=5-7; Fig. 19d). As AMPK and pAMPK were not immunoblotted in the same membranes, a ratio between AMPK and pAMPK could not be calculated.

Additionally, SESN2 levels are not altered in synaptosomes of APP/PS1 mice compared to WT mice (WT: 100.0 ± 15.5%; APP/PS1: 81.3 ± 7.7%; p=0.3123; n=5; Fig. 18e). However, a decrease in the SESN2 levels was found in total protein extracts of APP/PS1 compared to WT mice (WT: 100.0 ± 8.4%; APP/PS1: 69.8 ± 7.0%; p=0.0202; n=5-7; Fig. 19e).

Unfortunately, in 9 months old APP/PS1 mice only LC3-I could be analysed. Thus, with lacking analysis of LC3-II levels and LC3-II/L3-I ratio levels, we cannot infer information on the autophagic flux of the cell. However, we did find that LC3-I levels are not alter in both synaptosomes (WT: 100.0 ± 11.3%; APP/PS1: 88.4 ± 9.0%; p=0.4375; n=5-6; Fig. 18f) and total protein extracts (WT: 100.0 ± 7.0%; APP/PS1: 104.7 ± 4.1%; p=0.5588; n=5-6; Fig. 19f)

MFN2 levels were also determined, as MFN2 is involved in mitochondria fusion. No alteration of MFN2 levels were found in synaptosomes in APP/PS1 mice (WT: 100.0 ± 5.5%; APP/PS1: 97.3 ± 10.1%; p=0.8405; n=5-7; Fig. 18g). However, MFN2 levels are decreased in total protein extracts in APP/PS1 mice compared to WT mice (WT: 100.0 ± 3.8%; APP/PS1: 75.3 ± 4.8%; p=0.0037; n=5-7; Fig. 19g).

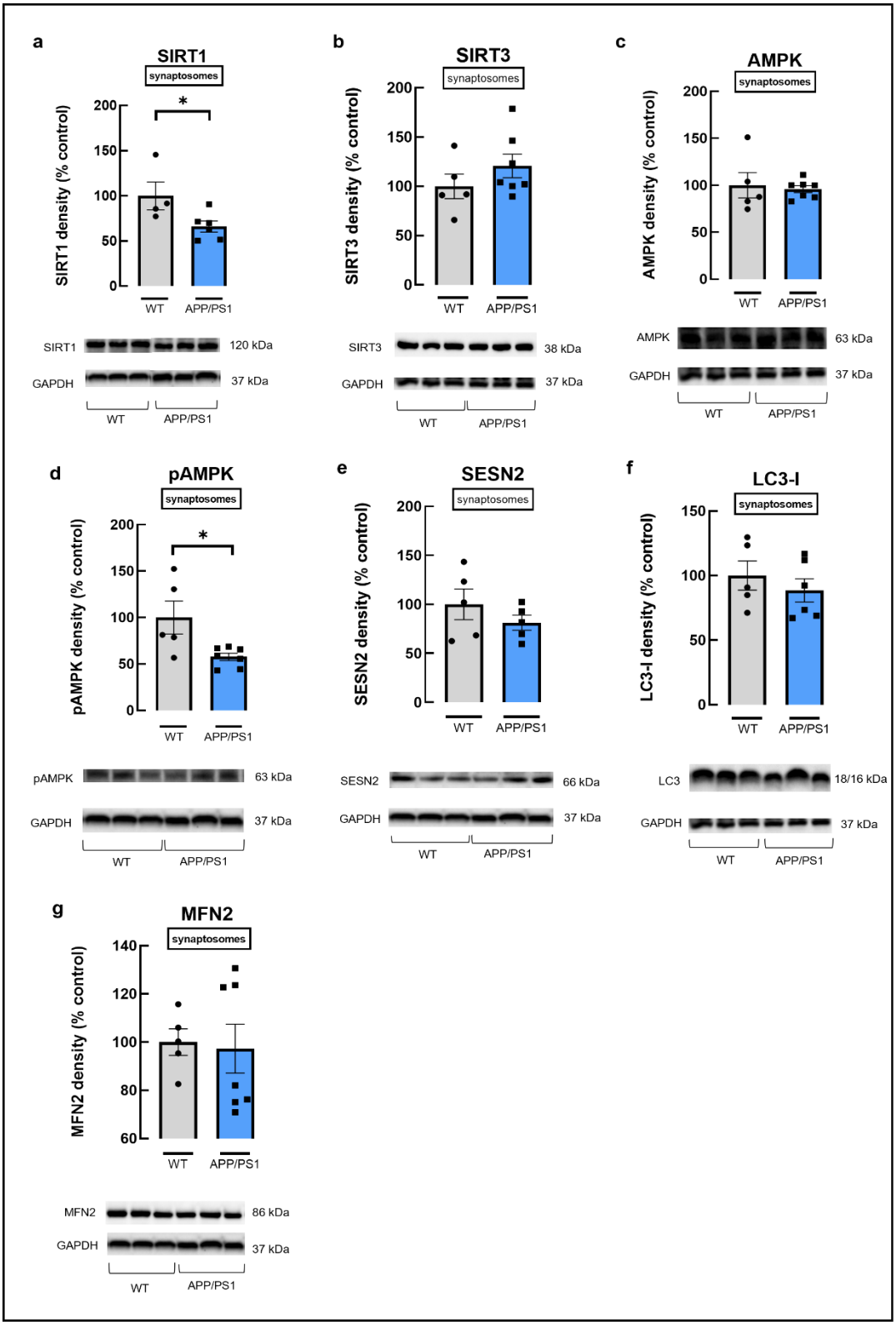

Figure 18 - Relative density of proteins **a.** SIRT1, **b.** SIRT3, **c.** AMPK, **d.** pAMPK, **e.** SESN2, **f.** LC3-I, **g.** MFN2 in cortical synaptosomes of 9 months old female APP/PS1 mice. GAPDH was used as a loading control, thus results as presented as a ratio between the density of the protein of interest and GAPDH. Results are presented as a percentage of values of control mice (WT), which was designated 100%. * $p<0.05$, using a Student's unpaired *t*-test. Values are mean ± SEM of 4-5 WT and 5-7 APP/PS1 mice. A significant decrease in the levels of SIRT1, pAMPK and SESN2 were found in APP/PS1 mice compared to control WT mice. No significant alterations were found in the levels of SIRT3, AMPK, LC3-I and MFN2.

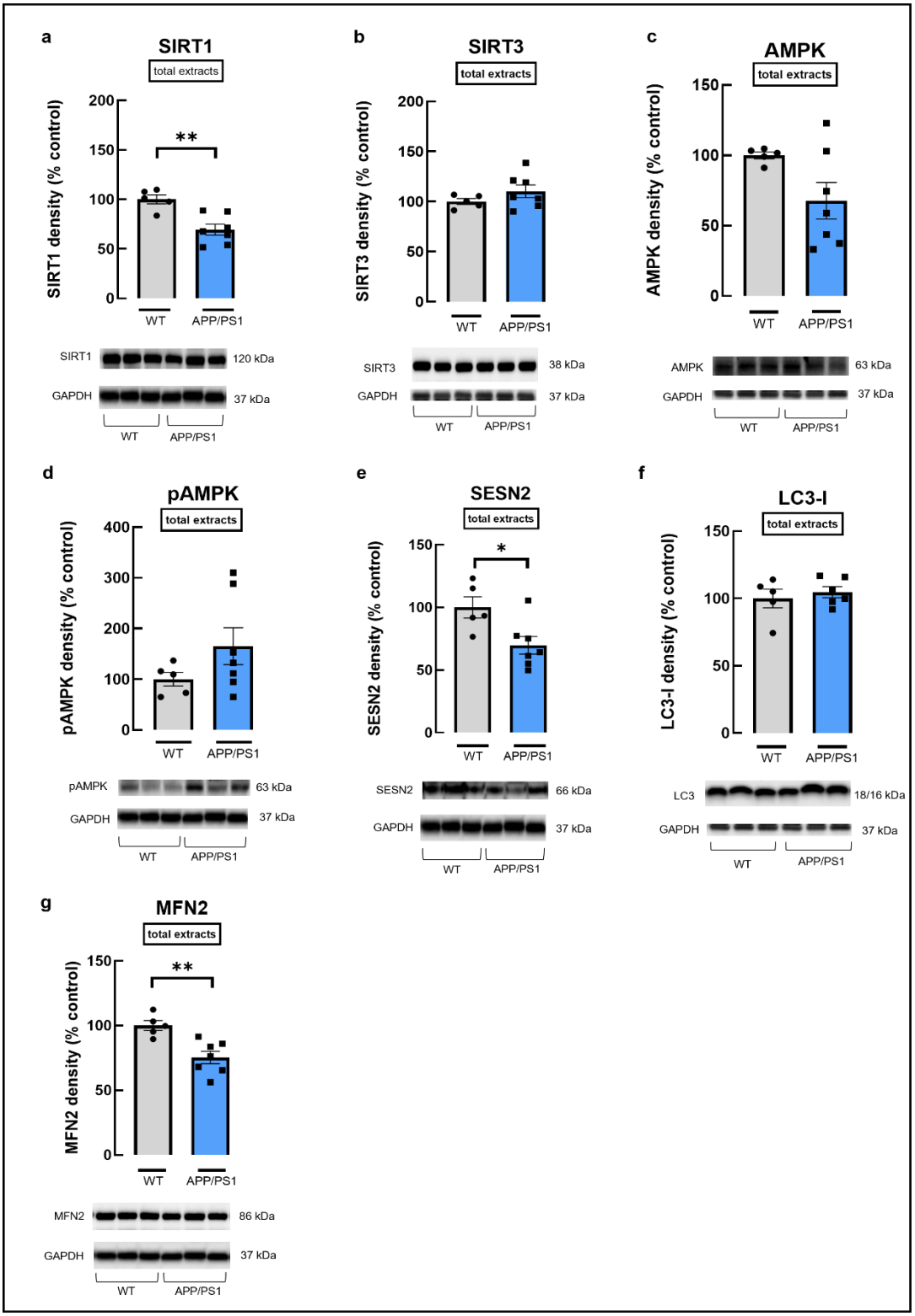

Figure 19 - Relative density of proteins **a.** SIRT1, **b.** SIRT3, **c.** AMPK, **d.** pAMPK, **e.** SESN2, **f.** LC3-I, **g.** MFN2 in cortical protein extracts of 9 months old female APP/PS1 mice. GAPDH was used as a loading control, thus results as presented as a ratio between the density of the protein of interest and GAPDH. Results are presented as a percentage of values of control mice (WT), which was designated 100%. * $p<0.05$, using a Student's unpaired *t*-test. Values are mean ± SEM of 4-5 WT and 6-7 APP/PS1 mice. A significant decrease in the levels of SIRT1, SESN2 and MFN2 were found in APP/PS1 mice compared to control WT mice. No significant alterations were found in the levels of SIRT3, AMPK, pAMPK and LC3-I.

At 9 months old, an evaluation of synaptic proteins markers was performed. We found that there was no alteration in the levels of SNAP-25 (WT: 100.0 ± 3.9%; APP/PS1: 113.6 ± 4.4%; p=0.0520; n=5-7; Fig. 20a), syntaxin (WT: 100.0 ± 1.8%; APP/PS1: 118.4 ± 9.2%; p=0.1276; n=5-7; Fig. 20b), synaptophysin (WT: 100.0 ± 12.7%; APP/PS1: 114.5 ± 5.5%; p=0.3270; n=5; Fig. 20c) and PSD-95 (WT: 100.0 ± 3.7%; APP/PS1: 91.9 ± 5.1%; p=0.2835; n=4-6; Fig. 20d). These results indicate that at this time point the animals do not seem to display a loss of synaptic proteins in viable synapses in the cerebral cortex.

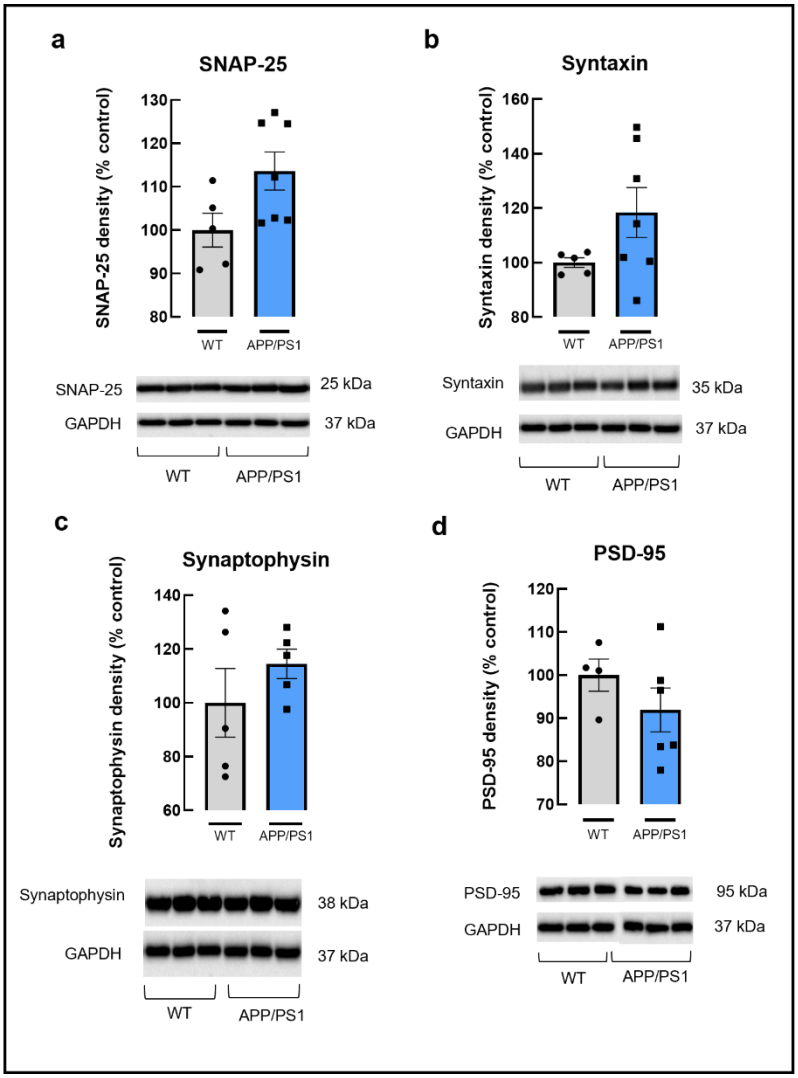

Figure 20 - Relative density of synaptic markers in cortical synaptosomes of 9 months old female APP/PS1 mice. Immunocontent of **a.** SNAP-25, **b.** syntaxin, **c.** synaptophysin and **d.** PSD-95. GAPDH was used as a loading control, thus results as presented as a ratio between the density of the protein of interest and GAPDH. Results are presented as a percentage of values of control mice (WT), which was designated 100%. A Student's unpaired *t*-test was performed and significance of 0.05 was not reached in any analysis. Values are mean ± SEM of 4-5 WT and 5-7 APP/PS1 mice.

A summary of the alterations found in cortical synapses of female APP/PS1 at 9 months old is presented in Table 10.

Table 10 - Summary of the alterations of levels of SIRT1, SIRT3, SESN2, AMPK, pAMPK, MFN2, LC3 and synaptic proteins SNAP-25, syntaxin, synaptophysin and PSD-95 in cortical synaptosomes and cortical total protein extracts of 9 months old female APP/PS1 mice compared to control WT mice; = represents no alterations found, ↑ represents an increase and ↓ represents a decrease.

		Cortical synaptosomes of 9 months old mice	Cortical total protein extracts of 9 months old mice
Protein	Process involved or localization	ΔAPP/PS1 vs. WT	
SIRT1	Metabolism	↓	↓
SIRT3	Metabolism	=	=
SESN2	Stress response	=	↓
AMPK	Sensor of energy	=	=
pAMPK	Sensor of energy	↓	=
MFN2	Mitochondria fusion	=	↓
LC3	Autophagy	=	=
SNAP-25	Pre-synaptic	=	
Syntaxin	Pre-synaptic	=	
Synaptophysin	Pre-synaptic vesicle and extra-synaptic	=	
PSD-95	Post-synaptic	=	

5. Neurochemical Characterization of $A\beta_{1-42}$-Injected Mice (14 Days)

To understand if different models of AD exhibit the same alterations in cerebral cortical synapses, a mouse model of AD that was subject to a $A\beta_{1-42}$ injection was used. Sacrifice of the animals occurred 14 days after the injection. Cortical synaptosomes and total protein extracts were prepared and used for Western blotting analysis.

No alterations were found in levels of SIRT1 in synaptosomes between $A\beta_{1-42}$-injected mice (Aβ) and control mice injected with a saline solution (vehicle mice, VEH) (VEH: 100.0 ± 12.4%; Aβ: 113.5 ± 21.5%; p=0.5824; n=7-8; Fig. 21a). Levels of SIRT3 were also not altered between $A\beta_{1-42}$-injected and VEH animals, in synaptosomes (VEH: 100.0 ± 6.1%; Aβ: 107.1 ± 8.2%; p=0.4893; n=8-10; Fig. 21b) nor in total protein extracts (VEH: 100.0 ± 8.0%; Aβ: 80.3 ± 12.6%; p=0.2152; n=6; Fig. 22a) of $A\beta_{1-42}$-injected mice.

As for SESN2 density in $A\beta_{1-42}$-injected mice, no alterations were found in both synaptosomes (VEH: 100.0 ± 0.8%; Aβ: 87.6 ± 7.0%; p=0.1954; n=3-4; Fig. 21e) or total protein extracts (VEH: 100.0 ± 5.6%; Aβ: 111.7 ± 26.7%; p=0.6802; n=5; Fig. 22b).

In synaptosomes, no alterations were found in AMPK density (VEH: 100.0 ± 11.9%; Aβ: 131.9 ± 32.7%; p=0.2663; n=4-10; Fig. 21c), nor in phosphorylated AMPK density (VEH: 100.0 ± 11.6%; Aβ: 68.1 ± 9.6%; p=0.0614; n=7-9; Fig. 21d) in the $A\beta_{1-42}$-injected mice.

Furthermore, levels of MFN2 were not altered in synaptosomes of the $A\beta_{1-42}$-injected mice (VEH: 100.0 ± 2.3%; Aβ: 98.9 ± 6.0%; p=0.8510; n=7-9; Fig. 21g).

Finally, we could only evaluate LC3-I levels, which we found to be not altered both in synaptosomes (VEH: 100.0 ± 3.2%; Aβ: 93.5 ± 7.9%; p=0.4215; n=08-10; Fig. 21f) and total protein extracts (VEH: 100.0 ± 7.3%; Aβ: 138.4 ± 17.8%; p=0.1326; n=4-6; Fig. 22c) in $A\beta_{1-42}$-injected mice.

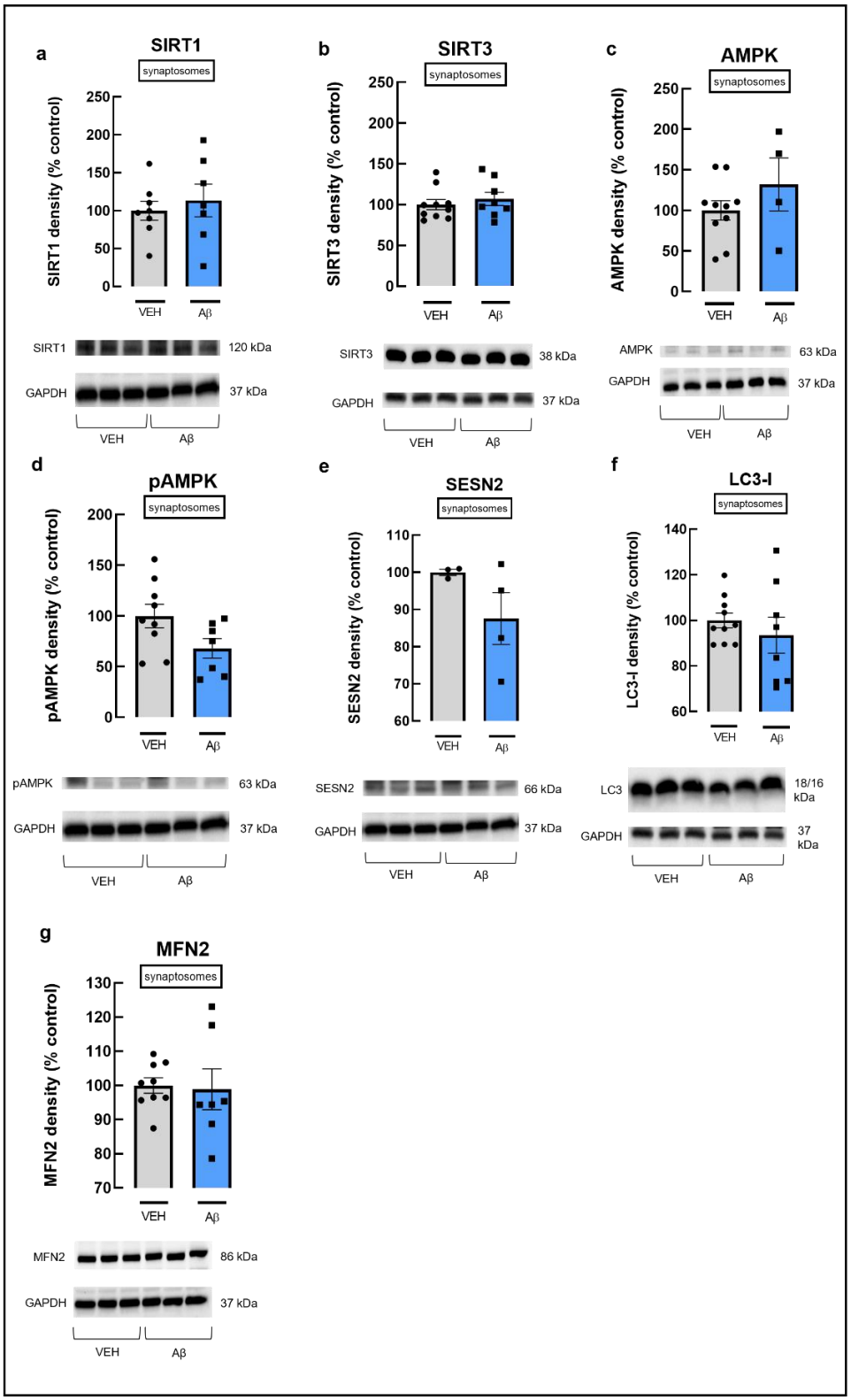

Figure 21 - Relative density of proteins **a.** SIRT1, **b.** SIRT3, **c.** AMPK, **d.** pAMPK, **e.** SESN2, **f.** LC3-I and **g.** MFN2 in cortical synaptosomes of the $A\beta_{1-42}$-injected model mice of AD, prepared 14 days after injection. GAPDH was used as a loading control, thus results as presented as a ratio between the density of the protein of interest and GAPDH. Results are presented as a percentage of values of control mice (vehicle), which was designated 100%. A Student's unpaired *t*-test was performed and significance of 0.05 was not reached in any analysis. Values are mean ± SEM of 3-10 WT and 4-8 APP/PS1 mice.

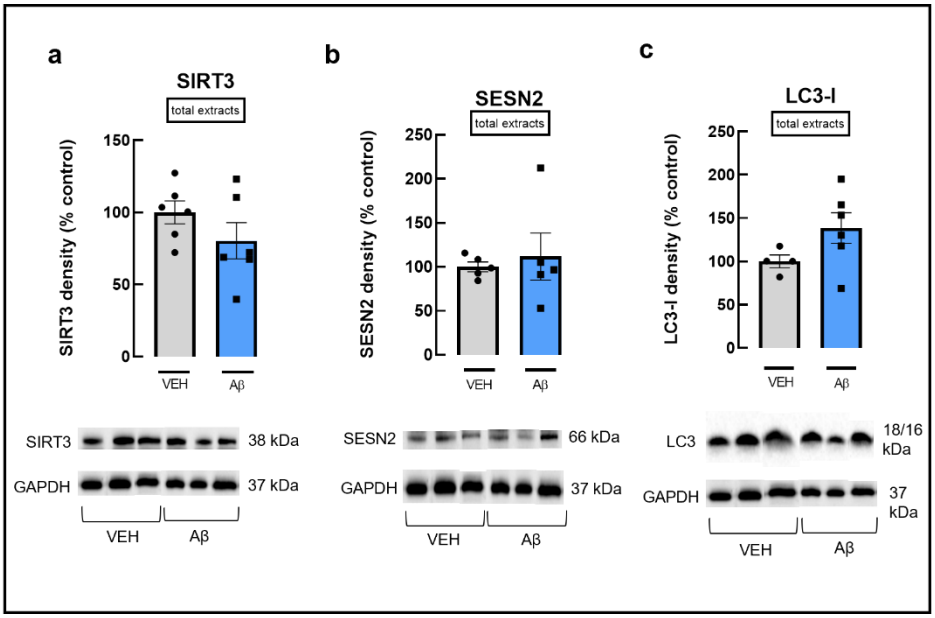

Figure 22 - Relative density of proteins **a.** SIRT3, **b.** SESN2 and **c.** LC3-I in cortical protein total extracts of $A\beta_{1-42}$-injected model mice of AD, prepared 14 days after injection. A Student's unpaired *t*-test was performed and significance of 0.05 was not reached in any analysis. GAPDH was used as a loading control, thus results as presented as a ratio between the density of the protein of interest and GAPDH. Results are presented as a percentage of values of control mice (vehicle), which was designated 100%. Values are mean ± SEM of 4-6 WT and 5-6 APP/PS1 mice.

Levels of synaptic protein markers were evaluated by Western blotting. An increase in pre-synaptic proteins SNAP-25 (VEH: 100.0 ± 1.1%; Aβ: 163.3 ± 27.1%; p=0.0184; n=8-10; Fig. 23a) and syntaxin (VEH: 100.0 ± 2.1%; Aβ: 215.6 ± 39.3%; p=0.0045; n=8-10; Fig. 23b) was found in $A\beta_{1-42}$-injected mice compared to VEH mice. Furthermore, an increase in pre-synaptic vesicles membrane-bound protein synaptophysin (VEH: 100.0 ± 3.8%; Aβ: 181.4 ± 43.6%; p=0.0401; n=7-10; Fig. 23c) and an increase in post-synaptic protein PSD-95 (VEH: 100.0 ± 4.0%; Aβ: 178.5 ± 34.4%; p=0.0216; n=8-10; Fig. 23d) were also found in $A\beta_{1-42}$-injected mice compared to VEH mice.

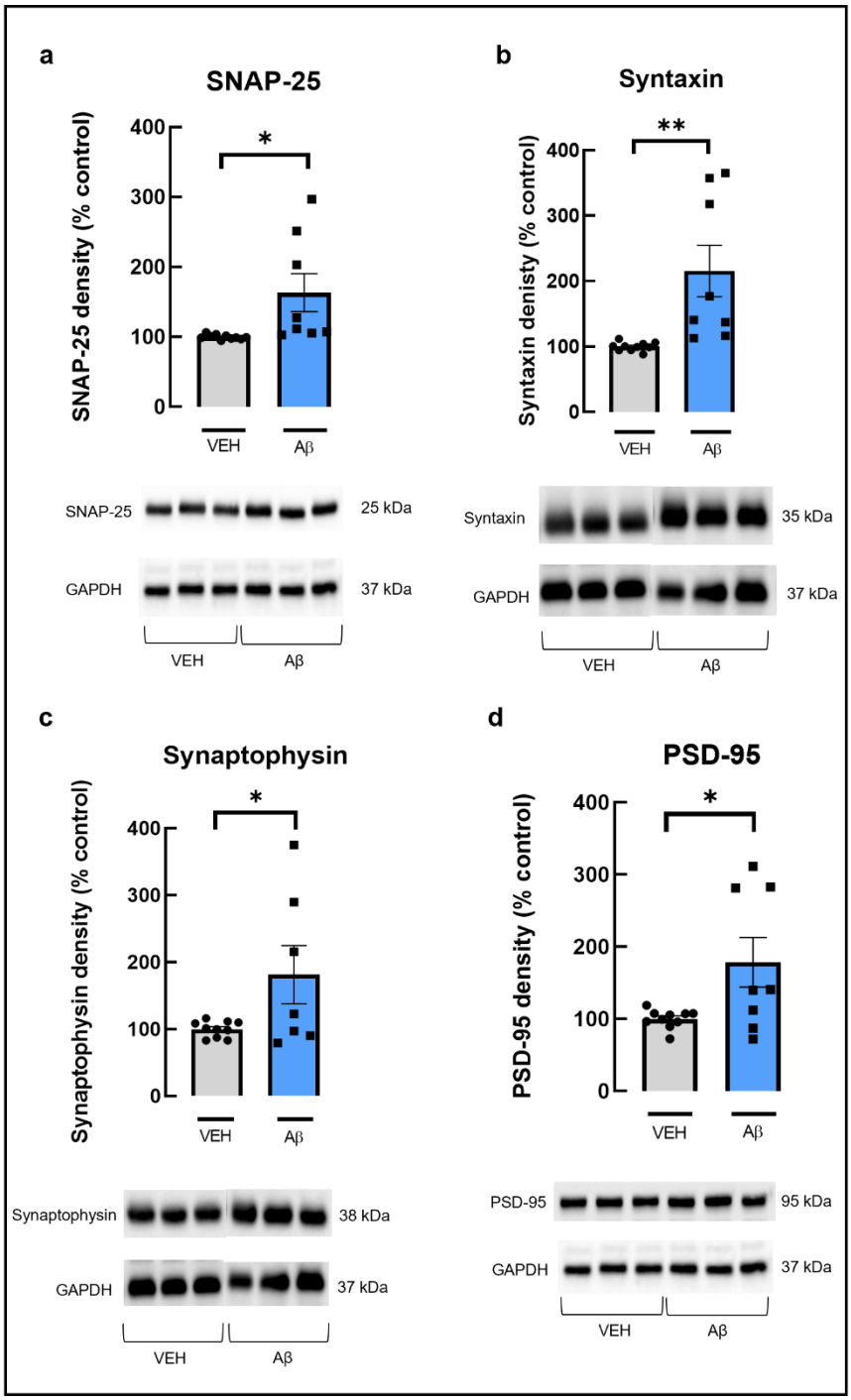

Figure 23 - Relative density of synaptic markers in cortical synaptosomes of $A\beta_{1-42}$-injected model mice of AD, prepared 14 days after injection. Immunocontent of **a.** SNAP-25, **b.** syntaxin, **c.** synaptophysin and **d.** PSD-95. * p< 0.05; ** p< 0.005, using a Student's unpaired *t*-test. GAPDH was used as a loading control, thus results as presented as a ratio between the density of the protein of interest and GAPDH. Results are presented as a percentage of values of control mice (vehicle), which was designated 100%. Values are mean ± SEM of 10 WT and 7-8 APP/PS1 mice. A significant increase in the levels of SNAP-25, syntaxin, synaptophysin and PSD-95 was found in the Aβ injected mice compared to control mice

A summary of the alterations found in the $A\beta_{1-42}$-injected mice model of AD, 14 days after injection are presented in Table 11.

Table 11 - Summary of the alterations of levels of SIRT1, SIRT3, SESN2, AMPK, pAMPK, MFN2, LC3 and synaptic proteins SNAP-25, syntaxin, synaptophysin and PSD-95 in cortical synaptosomes and cortical total protein extracts of the $A\beta_{1-42}$ icv mice model of AD (14 days) compared to control mice; = represents no alterations found, ↑ represents an increase and ↓ represents a decrease.

		Cortical synaptosomes of $A\beta_{1-42}$-injected mice (14 days)	Cortical total protein extracts of $A\beta_{1-42}$-injected mice (14 days)
Protein	Process involved or localization	ΔAPP/PS1 vs. WT	
SIRT1	Metabolism	=	
SIRT3	Metabolism	=	=
SESN2	Stress response	=	=
AMPK	Sensor of energy	=	
pAMPK	Sensor of energy	=	
MFN2	Mitochondria fusion	=	
LC3-I	Autophagy	=	=
SNAP-25	Pre-synaptic	↑	
Syntaxin	Pre-synaptic	↑	
Synaptophysin	Pre-synaptic vesicle and extra-synaptic	↑	
PSD-95	Post-synaptic	↑	

6. Neurochemical Characterization of $A\beta_{1-42}$-Injected Mice (20 Days)

Given the results obtained with the AD model with the injection of $A\beta_{1-42}$ and sacrifice after 14 days, we decided to use two different time points to evaluate neurochemical alterations, thus using animals whose animal sacrifice occurred 20 days after $A\beta_{1-42}$ injection. Cortical synaptosomes were prepared and used for Western blotting of the various potential senescence markers.

We found no alterations in densities of the proteins related to metabolism SIRT1 (VEH: 100.0 ± 10.1%; Aβ: 80.8 ± 7.8%; p=0.1646; n=6; Fig. 24a), SIRT3 (VEH: 100.0 ± 6.8%; Aβ: 123.5 ± 37.1%; p=0.5979; n=4-5; Fig. 24b), SESN2 (VEH: 100.0 ± 8.1%; Aβ: 82.6 ± 10.8%; p=0.2272; n=6; Fig. 24e) and pAMPK (VEH: 100.0 ± 10.9%; Aβ: 88.6 ± 16.7%; p=0.5809; n=6; Fig. 24d) in synaptosomes of $A\beta_{1-42}$-injected mice. In Figure 19c preliminary data of AMPK levels is presented (n=1-2).

We found a decrease in MFN2 levels in synaptosomes of $A\beta_{1-42}$-injected mice compared to VEH mice (VEH: 100.0 ± 15.0%; Aβ: 60.9 ± 7.4%; p=0.0417; n=6; Fig. 24i), which could suggest impaired mitochondria fusion.

As for the autophagy marker, LC3, no alterations were found in both LC3-I (VEH: 100.0 ± 14.9%; Aβ: 119.8 ± 4.0%; p=0.1981; n=3-4; Fig. 24f) nor LC3-II (VEH: 100.0 ± 8.0%; Aβ: 117.9 ± 1.6%; p=0.0650; n=2-3; Fig. 24g) levels in synaptosomes of $A\beta_{1-42}$-injected mice. Furthermore, LC3-II/LC3-I ratio is also not altered in $A\beta_{1-42}$-injected mice (VEH: 0.9 ± 0.1; Aβ: 1.2 ± 0.3; p=0.4091; n=2-3; Fig. 24h).

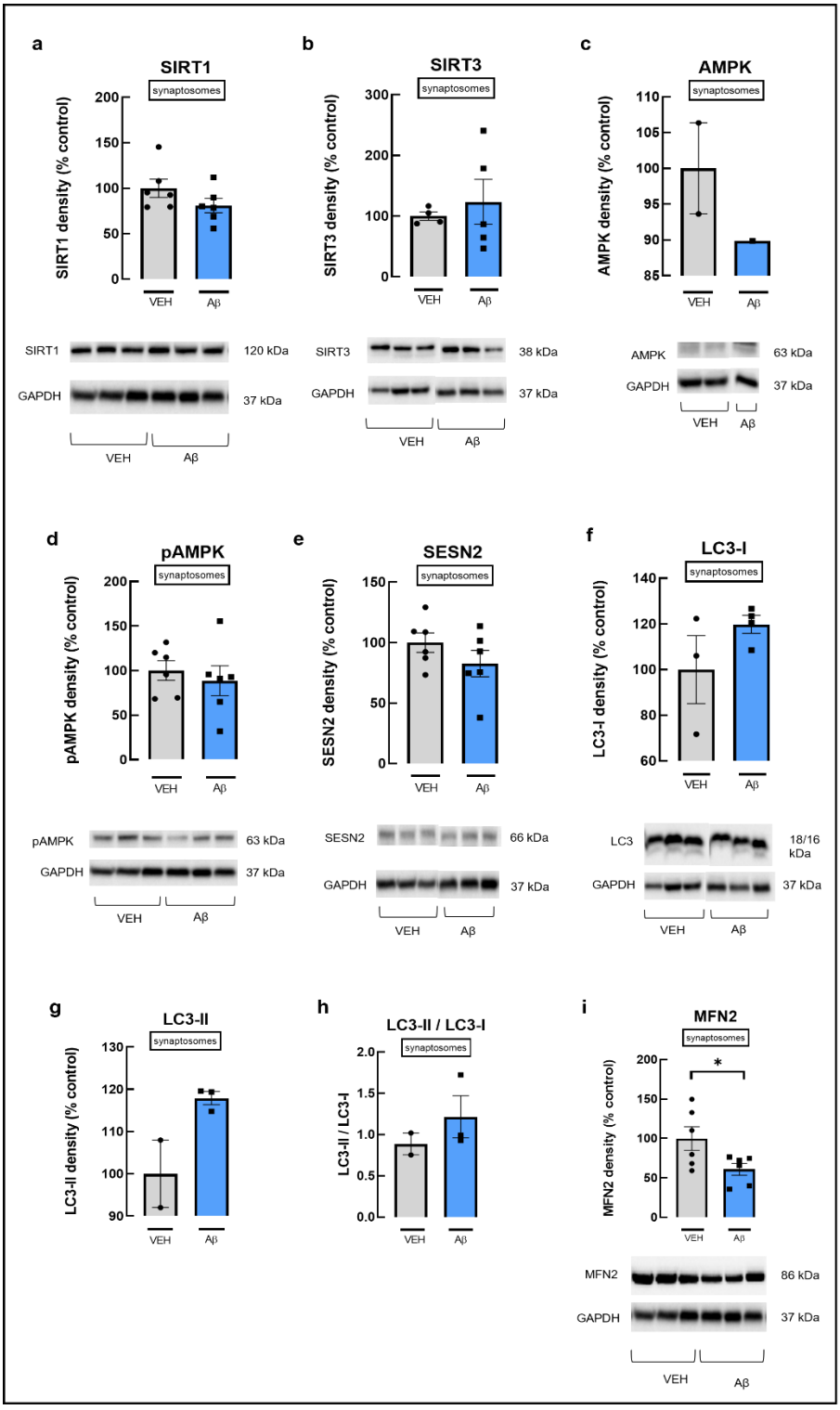

Figure 24 - Relative density of proteins **a.** SIRT1, **b.** SIRT3, **c.** AMPK, **d.** pAMPK, **e.** SESN2, **f.** LC3-I, **g.** LC3-II, **h.** LC3-II/LC3-I and **i.** MFN2 in cortical synaptosomes of $A\beta_{1-42}$-injected model mice of AD, prepared 20 days after injection. GAPDH was used as a loading control, thus results as presented as a ratio between the density of the protein of interest and GAPDH. Results are presented as a percentage of values of control mice (vehicle), which was designated 100%. Values are mean ± SEM of 2-6 WT and 1-6 APP/PS1 mice. * $p< 0.05$, using a Student's unpaired *t*-test. No significant alterations were found in the levels of these proteins, except for MFN2, were a significant decrease was observed in Aβ injected mice compared to control.

Levels of synaptic protein markers SNAP-25, syntaxin, synaptophysin and PSD-95 were estimated by Western blotting. No alteration was found in the levels of these proteins, suggesting that markers of synaptic dysregulation may not yet be present in cortical regions of this animal model (SNAP-25: VEH: 100.0 ± 15.1%; Aβ: 153.8 ± 33.6%; p=0.1548, n=5-6; Syntaxin: VEH: 100.0 ± 18.6%; Aβ: 185.7 ± 35.5%; p=0.0512, n=5-6; Synaptophysin: VEH: 100.0 ± 5.9%; Aβ: 132.3 ± 15.2%; p=0.0629, n=5-6; and PSD-95: VEH: 100.0 ± 19.7%; Aβ: 119.7 ± 32.3%; p=0.6002, n=5-6; Fig.25).

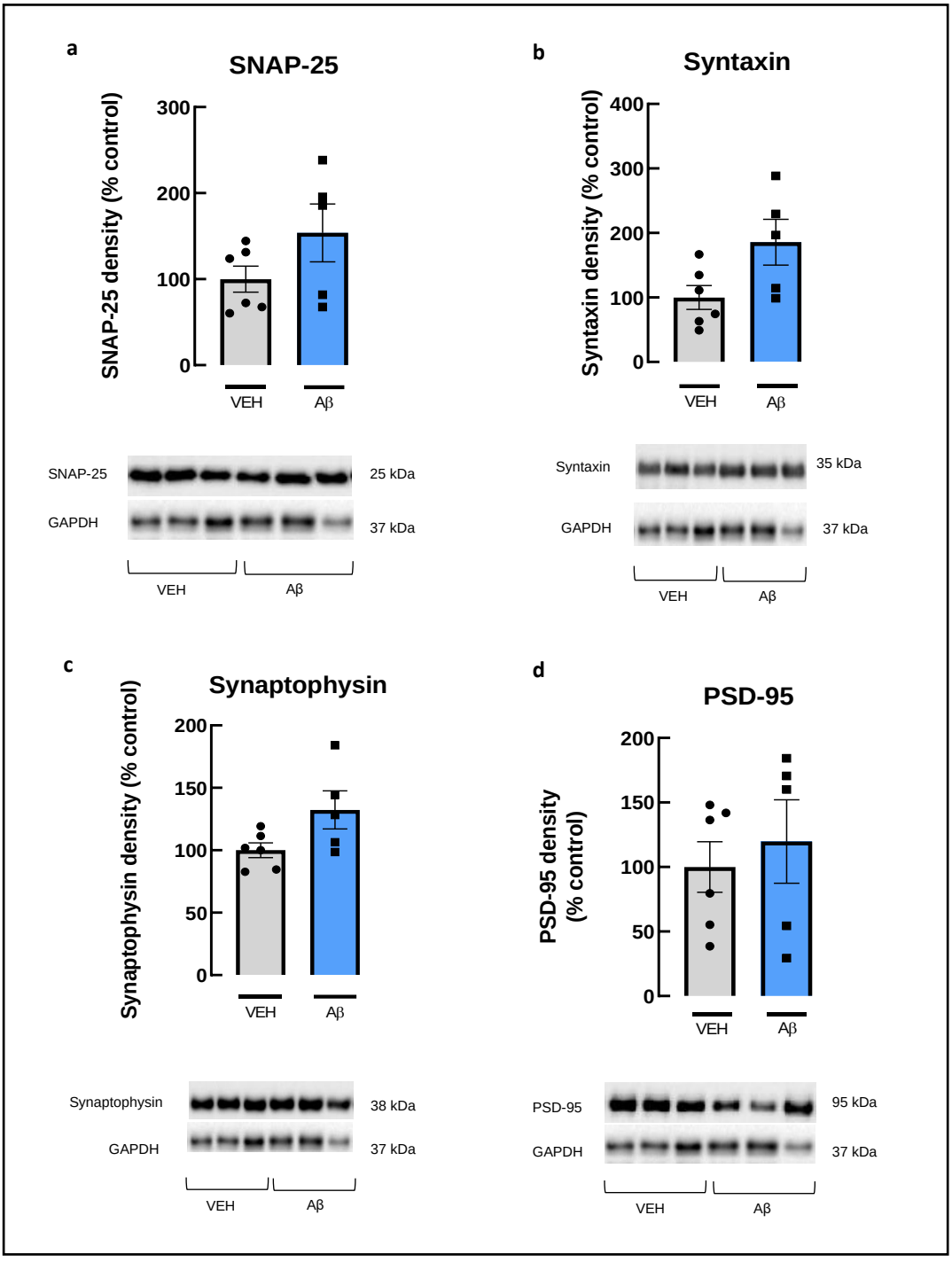

Figure 25 - Relative density of synaptic markers in cortical synaptosomes of $A\beta_{1-42}$-injected model mice of AD, prepared 20 days after injection. Immunocontent and representative images of the Western blots analysis of **a.** SNAP-25, **b.** syntaxin, **c.** synaptophysin and **d.** PSD-95. GAPDH was used as a loading control, thus results as presented as a ratio between the density of the protein of interest and GAPDH. Results are presented as a percentage of values of control mice (vehicle), which was designated 100%. Values are mean ± SEM of 6 WT and 5 APP/PS1 mice. A Student's unpaired *t*-test was performed and significance of 0.05 was not reached in any analysis

A summary of the alterations found in the cortical synapses of the $A\beta_{1-42}$-injected model mice of AD, prepared 20 days after injection, is presented in Table 12.

Table 12 - Summary of the alterations of levels of SIRT1, SIRT3, SESN2, AMPK, pAMPK, MFN2, LC3 and synaptic proteins SNAP-25, syntaxin, synaptophysin and PSD-95 in cortical synaptosomes and cortical total protein extracts of the $A\beta_{1-42}$ icv mice model of AD (20 days) compared to control mice; = represents no alterations found, ↑ represents an increase and ↓ represents a decrease.

		Cortical synaptosomes of $A\beta_{1-42}$-injected mice (20 days)
Protein	Process involved or localization	ΔAPP/PS1 vs. WT
SIRT1	Metabolism	=
SIRT3	Metabolism	=
SESN2	Stress response	=
AMPK	Sensor of energy	=
pAMPK	Sensor of energy	=
MFN2	Mitochondria fusion	↓
LC3-I LC3-II LC3-II/LC3-I	Autophagy	= = =
SNAP-25	Pre-synaptic	=
Syntaxin	Pre-synaptic	=
Synaptophysin	Pre-synaptic vesicle and extra-synaptic	=
PSD-95	Post-synaptic	=

Discussion

Aging is the major risk factor for neurodegenerative diseases, and with aging and neurodegenerative diseases it is observed an increase in cellular senescence (Martínez-Cué & Rueda, 2020). AD starts with synaptic and mitochondrial dysfunctions, thus, understanding the molecular processes behind these early dysfunctions could help finding treatments for AD in its early stages (Selkoe, 2002; Swerdlow, 2018).

Here, we assessed the levels of proteins related to metabolism, autophagy and mitochondrial dynamics, in cortical synaptosomes, in order to understand if they are related to the dysfunction characteristic of the synapses in AD.

First, we performed a behaviour characterization of 6 months-old female APP/PS1 mice, a mice model of familial AD. It is known that females have a higher risk for AD than males (Andrew & Tierney, 2018). This time-point was chosen considering that, previously, Viana da Silva *et al*. (2016) conducted behaviour tests in male APP/PS1 mice with 6 months and found that male mice already show an impairment in spatial memory, evaluated by the Y-maze test, as APP/PS1 mice spent less time exploring the novel arm of the apparatus. Furthermore, this model shows Aβ plaques at as early as 6 months old (Jankowsky *et al*., 2003)

Therefore, we conducted various behaviour tests which assess both memory and mood now in female mice. Overall, we found that APP/PS1 female mice are more anxious than WT mice, as indicated by the less time spent by APP/PS1 mice in the center of the OF arena, a thigmotactic behaviour, and the smaller number of entries and time spent in the open arms of the EPM. Thigmotaxis is a behaviour characterized by a preference for the spaces close to walls in favor of open spaces and can be useful as an indicator of anxiety (Simon *et al.,* 1994). Rodents tend to avoid open unknown areas, giving preference for the periphery of the spaces they are in (Prut & Belzung, 2003). Thigmotaxis in the 5 minutes of the test is essential as it helps mice create a spatial representation of the apparatus to navigate the space (Simon *et al.,* 1994). For a longer period of test, mice that spend more time in the center of the apparatus or have a decreased latency to enter the center of the apparatus can be perceived as anxious. Consistently, Cheng *et al*. (2013) found an increase in anxiety in male APP/PS1 mice with 7 months evaluated by the EPM test.

On the other hand, 6 months old APP/PS1 female mice do not display notable memory impairments, as would be expected considering previous works with age-

matched male mice (Viana da Silva, 2016). However, this could be justified by the intrinsic differences of male and female mice, how the breeding of the colony was performed and the genetic background of the colony.

As AD starts with synaptic dysfunctions (Selkoe, 2002) and mitochondrial impairment is an early AD feature, we wanted to evaluate the estimated density of several metabolism related proteins in the synapses of APP/PS1 mice. Therefore, a Western blotting analysis was performed with synaptosomes obtained from the cerebral cortex of the animals.

Surprisingly, except for LC3-I, no alterations were found in the estimated densities of SIRT1, SIRT3, SESN2, AMPK, pAMPK and MFN2. As for the LC3-I increase density that was observed in APP/PS1 female mice, it cannot be implied as an alteration of the autophagy process, as the autophagic flux is estimated by the LC3-II/LC3-I ratio, that was not altered between genotypes. LC3 is widely used as an autophagy marker. François *et al*., (2014), reported that in APP/PS1 (APPswe/PSEN1dE9) male mice with 6 months no alterations in LC3-I and LC3-II levels in total cortical protein extracts were found.

In APP/PS1 mice, glucose metabolism is first affected in the entorhinal cortex and hippocampus, before cognitive decline (Li *et al*., 2016). In these regions, an initial (2-3.5 months) hypermetabolism occurs, as a compensatory mechanism. Later (5-8 months), the increase in glucose metabolism decreases, returning to basal values and then further decreases to a hypometabolism, due to neuron loss and Aβ overload (Li *et al*., 2016). Snellman *et al*. (2019) reported a trend in an increase in glucose uptake in 6 months old APP/PS1 mice. As for human patients, during aging, a hypometabolism of glucose is reported in brain (Loessner *et al*., 1995).

NMR analysis of metabolite profiles in the cortical synapses of APP/PS1 and control mice used in this study were performed by a teammate. They found no alteration in glucose consumption, lactate production nor the percentages of glycolysis and oxidation pathways (data not published), which suggests that metabolic activity is not altered in the cortical synapses of APP/PS1 mice at 6 months old.

Therefore, our lack of alterations in the potential senescence markers could be explained by various factors. First, the overall lack of metabolic alteration in the cortex of APP/PS1 mice; Second, since females are biologically different from males, at the age chosen for these tests metabolic alterations could not be present yet or are restricted to sub-populations, that cannot be detected by the used techniques.

As synaptic loss is a prominent early feature in AD (Selkoe, 2002), we assessed levels of various synaptic markers. SNAP-25 is located in the pre-synaptic membrane in the synapses and throughout the axon (Hodel, 1998). Together with syntaxin and synaptobrevin, they form the soluble N-ethylmaleimide sensitive factor attachment receptors (SNARE) complex, that mediates calcium-triggered exocytosis and neurotransmission (Ramakrishnan *et al*., 2012).

PSD-95 is a component of the postsynaptic density (PSD), a postsynaptic specialization (Hunt *et al*., 1996). PSD-95 interacts with various receptors, ion channels and cell-adhesion molecules in the synapses and cytoplasmic signalling molecules (Kim & Sheng, 2004). Furthermore, PSD-95 is involved in synapse stabilization and plasticity (El-Husseini *et al*., 2000).

Synaptophysin is a transmembrane protein associated with the membrane of synaptic vesicles (Thiel, 1993). Synaptophysin is essential for synaptic plasticity (Janz *et al*., 1999) and control of exocytosis (Edelmann *et al*., 1995).

We found no alterations in the levels of SNAP-25 and synaptophysin, a decrease in the levels of syntaxin and an increase in the levels of PSD-95 in 6 months old APP/PS1 mice. This deregulation in the levels of these synaptic markers could be an indicator of synaptic dysfunction.

It seems that alterations of the levels if the synaptic markers are region-specific. For instance, Leuba *et al.* (2008) found that PSD-95 levels are increased and synaptophysin levels are decreased in the entorhinal cortex of AD patients, while Pham *et al.* (2010) found that PSD-95 levels are decrease in the frontal cortex of both AD patients and APP transgenic mice. Furthermore, Sultana *et al.* (2009) found a decrease in PSD-95 levels in the hippocampus of mild cognitive impairment (MCI) patients and Poirel *et al*. (2018) found that PSD-95 and synaptophysin expression levels decrease in the prefrontal cortex of AD patients with disease progression. Moreover, altered synaptic markers levels is more pronounced in the frontal cortices than in the parietal cortex (Reddy *et al*., 2005), and presynaptic markers are more affected than postsynaptic markers (de Wilde *et al*., 2016).

Overall, at 6 months old, female APP/PS1 mice display a mild impairment, a dysregulation of the synaptic markers levels and no alterations in metabolism-related proteins (except for LC3-I).

Various works are published with this AD model behaviourally characterized by the MWM test, with reported impairments in learning in APP/PS1 mice as young as 4 months old in males (Jardanhazi-Kurutz *et al.*, 2011). We chose 9 months old as the next time-point to test these animals under the assumption that the onset of behavioural and neurochemical alterations might occur later in females of this AD mouse model (Donkin *et al*., 2010; Gong *et al*., 2019).

To understand if these APP/PS1 female mice have, in fact, a memory and/or mood alterations and could be used as an AD model, we performed the MWM test and FC test, in addition to the modified Y-Maze, EPM and OF tests performed at 6 months old, for a phenotype confirmation. As no alteration of density of the potential senescence markers was found in synaptosomes of APP/PS1 female mice at 6 months, we decided to, also, prepare total protein extracts of the cortex in APP/PS1 female mice with 9 months as a control.

At 9 months old, APP/PS1 female mice have memory impairments and are anxious. Anxiety-like behaviour was detected in 3 tests: the open field test, in which APP/PS1 female mice spent less time in the center of the arena than WT mice; in the EPM test, where they spent less time and entered less times in the open arms of the apparatus than WT mice; and in the MWM test, where APP/PS1 female mice spent more time swimming close to the walls than WT mice, an indicator of thigmotaxis.

A spatial memory and learning impairment was observed in the MWM test. First, learning is assessed in the acquisition phase of the test, where mice must use distal cues in order to locate the platform and navigate in a direct path to it (Vorhees & Williams, 2006). Here, APP/PS1 female mice had a longer latency to reach the platform whereas control mice could reach the platform in less than 20 seconds after 6 days of trials. Thus, APP/PS1 have not learned in an efficient way to locate the platform.

Reference memory is assessed during the probe day in which the platform is removed, and the mice are except to show bias for the quadrant in which the platform was and cross the platform site multiple times (Vorhees & Williams, 2006). APP/PS1 female mice did not show a bias for any quadrant but, indeed, crossed the site of the platform less times than control mice. This indicates that APP/PS1 female mice have a memory impairment compared to control mice. Gong *et al*., (2019) found similar results,

as 7-8 months old APP/PS1 male mice were slower than control mice to reach the platform in the acquisition phase and crossed the platform site less times than control mice. Donkin *et al*., (2010) observed that 9 months old APP/PS1 male mice showed a longer latency to reach the platform in the last day of acquisition than control mice.

Furthermore, search strategies used for locating the platform on the probe day were analysed. Mice can use hippocampus-dependent (allocentric; spatial) or non hippocampus-dependent (egocentric; unspatial) strategies. Allocentric knowledge relies on the relative position of one landmark to other for navigation and depends on the hippocampus. Egocentric knowledge relies on stimulus–response or procedural processing for navigation and depends on the dorsal striatum (O'keefe & Nadel., 1978).

It is expected that mice find the most efficient path for the hidden platform which can be achieved by directed searches or direct paths, which involve the hippocampus. These strategies are more accurate but can also be less precise (Garthe & Kempermann, 2013). However, when hippocampal lesions are present these allocentric strategies are not used (Eichenbaum *et al*., 1990). In this cases, egocentric strategies are used, which involve random search for the platform (Garthe & Kempermann, 2013). Therefore, APP/PS1 seem to have learning and memory impairments compared to control mice.

APP/PS1 female mice with 9 months old were also submitted to a fear conditioning test. This test evaluated both mood and memory and involved the hippocampus and the basolateral amygdala (Maren, 2001). In the acquisition phase of the test, we found no differences between APP/PS1 and control mice in the percentage of time they spent freezing, which means they have similar initial reaction to the stimuli presented. Thus, although not directly assessed it seems that there might not be evident differences in pain perception between genotypes.

In the context FC test, we found that APP/PS1 female mice spent longer times in freezing in 1 time-point of the test, compared to control mice. Janus *et al*. (2015) found a trend to a lower freezing response in APP/PS1 male mice with 8 months. However, duration of tone, intensity of foot shock and number of CS-US pairings are different from the ones used in this study.

In the cued FC test, 9 months old APP/PS1 female mice spent more time than control mice in freezing in the habituation phase of the test. This result could be an indicator of fear generalization. In this context, fear generalization occurs when, after learning the association between a noxious and an obnoxious stimulus, a defence

response is used even with similar but not identical obnoxious stimuli are present as they predict an aversive outcome (Dunsmoor & Paz, 2015). This is a natural adaptation important for survival. However, excess generalization is found in various anxiety disorders, such as post-traumatic stress (Dunsmoor & Paz, 2015). While our results are indicative of a possible generalized fear present in 9 months old APP/PS1 female mice, a specific protocol of FC for generalized fear must be used. Janus *et al*. (2015) found that APP/PS1 male mice at 8 months old, have an impaired performance in the FC test, as shown by the less time spent in freezing than control mice. Still additional experiments need to be performed to study fear generalization in animal models of AD. As for the rest of the test, no differences were observed in the time spent in freezing between genotypes. Janus *et al*. (2015) found that in the cued test, APP/PS1 male mice froze for longer than control mice. Overall, these results indicate that memory and mood alterations do not initiate at the same time in males and females of this AD mouse model. Memory impairments appear earlier in males (Viana da Silva *et al*., 2016), around 6 months of age, and later in females, with subtle impairment at 6 months of age and mild impairments at 9 months of age.

After behaviour characterization, older APP/PS1 female mice were used for a quantification by Western blot of various senescence-associated proteins.

Here, we found that SIRT1 levels are decreased in 9 months old APP/PS1 female mice. This decrease is found in the synaptic and in total homogenates. SIRT1 seems to be beneficial in AD. Qin *et al* (2006) showed that SIRT1 promotes the non-amyloidogenic pathway via its deacetylase activity. In this study, both neuronal SIRT1 activation and increased NAD^+/NAM ratios, that also result from calorie restriction, promote ROCK1 decreased expression. This leads to an increase in α-secretase activity, therefore promoting the non-amyloidogenic pathway, and inhibiting β-amyloid production. Furthermore, SIRT1 activated *ADAM10* gene transcription, a component of α-secretase, via activation of the retinoic acid receptor-β (RARβ) protein (Lee *et al*., 2014). Therefore, an increase in SIRT1 leads to an increase in α-secretase production which in turn contributes to the preference for the non-amyloidogenic pathway over the amyloidogenic one.

Kilic *et al*. (2018) found elevated levels of SIRT1 in patients with dementia. In Elibol & Kilic (2018) the authors hypothesize that the increase in SIRT1 levels could happen to alleviate the oxidative stress that come with aging and neurodegenerative diseases. Therefore, SIRT1 seems to have a neuroprotective effect early in AD. However, with disease progression, this protection seems to be overthrown.

Given our results, it seems that at 9 months, a decrease in SIRT1 is not restricted to the synapses. In accordance, SIRT1 expression decreases with AD progression in cortical homogenates of AD patients (Lutz *et al*., 2014). In the parietal cortex of AD patients, a decrease in SIRT1 and *Sirt1* mRNA levels were also found and correlated with Aβ and tau accumulation (Julien *et al*., 2009). Interestingly, moreover, SIRT1 was proposed as a predictive marker in AD patients, as its serum concentration decreases with age, and in a more pronounced way in MCI and AD patients (Kumar *et al*., 2013).

We found no alterations in the density levels of SIRT3 in the synapses of 6 months old and 9 months old APP/PS1 mice and in the cortical homogenates of 9 months old APP/PS1 mice.

Lee *et al*. (2017) found that *sirt3* mRNA and protein levels in the cortices of AD patients were decreased compared to controls. Weir *et al.* (2012) found that in the cortex of PDAPP mice, no alterations were found in the levels of *Sirt3* mRNA at 6 months old but an increase in these levels were found at 26 months old. In the hippocampus, at 6 months old, there is an increase in *Sirt3* mRNA, and the levels return to normal at 26 months old. The authors suggest that SIRT3 may have a protective role in the CNS.

Yang *et al*. (2015) found that *sirt3* mRNA and protein levels in the cortices of 12 months old APP/PS1 mice were decreased. Thus, overall, it seems that at the time points we chose, alterations in SIRT3 levels may yet not be present.

Mitochondrial morphology is regulated by its fusion and fission; thus, alteration of this dynamic process can be responsible for alterations in mitochondrial morphology. Indeed, it is also known that mitochondria morphology alterations are responsible for functional alterations, and that without fusion, cellular dysfunction occurs (Chen *et al*., 2005). Moreover, a decrease in mitochondrial fusion can potentiate mitochondrial fragmentation, which is known to be associated with AD as it causes neurodegeneration (Chen *et al*., 2005; Han *et al*., 2020)

We found no alteration in MFN2 levels in the synapses of 6 months old and 9 months old APP/PS1 mice and a decrease in MFN2 levels in cortical homogenates of 9 months old APP/PS1 mice.

Consistently, Manczak *et al*. (2018) found that in 12 months old APP mice, there is a decrease in mitochondrial fusion proteins and an increase in mitochondrial fission proteins. This impairment in mitochondria dynamics is accompanied by an increase in mitochondria and decrease in its length, suggesting mitochondrial fragmentation, and an

impairment in mitochondria functions. Similar results of decrease in mitochondrial fusion proteins and an increase in mitochondrial fission proteins were reported by Wang *et al*. (2009) in *in vitro* studies of hippocampus of AD patients. Our results are in accordance with these works, suggesting that mitochondrial dynamics are altered in cortical regions while mitochondrial fusion does not seem to be altered in cortical synapses.

However, inconsistently with other studies, Xu *et al.* (2017) found an increase in fusion proteins, including MFN2, and fission proteins in the hippocampus of male APPsw/PS1dE9 mice starting at 3 months. At 9 months-old an increase in MFN2 is also found. This study also revealed impaired mitochondrial morphology by an increase in its number and length at 3 months old. These alterations are found before cognitive decline evaluated by the MWM test. However, while this study used whole hippocampus of male mice, our analysis was conducted in the cortical synapses of female mice, which can explain the different results.

SESN2 is a protein involved in stress-response that activates the AMPK pathway (Chen *et al*., 2019). We found that SESN2 levels are decreased in total cortical extracts of 9 months old APP/PS1 mice. No alterations were found in cortical synaptosomes of 6 and 9 months old APP/PS1 mice.

Chen *et al*. (2014) demonstrated that in cortical lysates of 12 months old APP/PS1 mice, SESN2 is upregulated compared to control mice. Furthermore, mRNA SESN2 levels were shown to be increased in AD and MCI patients compared to controls (Rai *et al*., 2016). Given its role in prevention of oxidative stress, overall, it is possible that SESN2 may have a neuroprotective role in AD (Chen *et al*., 2019)

In our attempt to characterize the autophagic marker LC3 in APP/PS1 mice we found that levels of LC3-I where increased in synaptosomes of 6 months old APP/PS1 mice, with no alteration of LC3-II levels. Moreover, at 9 months old, LC3-I levels return to normal in synaptosomes of APP/PS1 mice and no alterations were found in cortical protein extracts.

François *et al*. (2014) found no alterations in LC3-I and LC3-II levels in APP/PS1 mice with 3, 6 and 9 months in both cortex and hippocampus. However, they did find an impairment in autophagy, as levels of Beclin-1 and p62, other autophagy markers, are reduced APP/PS1 mice at 12 months old. It is worth mentioning that this study was performed with males and the samples used are from cortical lysates of females, which could explain our different results compared to this study, even if the same AD model

and same age were chosen. Son *et al.* (2012) found that in 8 to 9 months old APP/PS1 mice, there is an increase in the LC3-II/LC3-I ration in the cortex.

AMPK is a key molecule for regulation of metabolism in the cells. It regulates autophagy and cell growth and promotes mitophagy and mitochondria biogenesis (Mihaylova & Shaw, 2011).

We found no alterations in the levels of AMPK and pAMPK in the synaptosomes of 6 months old APP/PS1 mice and in the cortical extracts of 9 months old APP/PS1 mice. In the synaptosomes of 9 months old APP/PS1 we found no alteration in the levels of AMPK and a decrease in the levels of pAMPK.

In 10 to 12 month old APP/PS1 male mice, phosphorylated AMPK is found to be increased in the hippocampus, but not in the cerebellum or prefrontal cortex (Ma *et al*., 2014). This increase was also observed in the hippocampus of AD patients. Son *et al*. (2012) found that in 8 to 9 months old APP/PS1 male mice, phosphorylated AMPK is increased in the cortex.

In this study, AMPK and pAMPK could not be immunoblotted in the same membrane, which means, we can not express pAMPK levels in relation to the AMPK levels. Thus, we cannot justify the decrease in pAMPK found in the synaptosomes of APP/PS1 mice as a decrease of activation of AMPK through phosphorylation.

As for synaptic markers, we found no alterations in the protein levels in APP/PS1 mice, meaning that the increased PSD-95 levels and decreased syntaxin levels found in 6 months old APP/PS1 mice, return to normal with disease progression.

To explore if these alterations were also found in other AD models, we neurochemically characterized a $A\beta_{1-42}$-injected model of AD at two different time-points. The time-points chosen were previously validated in our lab (Canas *et al*., 2009; Matos *et al*., 2012). Canas *et al.* (2009) found that $A\beta_{1-42}$-injected rats accumulate soluble Aβ peptides and do not form aggregates in the hippocampus, do not show microgliosis nor astrogliosis, and have a memory impairment evaluated by the Y-Maze and novel object recognition tests, 15 after injection. Matos *et al.* (2012) found that $A\beta_{1-42}$-injected rats have memory impairments evaluated by the Y-Maze test, an increased astrogliosis and a lower D-aspartate uptake 20 days after injection. The non-transgenic $A\beta_{1-42}$-injected model can be considered a model of sporadic AD as they do not need the specific mutations of familial AD to develop the AD pathology (Ranjan *et al*., 2018).

In the $A\beta_{1-42}$-injected 14 days model we found no alterations in any of the proteins evaluated, nor in synaptosomes nor in total extracts. However, we did found an increase in SNAP-25, PSD-95, syntaxin and synaptophysin in the cortical synapses of the $A\beta_{1-42}$-injected 14 days model. Interestingly, in this AD model, a decrease in synaptophysin and SNAP-25 levels in the hippocampus that is accompanied by a cognitive decline is reported (Canas *et al*., 2009).

In the $A\beta_{1-42}$-injected 20 days model, we found no alterations in the proteins evaluated except for MFN2, in which we found a decrease in its levels in the synaptosomes of the $A\beta_{1-42}$-injected mice. As for the synaptic markers levels, we found no alterations in any of them in this model.

Merlo *et al.* (2018), reviews what is described as a "biphasic trend" in AD. This is characterized by a temporary increase of synaptic proteins and metabolic activity in the early stages of the disease. Then, with disease progression, this compensation is disrupted and the characteristic decrease in synaptic protein and metabolism activity in AD occurs. These early alterations are found to be a compensatory mechanism, as an attempt to resist initial damage. Evidence supporting the existence of synaptic reorganization is also found in patients with AD (Arendt, 2009).

Consistently, our results show that with symptoms progression, in the $A\beta_{1-42}$ 20 days model, the increase found in the synaptic markers levels in the $A\beta_{1-42}$-injected 14 days model is attenuated. Therefore, it is possible that a compensatory mechanism for AD is present in the $A\beta_{1-42}$-injected model of AD with 14 days of timelag between injection and sacrifice. However, it is worth mentioning that alterations in synaptic markers levels seem to be region-specific (Leuba *et al.*, 2008; Pham *et al.*, 2010) and that here, we used the whole cortex for the preparation of the synaptosomes.

Overall, we only found alterations in the cortical synapses of the levels of SIRT1, pAMPK, LC3 and MFN2 across both AD models and time-points studied. Furthermore, as for SIRT1 these alterations were also found in total cortical extracts. Both SESN2 and MFN2 levels were found to be altered in the total cortical extracts but not in the cortical synaptosomes. Thus, it is possible that, the characteristic AD synaptic dysfunction, starts and is influenced by other regions other the synapse itself. Indeed, glial cells, such as astrocytes and microglia, are intrinsically involved in synapses formation, elimination and function and synaptic plasticity (Chung *et al*., 2015). Furthermore, microglial activation, neuroinflammation and reactive astrogliosis are features of AD (Chung *et al*., 2015).

SIRT1 is shown to be reduced in aging microglia, which contributes to memory deficits (Cho *et al*., 2015). Furthermore, activation of SIRT1 in astrocytes prevents astrogliosis and reduce inflammation in a model of AD (Scuderi *et al*., 2014). Incubation of SH-SY5Y cells with Aβ and glia maturation factor (GMF), a neuroinflammatory protein, led to a decrease of the levels of MFN2 and other fusion proteins and an increase of the levels of fission proteins (Ahmed *et al*., 2019). These results suggest that these proteins could be important contributors to neurodegeneration via functions action in glial cells.

Given our results, it is important to understand if activation of the proteins whose levels are decreased in AD models, can revert the memory and learning impairments observed. For example, various compounds have been described as sirtuins activators, such as the natural compound resveratrol (Howitz *et al*., 2003), compound SRT1720 (Milne *et al*., 2007) and various oxazolo[4,5-b]pyridines (Bemis *et al.,* 2009; Villalba & Alcaín, 2012). Resveratrol seems to have a neuroprotective effect against neurodegeneration as it also prevents learning impairment (Kim *et al*., 2007). Additionally, resveratrol is a powerful antioxidant (Rege *et al*., 2014).

Conclusion

Alzheimer's disease is a neurodegenerative disease affecting millions of people (Alzheimer's Disease International *et al*., 2020). Mitochondria dysfunction and synapse loss are alterations present even before the characteristic Aβ plaques found in AD (Selkoe, 2002; Swerdlow, 2018). Targeting the synapse and its modifications in metabolism, mitochondria dynamics and autophagy in the early stages of AD is crucial as it helps the development of new therapies, that could prevent or delay disease progression

In this study, we found that female APP/PS1 mice, a mice model of AD, have a mild memory impairment starting at 6 months, evaluated by the modified Y-Maze test, that is also present at 9 months old, evaluated by the Morris Water Maze test. Furthermore, APP/PS1 mice seem to be more anxious than control mice, as observed in the open field test and the elevated plus maze test at 6 months old and at 9 months old in the Morris Water Maze test. Thus, females of this AD mouse model, show memory and mood impairments later than males (Viana da Silva *et al*., 2016). At 6 months old, we found a decrease in autophagy marker LC3-I in cortical synaptosomes and a dysregulation of synaptic marker PSD-95 and syntaxin. At 9 months old, we found a decrease in the levels of SIRT1 and pAMPK in the cortical synaptosomes and a decrease in the levels of SIRT1, MFN2 and SESN2 in total cortical extracts. Therefore, it seems that metabolism might be altered in APP/PS1 synapses, and an altered metabolism and mitochondria dynamics might be present in the cortex of these mice.

Moreover, with a $A\beta_{1-42}$-injected model of AD, we found no alterations in the levels of the proteins evaluated except for MFN2, whose levels decrease in the cortical synaptosomes of the $A\beta_{1-42}$-injected model, 20 days after injection. An increase in the levels of synaptic markers SNAP-25, PSD-95, syntaxin and synaptophysin were observed in the $A\beta_{1-42}$-injected model 14 days after injection and these levels return to normal in the $A\beta_{1-42}$-injected model 20 days after injection. The cortex is a heterogeneous mass and densities of these synaptic markers can differ from one region to another. Furthermore, densities of these proteins also differ from one cerebral region to another, as for example, mice injected with $A\beta_{1-42}$ show a decrease in the densities of SNAP-25 and synaptophysin in the hippocampus (Canas *et al*., 2009).

These results are indicative of mitochondria dynamics and metabolism impairment in the cortex of APP/PS1 mice related to cognitive impairments. In the synapses, a metabolic impairment could be present. However, the synaptic dysfunction

characteristic of AD, could be initiated and influenced by other compartments and cell types than the synapse itself, as suggested by our alterations in the densities of the tested proteins in total cortical extracts but not in the synaptosomes. Furthermore, synaptic markers dysregulation was also found which could contribute to synapse loss.

Future Perspectives

In this work, an initial characterization of levels of different proteins was performed with APP/PS1 and $A\beta_{1-42}$-injected mice at 2 different time-points. However, for a robust characterization of these processes, various tests can be additionally performed.

First, for a more detailed understanding of synaptic senescence other senescence markers should be characterized, including cell cycle markers. As for an autophagy characterization, it is important to explore and characterize other autophagic markers, such as accumulation of p62, which can then give us more detailed information about the autophagy flux in the synapses of the AD models.

Furthermore, functional studies of mitochondria's metabolism, such as quantification of glucose uptake using positron emission tomography/computed tomography, could be performed. Moreover, mitochondria's morphology could be evaluated by, for example, assessing fission proteins, such as Dpr1, levels, so that the balance between mitochondria fusion and fission can be assessed.

To complement our results, we could identify the pathways involved in the alterations of the levels of SIRT1, MFN2, SESN2 and pAMPK found, for example, assessing the levels of mTOR and PGC-1α. Furthermore, as some of these alterations were found only in the cortical extracts, we could evaluate glial and neuroinflammation markers, such as glial fibrillary acidic protein (GFAP) for astrocytes and could use ionized calcium-binding adaptor protein-1 (IBA-1) for microglia cells.

Lastly, various activators of SIRT1 and SESN2 are already described and well characterized. It is important to test if these activators can revert the memory and learning impairments found in the mice that showed decreased levels of those two proteins.

References

Aguiar, A., Boemer, G., Rial, D., Cordova, F., Mancini, G., Walz, R., de Bem, A., Latini, A., Leal, R., Pinho, R., & Prediger, R. (2010). High-intensity physical exercise disrupts implicit memory in mice: involvement of the striatal glutathione antioxidant system and intracellular signaling. *Neuroscience*, *171*(4), 1216–1227. https://doi.org/10.1016/j.neuroscience.2010.09.053

Ahmed, M. E., Selvakumar, G. P., Kempuraj, D., Thangavel, R., Mentor, S., Dubova, I., Raikwar, S. P., Zaheer, S., Iyer, S., & Zaheer, A. (2019). Synergy in disruption of mitochondrial dynamics by Aβ (1–42) and glia maturation factor (GMF) in SH-SY5Y Cells Is Mediated Through Alterations in Fission and Fusion Proteins. *Molecular Neurobiology*, *56*(10), 6964–6975. https://doi.org/10.1007/s12035-019-1544-z

Alers, S., Löffler, A. S., Wesselborg, S., & Stork, B. (2012). Role of AMPK-mTOR-Ulk1/2 in the regulation of autophagy: Cross talk, shortcuts, and feedbacks. *Molecular and Cellular Biology*, *32*(1), 2–11. https://doi.org/10.1128/mcb.06159-11

Alzheimer's Disease International, Guerchet, M., Prince, M., & Prina, M. (2020, November 30). *Numbers of people with dementia worldwide*. Alzheimer's Disease International. https://www.alzint.org/resource/numbers-of-people-with-dementia-worldwide/

Anagnostaras, S. G. (2010). Automated assessment of Pavlovian conditioned freezing and shock reactivity in mice using the VideoFreeze system. *Frontiers in Behavioral Neuroscience*, *4*. https://doi.org/10.3389/fnbeh.2010.00158

Anamika, Khanna, A., Acharjee, P., Acharjee, A., & Trigun, S. K. (2019). Mitochondrial SIRT3 and neurodegenerative brain disorders. *Journal of Chemical Neuroanatomy*, *95*, 43–53. https://doi.org/10.1016/j.jchemneu.2017.11.009

Andrew, M. K., & Tierney, M. C. (2018). The puzzle of sex, gender and Alzheimer's disease: Why are women more often affected than men? *Women's Health*, *14*. https://doi.org/10.1177/1745506518817995

Antunes, M., & Biala, G. (2011). The novel object recognition memory: neurobiology, test procedure, and its modifications. *Cognitive Processing*, *13*(2), 93–110. https://doi.org/10.1007/s10339-011-0430-z

Arendt, T. (2009). Synaptic degeneration in Alzheimer's disease. *Acta Neuropathologica*, *118*(1), 167–179. https://doi.org/10.1007/s00401-009-0536-x

Armstrong, R. A. (2019). Risk factors for Alzheimer's disease. *Folia Neuropathologica*, *57*(2), 87–105. https://doi.org/10.5114/fn.2019.85929

Assini, F. L., Duzzioni, M., & Takahashi, R. N. (2009). Object location memory in mice: Pharmacological validation and further evidence of hippocampal CA1 participation. *Behavioural Brain Research*, *204*(1), 206–211. https://doi.org/10.1016/j.bbr.2009.06.005

Bae, S., Sung, S., Oh, S., Lim, J., Lee, S., Park, Y., Lee, H., Kang, D., & Rhee, S. (2013). Sestrins activate Nrf2 by promoting p62-dependent autophagic degradation of Keap1 and prevent oxidative liver damage. *Cell Metabolism*, *17*(1), 73–84. https://doi.org/10.1016/j.cmet.2012.12.002

Bemis, J. E., Vu, C. B., Xie, R., Nunes, J. J., Ng, P. Y., Disch, J. S., Milne, J. C., Carney, D. P., Lynch, A. V., Jin, L., Smith, J. J., Lavu, S., Iffland, A., Jirousek, M. R., & Perni, R. B. (2009). Discovery of oxazolo[4,5-b]pyridines and related

heterocyclic analogs as novel SIRT1 activators. *Bioorganic & Medicinal Chemistry Letters*, *19*(8), 2350–2353. https://doi.org/10.1016/j.bmcl.2008.11.106

Bilousova, T., Miller, C. A., Poon, W. W., Vinters, H. V., Corrada, M., Kawas, C., Hayden, E. Y., Teplow, D. B., Glabe, C., Albay, R., Cole, G. M., Teng, E., & Gylys, K. H. (2016). Synaptic amyloid-β oligomers precede p-Tau and differentiate high pathology control cases. *The American Journal of Pathology*, *186*(1), 185–198. https://doi.org/10.1016/j.ajpath.2015.09.018

Bordone, L., & Guarente, L. (2005). Calorie restriction, SIRT1 and metabolism: understanding longevity. *Nature Reviews Molecular Cell Biology*, *6*(4), 298–305. https://doi.org/10.1038/nrm1616

Braak, H., & Braak, E. (1991). Demonstration of amyloid deposits and neurofibrillary changes in whole brain sections. *Brain Pathology*, *1*(3), 213–216. https://doi.org/10.1111/j.1750-3639.1991.tb00661.x

Bramblett, G. T., Goedert, M., Jakes, R., Merrick, S. E., Trojanowski, J. Q., & Lee, V. M. (1993). Abnormal tau phosphorylation at Ser396 in alzheimer's disease recapitulates development and contributes to reduced microtubule binding. *Neuron*, *10*(6), 1089–1099. https://doi.org/10.1016/0896-6273(93)90057-x

Brenmoehl, J., & Hoeflich, A. (2013). Dual control of mitochondrial biogenesis by sirtuin 1 and sirtuin 3. *Mitochondrion*, *13*(6), 755–761. https://doi.org/10.1016/j.mito.2013.04.002

Budanov, A. V., & Karin, M. (2008). p53 target genes sestrin1 and sestrin2 connect genotoxic stress and mTOR signaling. *Cell*, *134*(3), 451–460. https://doi.org/10.1016/j.cell.2008.06.028

Caccamo, A., de Pinto, V., Messina, A., Branca, C., & Oddo, S. (2014). Genetic reduction of mammalian target of rapamycin ameliorates Alzheimer's disease-like cognitive and pathological deficits by restoring hippocampal gene expression signature. *Journal of Neuroscience*, *34*(23), 7988–7998. https://doi.org/10.1523/jneurosci.0777-14.2014

Cai, Q., & Jeong, Y. Y. (2020). Mitophagy in Alzheimer's disease and other age-related neurodegenerative diseases. *Cells*, *9*(1), 150. https://doi.org/10.3390/cells9010150

Cai, Q., & Tammineni, P. (2017). Mitochondrial aspects of synaptic dysfunction in Alzheimer's disease. *Journal of Alzheimer's Disease*, *57*(4), 1087–1103. https://doi.org/10.3233/jad-160726

Canas, P. M., Porciuncula, L. O., Cunha, G. M. A., Silva, C. G., Machado, N. J., Oliveira, J. M. A., Oliveira, C. R., & Cunha, R. A. (2009). Adenosine A_2A receptor blockade prevents synaptotoxicity and memory dysfunction caused by β-amyloid peptides via p38 mitogen-activated protein kinase pathway. *Journal of Neuroscience*, *29*(47), 14741–14751. https://doi.org/10.1523/jneurosci.3728-09.2009

Castellani, R. J., Rolston, R. K., & Smith, M. A. (2010). Alzheimer disease. *Disease-a-Month*, *56*(9), 484–546. https://doi.org/10.1016/j.disamonth.2010.06.001

Chen, C., Zhou, M., Ge, Y., & Wang, X. (2020). SIRT1 and aging related signaling pathways. *Mechanisms of Ageing and Development*, *187*, 111215. https://doi.org/10.1016/j.mad.2020.111215

Chen, H., Chomyn, A., & Chan, D. C. (2005). Disruption of fusion results in mitochondrial heterogeneity and dysfunction. *Journal of Biological Chemistry*, *280*(28), 26185–26192. https://doi.org/10.1074/jbc.m503062200

Chen, S. D., Yang, J. L., Lin, T. K., & Yang, D. I. (2019). Emerging roles of sestrins in neurodegenerative diseases: Counteracting oxidative stress and beyond. *Journal of clinical medicine*, *8*(7), 1001. https://doi.org/10.3390/jcm8071001

Chen, Y. S., Chen, S. D., Wu, C. L., Huang, S. S., & Yang, D. I. (2014). Induction of sestrin2 as an endogenous protective mechanism against amyloid beta-peptide neurotoxicity in primary cortical culture. *Experimental Neurology*, *253*, 63–71. https://doi.org/10.1016/j.expneurol.2013.12.009

Chen, Y., Liang, Z., Tian, Z., Blanchard, J., Dai, C. L., Chalbot, S., Iqbal, K., Liu, F., & Gong, C. X. (2013). Intracerebroventricular streptozotocin exacerbates Alzheimer-like changes of 3xTg-AD mice. *Molecular Neurobiology*, *49*(1), 547–562. https://doi.org/10.1007/s12035-013-8539-y

Cheng, D., Logge, W., Low, J. K., Garner, B., & Karl, T. (2013). Novel behavioural characteristics of the APPSwe/PS1ΔE9 transgenic mouse model of Alzheimer's disease. *Behavioural Brain Research*, *245*, 120–127. https://doi.org/10.1016/j.bbr.2013.02.008

Cho, S. H., Chen, J. A., Sayed, F., Ward, M. E., Gao, F., Nguyen, T. A., Krabbe, G., Sohn, P. D., Lo, I., Minami, S., Devidze, N., Zhou, Y., Coppola, G., & Gan, L. (2015). SIRT1 deficiency in microglia contributes to cognitive decline in aging and neurodegeneration via epigenetic regulation of IL-1β. *The Journal of Neuroscience*, *35*(2), 807–818. https://doi.org/10.1523/jneurosci.2939-14.2015

Chung, W. S., Welsh, C. A., Barres, B. A., & Stevens, B. (2015). Do glia drive synaptic and cognitive impairment in disease? *Nature Neuroscience*, *18*(11), 1539–1545. https://doi.org/10.1038/nn.4142

Citron, M., Diehl, T. S., Gordon, G., Biere, A. L., Seubert, P., & Selkoe, D. J. (1996b). Evidence that the 42- and 40-amino acid forms of amyloid protein are generated from the -amyloid precursor protein by different protease activities. *Proceedings of the National Academy of Sciences*, *93*(23), 13170–13175. https://doi.org/10.1073/pnas.93.23.13170

Cleary, J. P., Walsh, D. M., Hofmeister, J. J., Shankar, G. M., Kuskowski, M. A., Selkoe, D. J., & Ashe, K. H. (2004). Natural oligomers of the amyloid-β protein specifically disrupt cognitive function. *Nature Neuroscience*, *8*(1), 79–84. https://doi.org/10.1038/nn1372

Corder, E., Saunders, A., Strittmatter, W., Schmechel, D., Gaskell, P., Small, G., Roses, A., Haines, J., & Pericak-Vance, M. (1993). Gene dose of apolipoprotein E type 4 allele and the risk of Alzheimer's disease in late onset families. *Science*, *261*(5123), 921–923. https://doi.org/10.1126/science.8346443

Curry, D. W., Stutz, B., Andrews, Z. B., & Elsworth, J. D. (2018). Targeting AMPK signaling as a neuroprotective strategy in Parkinson's disease. *Journal of Parkinson's Disease*, *8*(2), 161–181. https://doi.org/10.3233/jpd-171296

Davies, C., Mann, D., Sumpter, P., & Yates, P. (1987). A quantitative morphometric analysis of the neuronal and synaptic content of the frontal and temporal cortex in patients with Alzheimer's disease. *Journal of the Neurological Sciences*, *78*(2), 151–164. https://doi.org/10.1016/0022-510x(87)90057-8

Davies, P., & Maloney, A. J. (1976). Selective loss of central cholinergic neurons in Alzheimer's disease. *Lancet (London, England)*, *2*(8000), 1403. https://doi.org/10.1016/s0140-6736(76)91936-x

de Brito, O. M., & Scorrano, L. (2008). Mitofusin 2 tethers endoplasmic reticulum to mitochondria. *Nature*, *456*(7222), 605–610. https://doi.org/10.1038/nature07534

de Wilde, M. C., Overk, C. R., Sijben, J. W., & Masliah, E. (2016). Meta-analysis of synaptic pathology in Alzheimer's disease reveals selective molecular vesicular machinery vulnerability. *Alzheimer's & Dementia*, *12*(6), 633–644. https://doi.org/10.1016/j.jalz.2015.12.005

Demidenko, Z. N., & Blagosklonny, M. V. (2009). At concentrations that inhibit mTOR, resveratrol suppresses cellular senescence. *Cell Cycle*, *8*(12), 1901–1904. https://doi.org/10.4161/cc.8.12.8810

Dias, L., Lopes, C. R., Gonçalves, F. Q., Nunes, A., Pochmann, D., Machado, N. J., Tomé, A. R., Agostinho, P., & Cunha, R. A. (2021). Crosstalk between ATP-P2X7 and adenosine A2A receptors controlling neuroinflammation in rats subject to repeated restraint stress. *Frontiers in Cellular Neuroscience*, *15*. https://doi.org/10.3389/fncel.2021.639322

Dimri, G. P., Lee, X., Basile, G., Acosta, M., Scott, G., Roskelley, C., Medrano, E. E., Linskens, M., Rubelj, I., & Pereira-Smith, O. (1995). A biomarker that identifies senescent human cells in culture and in aging skin *in vivo*. *Proceedings of the National Academy of Sciences*, *92*(20), 9363–9367. https://doi.org/10.1073/pnas.92.20.9363

Dong, W., Cheng, S., Huang, F., Fan, W., Chen, Y., Shi, H., & He, H. (2011). Mitochondrial dysfunction in long-term neuronal cultures mimics changes with aging. *Medical Science Monitor*, *17*(4), BR91–BR96. https://doi.org/10.12659/msm.881706

Donkin, J. J., Stukas, S., Hirsch-Reinshagen, V., Namjoshi, D., Wilkinson, A., May, S., Chan, J., Fan, J., Collins, J., & Wellington, C. L. (2010). ATP-binding cassette transporter A1 mediates the beneficial effects of the liver X receptor agonist GW3965 on object recognition memory and amyloid burden in amyloid precursor protein/presenilin 1 mice*. *Journal of Biological Chemistry*, *285*(44), 34144–34154. https://doi.org/10.1074/jbc.m110.108100

Dunkley, P. R., Jarvie, P. E., & Robinson, P. J. (2008). A rapid Percoll gradient procedure for preparation of synaptosomes. *Nature Protocols*, *3*(11), 1718–1728. https://doi.org/10.1038/nprot.2008.171

Dunsmoor, J. E., & Paz, R. (2015). Fear generalization and anxiety: Behavioral and neural mechanisms. *Biological Psychiatry*, *78*(5), 336–343. https://doi.org/10.1016/j.biopsych.2015.04.010

Edelmann, L., Hanson, P., Chapman, E., & Jahn, R. (1995). Synaptobrevin binding to synaptophysin: a potential mechanism for controlling the exocytotic fusion machine. *The EMBO Journal*, *14*(2), 224–231. https://doi.org/10.1002/j.1460-2075.1995.tb06995.x

Egan, D. F., Shackelford, D. B., Mihaylova, M. M., Gelino, S., Kohnz, R. A., Mair, W., Vasquez, D. S., Joshi, A., Gwinn, D. M., Taylor, R., Asara, J. M., Fitzpatrick, J., Dillin, A., Viollet, B., Kundu, M., Hansen, M., & Shaw, R. J. (2010). Phosphorylation of ULK1 (hATG1) by AMP-Activated protein kinase connects energy sensing to mitophagy. *Science*, *331*(6016), 456–461. https://doi.org/10.1126/science.1196371

Eichenbaum, H., Stewart, C., & Morris, R. G. (1990). Hippocampal representation in place learning. *Journal of Neuroscience*, *10*(11), 3531-3542.

Elder, G. A., Gama Sosa, M. A., & de Gasperi, R. (2010). Transgenic mouse models of Alzheimer's disease. *Mount Sinai Journal of Medicine: A Journal of Translational and Personalized Medicine*, *77*(1), 69–81. https://doi.org/10.1002/msj.20159

El-Husseini, A. E., Schnell, E., Chetkovich, D. M., Nicoll, R. A., & Bredt, D. S. (2000). PSD-95 involvement in maturation of excitatory synapses. *Science (New York, N.Y.)*, *290*(5495), 1364–1368. https://doi.org/10.1126/science.290.5495.1364

Elibol, B., & Kilic, U. (2018). High levels of SIRT1 expression as a protective mechanism against disease-related conditions. *Frontiers in Endocrinology*, *9*. https://doi.org/10.3389/fendo.2018.00614

Ennaceur, A., & Delacour, J. (1988). A new one-trial test for neurobiological studies of memory in rats. 1: Behavioral data. *Behavioural Brain Research*, *31*(1), 47–59. https://doi.org/10.1016/0166-4328(88)90157-x

Esquerda-Canals, G., Montoliu-Gaya, L., Güell-Bosch, J., & Villegas, S. (2017). Mouse models of Alzheimer's disease. *Journal of Alzheimer's disease, JAD*, *57*(4), 1171–1183. https://doi.org/10.3233/JAD-170045

Evans G. J. (2015). The synaptosome as a model system for studying synaptic physiology. *Cold Spring Harbor protocols*, *2015*(5), 421–424. https://doi.org/10.1101/pdb.top074450

Fang, E. F., Hou, Y., Palikaras, K., Adriaanse, B. A., Kerr, J. S., Yang, B., Lautrup, S., Hasan-Olive, M. M., Caponio, D., Dan, X., Rocktäschel, P., Croteau, D. L., Akbari, M., Greig, N. H., Fladby, T., Nilsen, H., Cader, M. Z., Mattson, M. P., Tavernarakis, N., & Bohr, V. A. (2019). Mitophagy inhibits amyloid-β and tau pathology and reverses cognitive deficits in models of Alzheimer's disease. *Nature Neuroscience*, *22*(3), 401–412. https://doi.org/10.1038/s41593-018-0332-9

Ferreira-Vieira, T. H., Guimaraes, I. M., Silva, F. R., & Ribeiro, F. M. (2016). Alzheimer's disease: Targeting the Cholinergic System. *Current neuropharmacology*, *14*(1), 101–115. https://doi.org/10.2174/1570159x13666150716165726

François, A., Rioux Bilan, A., Quellard, N., Fernandez, B., Janet, T., Chassaing, D., Paccalin, M., Terro, F., & Page, G. (2014). Longitudinal follow-up of autophagy and inflammation in brain of APPswePS1dE9 transgenic mice. *Journal of Neuroinflammation*, *11*(1). https://doi.org/10.1186/s12974-014-0139-x

Freund, A., Laberge, R. M., Demaria, M., & Campisi, J. (2012). Lamin B1 loss is a senescence-associated biomarker. *Molecular Biology of the Cell*, *23*(11), 2066–2075. https://doi.org/10.1091/mbc.e11-10-0884

Frost, B., Jacks, R. L., & Diamond, M. I. (2009). Propagation of tau misfolding from the outside to the inside of a cell. *Journal of Biological Chemistry*, *284*(19), 12845–12852. https://doi.org/10.1074/jbc.m808759200

Garcia-Alloza, M., Robbins, E. M., Zhang-Nunes, S. X., Purcell, S. M., Betensky, R. A., Raju, S., Prada, C., Greenberg, S. M., Bacskai, B. J., & Frosch, M. P. (2006). Characterization of amyloid deposition in the APPswe/PS1dE9 mouse model of Alzheimer disease. *Neurobiology of Disease*, *24*(3), 516–524. https://doi.org/10.1016/j.nbd.2006.08.017

Garthe, A., & Kempermann, G. (2013). An old test for new neurons: refining the Morris water maze to study the functional relevance of adult hippocampal neurogenesis. *Frontiers in Neuroscience*, *7*. https://doi.org/10.3389/fnins.2013.00063

Garza-Lombó, C., Schroder, A., Reyes-Reyes, E. M., & Franco, R. (2018). mTOR/AMPK signaling in the brain: Cell metabolism, proteostasis and survival. *Current Opinion in Toxicology*, *8*, 102–110. https://doi.org/10.1016/j.cotox.2018.05.002

Glick, D., Barth, S., & Macleod, K. F. (2010). Autophagy: cellular and molecular mechanisms. *The Journal of Pathology*, *221*(1), 3–12. https://doi.org/10.1002/path.2697

Gonçalves, F. Q., Lopes, J. P., Silva, H. B., Lemos, C., Silva, A. C., Gonçalves, N., Tomé, N. R., Ferreira, S. G., Canas, P. M., Rial, D., Agostinho, P., & Cunha, R. A. (2019). Synaptic and memory dysfunction in a β-amyloid model of early Alzheimer's disease depends on increased formation of ATP-derived extracellular adenosine. *Neurobiology of Disease*, *132*, 104570. https://doi.org/10.1016/j.nbd.2019.104570

Gong, Z., Huang, J., Xu, B., Ou, Z., Zhang, L., Lin, X., Ye, X., Kong, X., Long, D., Sun, X., He, X., Xu, L., Li, Q., & Xuan, A. (2019). Urolithin A attenuates memory impairment and neuroinflammation in APP/PS1 mice. *Journal of Neuroinflammation*, *16*(1). https://doi.org/10.1186/s12974-019-1450-3

González-Gualda, E., Baker, A. G., Fruk, L., & Muñoz-Espín, D. (2020). A guide to assessing cellular senescence *in vitro* and *in vivo*. *The FEBS Journal*, *288*(1), 56–80. https://doi.org/10.1111/febs.15570

Götz, J., Bodea, L. G., & Goedert, M. (2018). Rodent models for Alzheimer disease. *Nature Reviews Neuroscience*, *19*(10), 583–598. https://doi.org/10.1038/s41583-018-0054-8

Grasso, D., Ropolo, A., & Vaccaro, M. I. (2015). Autophagy in cell fate and diseases. *Cell Death-Autophagy, Apoptosis and Necrosis*, *1*, 3-26. https://doi.org/10.5772/61553

Gwinn, D. M., Shackelford, D. B., Egan, D. F., Mihaylova, M. M., Mery, A., Vasquez, D. S., Turk, B. E., & Shaw, R. J. (2008). AMPK phosphorylation of raptor mediates a metabolic checkpoint. *Molecular Cell*, *30*(2), 214–226. https://doi.org/10.1016/j.molcel.2008.03.003

Haass, C., & Selkoe, D. J. (2007). Soluble protein oligomers in neurodegeneration: lessons from the Alzheimer's amyloid β-peptide. *Nature Reviews Molecular Cell Biology*, *8*(2), 101–112. https://doi.org/10.1038/nrm2101

Haass, C., Kaether, C., Thinakaran, G., & Sisodia, S. (2012). Trafficking and proteolytic processing of APP. *Cold Spring Harbor Perspectives in Medicine*, *2*(5), a006270. https://doi.org/10.1101/cshperspect.a006270

Hall, C. S. (1934). Emotional behavior in the rat. I. Defecation and urination as measures of individual differences in emotionality. *Journal of Comparative Psychology*, *18*(3), 385–403. https://doi.org/10.1037/h0071444

Han, S., Nandy, P., Austria, Q., Siedlak, S. L., Torres, S., Fujioka, H., Wang, W., & Zhu, X. (2020). Mfn2 ablation in the adult mouse hippocampus and cortex causes neuronal death. *Cells*, *9*(1), 116. https://doi.org/10.3390/cells9010116

Hardie, D. G., Ross, F. A., & Hawley, S. A. (2012). AMPK: a nutrient and energy sensor that maintains energy homeostasis. *Nature Reviews Molecular Cell Biology*, *13*(4), 251–262. https://doi.org/10.1038/nrm3311

Hardy, J., & Allsop, D. (1991). Amyloid deposition as the central event in the aetiology of Alzheimer's disease. *Trends in Pharmacological Sciences*, *12*, 383–388. https://doi.org/10.1016/0165-6147(91)90609-v

Hardy, J., & Higgins, G. (1992). Alzheimer's disease: the amyloid cascade hypothesis. *Science*, *256*(5054), 184–185. https://doi.org/10.1126/science.1566067

Hirai, K., Aliev, G., Nunomura, A., Fujioka, H., Russell, R. L., Atwood, C. S., Johnson, A. B., Kress, Y., Vinters, H. V., Tabaton, M., Shimohama, S., Cash, A. D., Siedlak, S. L., Harris, P. L. R., Jones, P. K., Petersen, R. B., Perry, G., & Smith, M. A. (2001). Mitochondrial abnormalities in Alzheimer's disease. *The Journal of Neuroscience*, *21*(9), 3017–3023. https://doi.org/10.1523/jneurosci.21-09-03017.2001

Hodel, A. (1998). SNAP-25. *The International Journal of Biochemistry & Cell Biology*, *30*(10), 1069–1073. https://doi.org/10.1016/s1357-2725(98)00079-x

Hou, Y., Dan, X., Babbar, M., Wei, Y., Hasselbalch, S. G., Croteau, D. L., & Bohr, V. A. (2019). Ageing as a risk factor for neurodegenerative disease. *Nature Reviews Neurology*, *15*(10), 565–581. https://doi.org/10.1038/s41582-019-0244-7

Howitz, K. T., Bitterman, K. J., Cohen, H. Y., Lamming, D. W., Lavu, S., Wood, J. G., Zipkin, R. E., Chung, P., Kisielewski, A., Zhang, L. L., Scherer, B., & Sinclair, D. A. (2003). Small molecule activators of sirtuins extend *Saccharomyces cerevisiae* lifespan. *Nature*, *425*(6954), 191–196. https://doi.org/10.1038/nature01960

Hsia, A. Y., Masliah, E., McConlogue, L., Yu, G. Q., Tatsuno, G., Hu, K., Kholodenko, D., Malenka, R. C., Nicoll, R. A., & Mucke, L. (1999). Plaque-independent disruption of neural circuits in Alzheimer's disease mouse models. *Proceedings of the National Academy of Sciences of the United States of America*, *96*(6), 3228–3233. https://doi.org/10.1073/pnas.96.6.3228

Hunt, C., Schenker, L., & Kennedy, M. (1996). PSD-95 is associated with the postsynaptic density and not with the presynaptic membrane at forebrain synapses. *The Journal of Neuroscience*, *16*(4), 1380–1388. https://doi.org/10.1523/jneurosci.16-04-01380.1996

Imai, S. I., Armstrong, C. M., Kaeberlein, M., & Guarente, L. (2000). Transcriptional silencing and longevity protein Sir2 is an NAD-dependent histone deacetylase. *Nature*, *403*(6771), 795–800. https://doi.org/10.1038/35001622

Inoki, K., Zhu, T., & Guan, K. L. (2003). TSC2 mediates cellular energy response to control cell growth and survival. *Cell*, *115*(5), 577–590. https://doi.org/10.1016/s0092-8674(03)00929-2

Jager, S., Handschin, C., St.-Pierre, J., & Spiegelman, B. M. (2007). AMP-activated protein kinase (AMPK) action in skeletal muscle via direct phosphorylation of PGC-1. *Proceedings of the National Academy of Sciences*, *104*(29), 12017–12022. https://doi.org/10.1073/pnas.0705070104

Jankowsky, J. L., Fadale, D. J., Anderson, J., Xu, G. M., Gonzales, V., Jenkins, N. A., Copeland, N. G., Lee, M. K., Younkin, L. H., Wagner, S. L., Younkin, S. G., & Borchelt, D. R. (2003). Mutant presenilins specifically elevate the levels of the 42 residue β-amyloid peptide in vivo: evidence for augmentation of a 42-specific γ secretase. *Human Molecular Genetics*, *13*(2), 159–170. https://doi.org/10.1093/hmg/ddh019

Jankowsky, J. L., Slunt, H. H., Ratovitski, T., Jenkins, N. A., Copeland, N. G., & Borchelt, D. R. (2001). Co-expression of multiple transgenes in mouse CNS: a comparison of strategies. *Biomolecular Engineering*, *17*(6), 157–165. https://doi.org/10.1016/s1389-0344(01)00067-3

Janus, C. (2004). Search strategies used by APP transgenic mice during navigation in the Morris Water Maze. *Learning & Memory*, *11*(3), 337–346. https://doi.org/10.1101/lm.70104

Janus, C., Flores, A. Y., Xu, G., & Borchelt, D. R. (2015). Behavioral abnormalities in APPSwe/PS1dE9 mouse model of AD-like pathology: comparative analysis across multiple behavioral domains. *Neurobiology of Aging*, *36*(9), 2519–2532. https://doi.org/10.1016/j.neurobiolaging.2015.05.010

Janz, R., Südhof, T. C., Hammer, R. E., Unni, V., Siegelbaum, S. A., & Bolshakov, V. Y. (1999). Essential roles in synaptic plasticity for synaptogyrin I and synaptophysin I. *Neuron*, *24*(3), 687–700. https://doi.org/10.1016/s0896-6273(00)81122-8

Jardanhazi-Kurutz, D., Kummer, M., Terwel, D., Vogel, K., Thiele, A., & Heneka, M. (2011). Distinct adrenergic system changes and neuroinflammation in response to induced locus ceruleus degeneration in APP/PS1 transgenic mice. *Neuroscience*, *176*, 396–407. https://doi.org/10.1016/j.neuroscience.2010.11.052

Jarrett, J. T., Berger, E. P., & Lansbury, P. T. (1993). The carboxy terminus of the.beta. amyloid protein is critical for the seeding of amyloid formation: Implications for the pathogenesis of Alzheimer's disease. *Biochemistry*, *32*(18), 4693–4697. https://doi.org/10.1021/bi00069a001

Jeong S. (2017). Molecular and cellular basis of neurodegeneration in Alzheimer's disease. *Molecules and cells*, *40*(9), 613–620. https://doi.org/10.14348/molcells.2017.0096

John, A., & Reddy, P. H. (2021). Synaptic basis of Alzheimer's disease: Focus on synaptic amyloid beta, P-tau and mitochondria. *Ageing Research Reviews*, *65*, 101208. https://doi.org/10.1016/j.arr.2020.101208

Johnson, J., Mercado-Ayon, E., Mercado-Ayon, Y., Dong, Y. N., Halawani, S., Ngaba, L., & Lynch, D. R. (2021). Mitochondrial dysfunction in the development and progression of neurodegenerative diseases. *Archives of Biochemistry and Biophysics*, *702*, 108698. https://doi.org/10.1016/j.abb.2020.108698

Julien, C., Tremblay, C., ÉMond, V., Lebbadi, M., Salem, N., Bennett, D. A., & Calon, F. (2009). Sirtuin 1 reduction parallels the accumulation of tau in Alzheimer disease. *Journal of Neuropathology & Experimental Neurology*, *68*(1), 48–58. https://doi.org/10.1097/nen.0b013e3181922348

Jurk, D., Wang, C., Miwa, S., Maddick, M., Korolchuk, V., Tsolou, A., Gonos, E. S., Thrasivoulou, C., Jill Saffrey, M., Cameron, K., & von Zglinicki, T. (2012). Postmitotic neurons develop a p21-dependent senescence-like phenotype driven by a DNA damage response. *Aging Cell*, *11*(6), 996–1004. https://doi.org/10.1111/j.1474-9726.2012.00870.x

Kabeya, Y. (2000). LC3, a mammalian homologue of yeast Apg8p, is localized in autophagosome membranes after processing. *The EMBO Journal*, *19*(21), 5720–5728. https://doi.org/10.1093/emboj/19.21.5720

Kabeya, Y., Mizushima, N., Yamamoto, A., Oshitani-Okamoto, S., Ohsumi, Y., & Yoshimori, T. (2004). LC3, GABARAP and GATE16 localize to autophagosomal membrane depending on form-II formation. *Journal of Cell Science*, *117*(13), 2805–2812. https://doi.org/10.1242/jcs.01131

Kametani, F., & Hasegawa, M. (2018). Reconsideration of amyloid hypothesis and tau hypothesis in Alzheimer's disease. *Frontiers in Neuroscience*, *12*. https://doi.org/10.3389/fnins.2018.00025

Kashyap, G., Bapat, D., Das, D., Gowaikar, R., Amritkar, R. E., Rangarajan, G., Ravindranath, V., & Ambika, G. (2019). Synapse loss and progress of Alzheimer's disease -A network model. *Scientific Reports*, *9*(1). https://doi.org/10.1038/s41598-019-43076-y

Kilic, U., Elibol, B., Uysal, O., Kilic, E., Yulug, B., Sayin Sakul, A., & Babacan Yildiz, G. (2018). Specific alterations in the circulating levels of the SIRT1, TLR4, and IL7 proteins in patients with dementia. *Experimental Gerontology*, *111*, 203–209. https://doi.org/10.1016/j.exger.2018.07.018

Kim, D., Nguyen, M. D., Dobbin, M. M., Fischer, A., Sananbenesi, F., Rodgers, J. T., Delalle, I., Baur, J. A., Sui, G., Armour, S. M., Puigserver, P., Sinclair, D. A., & Tsai, L. H. (2007). SIRT1 deacetylase protects against neurodegeneration in models for Alzheimer's disease and amyotrophic lateral sclerosis. *The EMBO Journal*, *26*(13), 3169–3179. https://doi.org/10.1038/sj.emboj.7601758

Kim, E., & Sheng, M. (2004). PDZ domain proteins of synapses. *Nature Reviews Neuroscience*, *5*(10), 771–781. https://doi.org/10.1038/nrn1517

Kim, H. Y., Lee, D. K., Chung, B. R., Kim, H. V., & Kim, Y. (2016). Intracerebroventricular injection of amyloid-β peptides in normal mice to acutely induce Alzheimer-like cognitive deficits. *Journal of Visualized Experiments*, *109*. https://doi.org/10.3791/53308

Kirisako, T., Baba, M., Ishihara, N., Miyazawa, K., Ohsumi, M., Yoshimori, T., Noda, T., & Ohsumi, Y. (1999). Formation process of autophagosome is traced with Apg8/Aut7p in yeast. *Journal of Cell Biology*, *147*(2), 435–446. https://doi.org/10.1083/jcb.147.2.435

Knott, A. B., Perkins, G., Schwarzenbacher, R., & Bossy-Wetzel, E. (2008). Mitochondrial fragmentation in neurodegeneration. *Nature Reviews Neuroscience*, *9*(7), 505–518. https://doi.org/10.1038/nrn2417

Krishnamurthy, J., Torrice, C., Ramsey, M. R., Kovalev, G. I., Al-Regaiey, K., Su, L., & Sharpless, N. E. (2004). Ink4a/Arf expression is a biomarker of aging. *Journal of Clinical Investigation*, *114*(9), 1299–1307. https://doi.org/10.1172/jci22475

Kumar, R., Chaterjee, P., Sharma, P. K., Singh, A. K., Gupta, A., Gill, K., Tripathi, M., Dey, A. B., & Dey, S. (2013). Sirtuin1: A promising serum protein marker for early detection of Alzheimer's disease. *PLoS ONE*, *8*(4), e61560. https://doi.org/10.1371/journal.pone.0061560

Kumari, R., & Jat, P. (2021). Mechanisms of cellular senescence: Cell cycle arrest and senescence associated secretory phenotype. *Frontiers in Cell and Developmental Biology*, *9*. https://doi.org/10.3389/fcell.2021.645593

LeDoux, J. E. (2000). Emotion circuits in the brain. *Annual Review of Neuroscience*, *23*(1), 155–184. https://doi.org/10.1146/annurev.neuro.23.1.155

Lee, H. R., Shin, H. K., Park, S. Y., Kim, H. Y., Lee, W. S., Rhim, B. Y., Hong, K. W., & Kim, C. D. (2014). Cilostazol suppresses β-amyloid production by activating a disintegrin and metalloproteinase 10 via the upregulation of SIRT1-coupled retinoic acid receptor-β. *Journal of Neuroscience Research*, *92*(11), 1581–1590. https://doi.org/10.1002/jnr.23421

Lee, J., Kim, Y., Liu, T., Hwang, Y. J., Hyeon, S. J., Im, H., Lee, K., Alvarez, V. E., McKee, A. C., Um, S. J., Hur, M., Mook-Jung, I., Kowall, N. W., & Ryu, H. (2017). SIRT3 deregulation is linked to mitochondrial dysfunction in Alzheimer's disease. *Aging Cell*, *17*(1), e12679. https://doi.org/10.1111/acel.12679

Lee, S., Jeong, S. Y., Lim, W. C., Kim, S., Park, Y. Y., Sun, X., Youle, R. J., & Cho, H. (2007). Mitochondrial fission and fusion mediators, hFis1 and OPA1, modulate cellular senescence. *Journal of Biological Chemistry*, *282*(31), 22977–22983. https://doi.org/10.1074/jbc.m700679200

Leuba, G., Walzer, C., Vernay, A., Carnal, B., Kraftsik, R., Piotton, F., Marin, P., Bouras, C., & Savioz, A. (2008). Postsynaptic density protein PSD-95 expression in Alzheimer's disease and okadaic acid induced neuritic retraction. *Neurobiology of Disease*, *30*(3), 408–419. https://doi.org/10.1016/j.nbd.2008.02.012

Li, X. Y., Men, W. W., Zhu, H., Lei, J. F., Zuo, F. X., Wang, Z. J., Zhu, Z. H., Bao, X. J., & Wang, R. Z. (2016). Age- and brain region-specific changes of glucose metabolic disorder, learning, and memory dysfunction in early Alzheimer's disease assessed in APP/PS1 transgenic mice using ^{18}F-FDG-PET. *International Journal of Molecular Sciences*, *17*(10), 1707. https://doi.org/10.3390/ijms17101707

Liguori, I., Russo, G., Curcio, F., Bulli, G., Aran, L., Della-Morte, D., Gargiulo, G., Testa, G., Cacciatore, F., Bonaduce, D., & Abete, P. (2018). Oxidative stress, aging, and diseases. *Clinical Interventions in Aging*, *Volume 13*, 757–772. https://doi.org/10.2147/cia.s158513

Lin, S. J., Kaeberlein, M., Andalis, A. A., Sturtz, L. A., Defossez, P. A., Culotta, V. C., Fink, G. R., & Guarente, L. (2002). Calorie restriction extends *Saccharomyces cerevisiae* lifespan by increasing respiration. *Nature*, *418*(6895), 344–348. https://doi.org/10.1038/nature00829

Lister, R. (1987). The use of a plus-maze to measure anxiety in the mouse. *Psychopharmacology*, *92*(2), 180–185. https://doi.org/10.1007/bf00177912

Liu, P. P., Xie, Y., Meng, X. Y., & Kang, J. S. (2019). History and progress of hypotheses and clinical trials for Alzheimer's disease. *Signal Transduction and Targeted Therapy*, *4*(1). https://doi.org/10.1038/s41392-019-0063-8

Loessner, A., Alavi, A., Lewandrowski, K. U., Mozley, D., Souder, E., & Gur, R. E. (1995). Regional cerebral function determined by FDG-PET in healthy volunteers: normal patterns and changes with age. *Journal of nuclear medicine : official publication, Society of Nuclear Medicine*, *36*(7), 1141–1149.

Lopes-Paciencia, S., Saint-Germain, E., Rowell, M. C., Ruiz, A. F., Kalegari, P., & Ferbeyre, G. (2019). The senescence-associated secretory phenotype and its regulation. *Cytokine*, *117*, 15–22. https://doi.org/10.1016/j.cyto.2019.01.013

López-Otín, C., Blasco, M. A., Partridge, L., Serrano, M., & Kroemer, G. (2013). The hallmarks of aging. *Cell*, *153*(6), 1194–1217. https://doi.org/10.1016/j.cell.2013.05.039

Lu, J., Wu, D. M., Zheng, Y. L., Hu, B., Zhang, Z. F., Shan, Q., Zheng, Z. H., Liu, C. M., & Wang, Y. J. (2010). Quercetin activates AMP-activated protein kinase by reducing PP2C expression protecting old mouse brain against high cholesterol-induced neurotoxicity. *The Journal of Pathology*, *222*(2), 199–212. https://doi.org/10.1002/path.2754

Lutz, M. I., Milenkovic, I., Regelsberger, G., & Kovacs, G. G. (2014). Distinct patterns of sirtuin expression during progression of Alzheimer's disease. *NeuroMolecular Medicine*, *16*(2), 405–414. https://doi.org/10.1007/s12017-014-8288-8

Ma, T., Chen, Y., Vingtdeux, V., Zhao, H., Viollet, B., Marambaud, P., & Klann, E. (2014). Inhibition of AMP-activated protein kinase signaling alleviates impairments in hippocampal synaptic plasticity induced by amyloid. *Journal of Neuroscience*, *34*(36), 12230–12238. https://doi.org/10.1523/jneurosci.1694-14.2014

Manczak, M., Anekonda, T. S., Henson, E., Park, B. S., Quinn, J., & Reddy, P. H. (2006). Mitochondria are a direct site of Aβ accumulation in Alzheimer's disease neurons: implications for free radical generation and oxidative damage in disease progression. *Human Molecular Genetics*, *15*(9), 1437–1449. https://doi.org/10.1093/hmg/ddl066

Manczak, M., Kandimalla, R., Yin, X., & Reddy, P. H. (2018). Hippocampal mutant APP and amyloid beta-induced cognitive decline, dendritic spine loss, defective autophagy, mitophagy and mitochondrial abnormalities in a mouse model of Alzheimer's disease. *Human Molecular Genetics*, *27*(8), 1332–1342. https://doi.org/10.1093/hmg/ddy042

Maren, S. (2001). Neurobiology of Pavlovian fear conditioning. *Annual Review of Neuroscience*, *24*(1), 897–931. https://doi.org/10.1146/annurev.neuro.24.1.897

Martínez-Cué, C., & Rueda, N. (2020). Cellular senescence in neurodegenerative diseases. *Frontiers in Cellular Neuroscience*, *14*. https://doi.org/10.3389/fncel.2020.00016

Matilainen, O., Quirós, P. M., & Auwerx, J. (2017). Mitochondria and epigenetics – Crosstalk in homeostasis and stress. *Trends in Cell Biology*, *27*(6), 453–463. https://doi.org/10.1016/j.tcb.2017.02.004

Matos, M., Augusto, E., Machado, N. J., dos Santos-Rodrigues, A., Cunha, R. A., & Agostinho, P. (2012). Astrocytic adenosine A_2A receptors control the amyloid-β peptide-induced decrease of glutamate uptake. *Journal of Alzheimer's Disease*, *31*(3), 555–567. https://doi.org/10.3233/jad-2012-120469

Meng, H., Yan, W. Y., Lei, Y. H., Wan, Z., Hou, Y. Y., Sun, L. K., & Zhou, J. P. (2019). SIRT3 regulation of mitochondrial quality control in neurodegenerative diseases. *Frontiers in Aging Neuroscience*, *11*. https://doi.org/10.3389/fnagi.2019.00313

Merlo, S., Spampinato, S. F., & Sortino, M. A. (2018). Early compensatory responses against neuronal injury: A new therapeutic window of opportunity for Alzheimer's disease? *CNS Neuroscience & Therapeutics*, *25*(1), 5–13. https://doi.org/10.1111/cns.13050

Mhatre, S. D., Paddock, B. E., Saunders, A. J., & Marenda, D. R. (2012). Invertebrate models of Alzheimer's disease. *Journal of Alzheimer's Disease*, *33*(1), 3–16. https://doi.org/10.3233/jad-2012-121204

Michan, S., Li, Y., Chou, M. M. H., Parrella, E., Ge, H., Long, J. M., Allard, J. S., Lewis, K., Miller, M., Xu, W., Mervis, R. F., Chen, J., Guerin, K. I., Smith, L. E. H., McBurney, M. W., Sinclair, D. A., Baudry, M., de Cabo, R., & Longo, V. D. (2010). SIRT1 is essential for normal cognitive function and synaptic plasticity. *Journal of Neuroscience*, *30*(29), 9695–9707. https://doi.org/10.1523/jneurosci.0027-10.2010

Michishita, E., Park, J. Y., Burneskis, J. M., Barrett, J. C., & Horikawa, I. (2005). Evolutionarily conserved and nonconserved cellular localizations and functions of human SIRT proteins. *Molecular Biology of the Cell*, *16*(10), 4623–4635. https://doi.org/10.1091/mbc.e05-01-0033

Mihaylova, M. M., & Shaw, R. J. (2011). The AMPK signalling pathway coordinates cell growth, autophagy and metabolism. *Nature Cell Biology*, *13*(9), 1016–1023. https://doi.org/10.1038/ncb2329

Milne, J. C., Lambert, P. D., Schenk, S., Carney, D. P., Smith, J. J., Gagne, D. J., Jin, L., Boss, O., Perni, R. B., Vu, C. B., Bemis, J. E., Xie, R., Disch, J. S., Ng, P. Y., Nunes, J. J., Lynch, A. V., Yang, H., Galonek, H., Israelian, K., Choy, W., Iffland, A., Lavu, S., Medvedik, O., Sinclair., D. A., Olefsky, J. M., Jirousek, M. R., Elliott, P. J. & Westphal, C. H. (2007). Small molecule activators of SIRT1 as therapeutics for the treatment of type 2 diabetes. *Nature*, *450*(7170), 712–716. https://doi.org/10.1038/nature06261

Mizushima, N., & Yoshimori, T. (2007). How to interpret LC3 immunoblotting. *Autophagy*, *3*(6), 542–545. https://doi.org/10.4161/auto.4600

Moreira-de-Sá, A., Gonçalves, F. Q., Lopes, J. P., Silva, H. B., Tomé, N. R., Cunha, R. A., & Canas, P. M. (2020). Adenosine A2A receptors format long-term depression and memory strategies in a mouse model of Angelman syndrome. *Neurobiology of Disease*, *146*, 105137. https://doi.org/10.1016/j.nbd.2020.105137

Moreira-de-Sá, A., Gonçalves, F. Q., Lopes, J. P., Silva, H. B., Tomé, N. R., Cunha, R. A., & Canas, P. M. (2021). Motor deficits coupled to cerebellar and striatal alterations in Ube3a$^{m-/p+}$ mice modelling Angelman Syndrome are

attenuated by adenosine A_2A receptor blockade. *Molecular Neurobiology*, *58*(6), 2543–2557. https://doi.org/10.1007/s12035-020-02275-9

Morris, R. (1984). Developments of a water-maze procedure for studying spatial learning in the rat. *Journal of Neuroscience Methods*, *11*(1), 47–60. https://doi.org/10.1016/0165-0270(84)90007-4

Morris, R. G. (1981). Spatial localization does not require the presence of local cues. *Learning and Motivation*, *12*(2), 239–260. https://doi.org/10.1016/0023-9690(81)90020-5

Mucke, L., & Selkoe, D. J. (2012). Neurotoxicity of amyloid β-protein: synaptic and network dysfunction. *Cold Spring Harbor perspectives in medicine*, *2*(7), a006338. https://doi.org/10.1101/cshperspect.a006338

Muñoz-Espín, D., & Serrano, M. (2014). Cellular senescence: from physiology to pathology. *Nature Reviews Molecular Cell Biology*, *15*(7), 482–496. https://doi.org/10.1038/nrm3823

Nativio, R., Donahue, G., Berson, A., Lan, Y., Amlie-Wolf, A., Tuzer, F., Toledo, J. B., Gosai, S. J., Gregory, B. D., Torres, C., Trojanowski, J. Q., Wang, L. S., Johnson, F. B., Bonini, N. M., & Berger, S. L. (2018). Dysregulation of the epigenetic landscape of normal aging in Alzheimer's disease. *Nature Neuroscience*, *21*(4), 497–505. https://doi.org/10.1038/s41593-018-0101-9

Negrón-Oyarzo, I., Espinosa, N., Aguilar-Rivera, M., Fuenzalida, M., Aboitiz, F., & Fuentealba, P. (2018). Coordinated prefrontal–hippocampal activity and navigation strategy-related prefrontal firing during spatial memory formation. *Proceedings of the National Academy of Sciences*, *115*(27), 7123–7128. https://doi.org/10.1073/pnas.1720117115

North, B. J., Marshall, B. L., Borra, M. T., Denu, J. M., & Verdin, E. (2003). The human Sir2 ortholog, SIRT2, is an NAD^+-dependent tubulin deacetylase. *Molecular Cell*, *11*(2), 437–444. https://doi.org/10.1016/s1097-2765(03)00038-8

O'keefe, J., & Nadel, L. (1978). The hippocampus as a cognitive map. Oxford university press.

Onyango, P., Celic, I., McCaffery, J. M., Boeke, J. D., & Feinberg, A. P. (2002). SIRT3, a human SIR2 homologue, is an NAD- dependent deacetylase localized to mitochondria. *Proceedings of the National Academy of Sciences*, *99*(21), 13653–13658. https://doi.org/10.1073/pnas.222538099

Park, H., Kang, J. H., & Lee, S. (2020). Autophagy in neurodegenerative diseases: A hunter for aggregates. *International Journal of Molecular Sciences*, *21*(9), 3369. https://doi.org/10.3390/ijms21093369

Parzych, K. R., & Klionsky, D. J. (2014). An overview of autophagy: morphology, mechanism, and regulation. *Antioxidants & Redox Signaling*, *20*(3), 460–473. https://doi.org/10.1089/ars.2013.5371

Pavlov, I. P. (1927). Conditioned reflexes: an investigation of the physiological activity of the cerebral cortex. *Oxford Univ. Press.*

Penney, J., Ralvenius, W. T., & Tsai, L. H. (2019). Modeling Alzheimer's disease with iPSC-derived brain cells. *Molecular Psychiatry*, *25*(1), 148–167. https://doi.org/10.1038/s41380-019-0468-3

Perlman, R. L. (2016). Mouse models of human disease: An evolutionary perspective. *Evolution, Medicine, and Public Health*, eow014. https://doi.org/10.1093/emph/eow014

Pham, E., Crews, L., Ubhi, K., Hansen, L., Adame, A., Cartier, A., Salmon, D., Galasko, D., Michael, S., Savas, J. N., Yates, J. R., Glabe, C., & Masliah, E. (2010). Progressive accumulation of amyloid-β oligomers in Alzheimer's

disease and in amyloid precursor protein transgenic mice is accompanied by selective alterations in synaptic scaffold proteins. *FEBS Journal*, *277*(14), 3051–3067. https://doi.org/10.1111/j.1742-4658.2010.07719.x

Piechota, M., Sunderland, P., Wysocka, A., Nalberczak, M., Sliwinska, M. A., Radwanska, K., & Sikora, E. (2016). Is senescence-associated β-galactosidase a marker of neuronal senescence? *Oncotarget*, *7*(49), 81099–81109. https://doi.org/10.18632/oncotarget.12752

Poirel, O., Mella, S., Videau, C., Ramet, L., Davoli, M. A., Herzog, E., Katsel, P., Mechawar, N., Haroutunian, V., Epelbaum, J., Daumas, S., & el Mestikawy, S. (2018). Moderate decline in select synaptic markers in the prefrontal cortex (BA9) of patients with Alzheimer's disease at various cognitive stages. *Scientific Reports*, *8*(1). https://doi.org/10.1038/s41598-018-19154-y

Prut, L., & Belzung, C. (2003). The open field as a paradigm to measure the effects of drugs on anxiety-like behaviors: a review. *European Journal of Pharmacology*, *463*(1–3), 3–33. https://doi.org/10.1016/s0014-2999(03)01272-x

Qin, W., Yang, T., Ho, L., Zhao, Z., Wang, J., Chen, L., Zhao, W., Thiyagarajan, M., MacGrogan, D., Rodgers, J. T., Puigserver, P., Sadoshima, J., Deng, H., Pedrini, S., Gandy, S., Sauve, A. A., & Pasinetti, G. M. (2006). Neuronal SIRT1 activation as a novel mechanism underlying the prevention of Alzheimer disease amyloid neuropathology by calorie restriction*. *Journal of Biological Chemistry*, *281*(31), 21745–21754. https://doi.org/10.1074/jbc.m602909200

Rai, N., Kumar, R., Desai, G. R., Venugopalan, G., Shekhar, S., Chatterjee, P., Tripathi, M., Upadhyay, A. D., Dwivedi, S., Dey, A. B., & Dey, S. (2016). Relative alterations in blood-based levels of sestrin in Alzheimer's disease and mild cognitive impairment patients. *Journal of Alzheimer's Disease*, *54*(3), 1147–1155. https://doi.org/10.3233/jad-160479

Ramakrishnan, N. A., Drescher, M. J., & Drescher, D. G. (2012). The SNARE complex in neuronal and sensory cells. *Molecular and cellular neurosciences*, *50*(1), 58–69. https://doi.org/10.1016/j.mcn.2012.03.009

Ranjan, V. D., Qiu, L., Tan, E. K., Zeng, L., & Zhang, Y. (2018). Modelling Alzheimer's disease: Insights from in vivo to in vitro three-dimensional culture platforms. *Journal of Tissue Engineering and Regenerative Medicine*, *12*(9), 1944–1958. https://doi.org/10.1002/term.2728

Ransohoff, R. M. (2016). How neuroinflammation contributes to neurodegeneration. *Science*, *353*(6301), 777–783. https://doi.org/10.1126/science.aag2590

Ray, P. D., Huang, B. W., & Tsuji, Y. (2012). Reactive oxygen species (ROS) homeostasis and redox regulation in cellular signaling. *Cellular Signalling*, *24*(5), 981–990. https://doi.org/10.1016/j.cellsig.2012.01.008

Rebola, N., Canas, P., Oliveira, C., & Cunha, R. (2005). Different synaptic and subsynaptic localization of adenosine A_2A receptors in the hippocampus and striatum of the rat. *Neuroscience*, *132*(4), 893–903. https://doi.org/10.1016/j.neuroscience.2005.01.014

Reddy, P. H. (2009). Role of mitochondria in neurodegenerative diseases: mitochondria as a therapeutic target in Alzheimer's disease. *CNS Spectrums*, *14*(S7), 8–13. https://doi.org/10.1017/s1092852900024901

Reddy, P. H. (2011). Abnormal tau, mitochondrial dysfunction, impaired axonal transport of mitochondria, and synaptic deprivation in Alzheimer's disease. *Brain Research*, *1415*, 136–148. https://doi.org/10.1016/j.brainres.2011.07.052

Reddy, P. H., & Beal, M. F. (2008). Amyloid beta, mitochondrial dysfunction and synaptic damage: implications for cognitive decline in aging and Alzheimer's disease. *Trends in Molecular Medicine*, *14*(2), 45–53. https://doi.org/10.1016/j.molmed.2007.12.002

Reddy, P. H., & Oliver, D. M. (2019). Amyloid beta and phosphorylated tau-induced defective autophagy and mitophagy in Alzheimer's disease. *Cells*, *8*(5), 488. https://doi.org/10.3390/cells8050488

Reddy, P. H., Mani, G., Park, B. S., Jacques, J., Murdoch, G., Whetsell, W., Kaye, J., & Manczak, M. (2005). Differential loss of synaptic proteins in Alzheimer's disease: Implications for synaptic dysfunction. *Journal of Alzheimer's Disease*, *7*(2), 103–117. https://doi.org/10.3233/jad-2005-7203

Rege, S. D., Geetha, T., Griffin, G. D., Broderick, T. L., & Babu, J. R. (2014). Neuroprotective effects of resveratrol in Alzheimer disease pathology. *Frontiers in Aging Neuroscience*, *6*. https://doi.org/10.3389/fnagi.2014.00218

Rizzi, L., & Roriz-Cruz, M. (2018). Sirtuin 1 and Alzheimer's disease: An up-to-date review. *Neuropeptides*, *71*, 54–60. https://doi.org/10.1016/j.npep.2018.07.001

Romagosa, C., Simonetti, S., López-Vicente, L., Mazo, A., Lleonart, M. E., Castellvi, J., & Ramon Y Cajal, S. (2011). $p16^{Ink4a}$ overexpression in cancer: a tumor suppressor gene associated with senescence and high-grade tumors. *Oncogene*, *30*(18), 2087–2097. https://doi.org/10.1038/onc.2010.614

Sabuncu, M. R. (2011). The dynamics of cortical and hippocampal atrophy in Alzheimer disease. *Archives of Neurology*, *68*(8), 1040. https://doi.org/10.1001/archneurol.2011.167

Saez-Atienzar, S., & Masliah, E. (2020). Cellular senescence and Alzheimer disease: the egg and the chicken scenario. *Nature Reviews Neuroscience*, *21*(8), 433–444. https://doi.org/10.1038/s41583-020-0325-z

Scuderi, C., Stecca, C., Bronzuoli, M. R., Rotili, D., Valente, S., Mai, A., & Steardo, L. (2014). Sirtuin modulators control reactive gliosis in an in vitro model of Alzheimer's disease. *Frontiers in Pharmacology*, *5*. https://doi.org/10.3389/fphar.2014.00089

Selkoe, D. J. (2002). Alzheimer's disease is a synaptic failure. *Science*, *298*(5594), 789–791. https://doi.org/10.1126/science.1074069

Selkoe, D. J. (2008). Soluble oligomers of the amyloid β-protein impair synaptic plasticity and behavior. *Behavioural Brain Research*, *192*(1), 106–113. https://doi.org/10.1016/j.bbr.2008.02.016

Serrano-Pozo, A., Frosch, M. P., Masliah, E., & Hyman, B. T. (2011). Neuropathological alterations in Alzheimer disease. *Cold Spring Harbor Perspectives in Medicine*, *1*(1), a006189. https://doi.org/10.1101/cshperspect.a006189

Simon, P., Dupuis, R., & Costentin, J. (1994). Thigmotaxis as an index of anxiety in mice. Influence of dopaminergic transmissions. *Behavioural Brain Research*, *61*(1), 59–64. https://doi.org/10.1016/0166-4328(94)90008-6

Sita, G., Hrelia, P., Graziosi, A., & Morroni, F. (2020). Back to the fusion: Mitofusin-2 in Alzheimer's disease. *Journal of Clinical Medicine*, *9*(1), 126. https://doi.org/10.3390/jcm9010126

Slanzi, A., Iannoto, G., Rossi, B., Zenaro, E., & Constantin, G. (2020). In vitro models of neurodegenerative diseases. *Frontiers in Cell and Developmental Biology*, *8*. https://doi.org/10.3389/fcell.2020.00328

Small, D. H., Mok, S. S., & Bornstein, J. C. (2001). Alzheimer's disease and Aβ toxicity: from top to bottom. *Nature Reviews Neuroscience*, *2*(8), 595–598. https://doi.org/10.1038/35086072

Snellman, A., Takkinen, J. S., López-Picón, F. R., Eskola, O., Solin, O., Rinne, J. O., & Haaparanta-Solin, M. (2019). Effect of genotype and age on cerebral [^{18}F]FDG uptake varies between transgenic APP_{Swe}-$PS1_{dE9}$ and Tg2576 mouse models of Alzheimer's disease. *Scientific Reports*, *9*(1). https://doi.org/10.1038/s41598-019-42074-4

Son, S. M., Jung, E. S., Shin, H. J., Byun, J., & Mook-Jung, I. (2012). Aβ-induced formation of autophagosomes is mediated by RAGE-CaMKKβ-AMPK signaling. *Neurobiology of Aging*, *33*(5), 1006.e11-1006.e23. https://doi.org/10.1016/j.neurobiolaging.2011.09.039

Soontornniyomkij, V., Soontornniyomkij, B., Moore, D. J., Gouaux, B., Masliah, E., Tung, S., Vinters, H. V., Grant, I., & Achim, C. L. (2012). Antioxidant sestrin-2 redistribution to neuronal soma in human immunodeficiency virus-associated neurocognitive disorders. *Journal of Neuroimmune Pharmacology*, *7*(3), 579–590. https://doi.org/10.1007/s11481-012-9357-0

Spillantini, M. G., & Goedert, M. (2013). Tau pathology and neurodegeneration. *The Lancet. Neurology*, *12*(6), 609–622. https://doi.org/10.1016/S1474-4422(13)70090-5

Spilman, P., Podlutskaya, N., Hart, M. J., Debnath, J., Gorostiza, O., Bredesen, D., Richardson, A., Strong, R., & Galvan, V. (2010). Inhibition of mTOR by rapamycin abolishes cognitive deficits and reduces amyloid-β levels in a mouse model of Alzheimer's disease. *PLoS ONE*, *5*(4), e9979. https://doi.org/10.1371/journal.pone.0009979

Sultana, R., Banks, W. A., & Butterfield, D. A. (2009). Decreased levels of PSD95 and two associated proteins and increased levels of BCl2and caspase 3 in hippocampus from subjects with amnestic mild cognitive impairment: Insights into their potential roles for loss of synapses and memory, accumulation of Aβ, and neurodegeneration in a prodromal stage of Alzheimer's disease. *Journal of Neuroscience Research*, NA. https://doi.org/10.1002/jnr.22227

Swerdlow, R. H. (2018). Mitochondria and mitochondrial cascades in Alzheimer's disease. *Journal of Alzheimer's Disease*, *62*(3), 1403–1416. https://doi.org/10.3233/jad-170585

Swerdlow, R. H., & Khan, S. M. (2004). A "mitochondrial cascade hypothesis" for sporadic Alzheimer's disease. *Medical Hypotheses*, *63*(1), 8–20. https://doi.org/10.1016/j.mehy.2003.12.045

Swerdlow, R. H., Burns, J. M., & Khan, S. M. (2014). The Alzheimer's disease mitochondrial cascade hypothesis: Progress and perspectives. *Biochimica et Biophysica Acta (BBA) - Molecular Basis of Disease*, *1842*(8), 1219–1231. https://doi.org/10.1016/j.bbadis.2013.09.010

Switon, K., Kotulska, K., Janusz-Kaminska, A., Zmorzynska, J., & Jaworski, J. (2017). Molecular neurobiology of mTOR. *Neuroscience*, *341*, 112–153. https://doi.org/10.1016/j.neuroscience.2016.11.017

Tan, F. C. C., Hutchison, E. R., Eitan, E., & Mattson, M. P. (2014). Are there roles for brain cell senescence in aging and neurodegenerative disorders? *Biogerontology*, *15*(6), 643–660. https://doi.org/10.1007/s10522-014-9532-1

Tanno, M., Sakamoto, J., Miura, T., Shimamoto, K., & Horio, Y. (2007). Nucleocytoplasmic shuttling of the NAD^+-dependent histone deacetylase SIRT1. *Journal of Biological Chemistry*, *282*(9), 6823–6832. https://doi.org/10.1074/jbc.m609554200

Terry, R. D., Masliah, E., Salmon, D. P., Butters, N., DeTeresa, R., Hill, R., Hansen, L. A., & Katzman, R. (1991). Physical basis of cognitive alterations in Alzheimer's disease: Synapse loss is the major correlate of cognitive impairment. *Annals of Neurology*, *30*(4), 572–580. https://doi.org/10.1002/ana.410300410

Thiel, G. (1993). Synapsin I, synapsin II, and synaptophysin: Marker proteins of synaptic vesicles. *Brain Pathology*, *3*(1), 87–95. https://doi.org/10.1111/j.1750-3639.1993.tb00729.x

Uttara, B., Singh, A. V., Zamboni, P., & Mahajan, R. T. (2009). Oxidative stress and neurodegenerative diseases: a review of upstream and downstream antioxidant therapeutic options. *Current neuropharmacology*, *7*(1), 65–74. https://doi.org/10.2174/157015909787602823

Vaquero, A., Scher, M., Lee, D., Erdjument-Bromage, H., Tempst, P., & Reinberg, D. (2004). Human SirT1 interacts with histone H1 and promotes formation of facultative heterochromatin. *Molecular Cell*, *16*(1), 93–105. https://doi.org/10.1016/j.molcel.2004.08.031

Viana Da Silva, S., Haberl, M. G., Zhang, P., Bethge, P., Lemos, C., Gonçalves, N., Gorlewicz, A., Malezieux, M., Gonçalves, F. Q., Grosjean, N., Blanchet, C., Frick, A., Nägerl, U. V., Cunha, R. A., & Mulle, C. (2016). Early synaptic deficits in the APP/PS1 mouse model of Alzheimer's disease involve neuronal adenosine A_2A receptors. *Nature Communications*, *7*(1). https://doi.org/10.1038/ncomms11915

Villalba, J. M., & Alcaín, F. J. (2012). Sirtuin activators and inhibitors. *BioFactors*, *38*(5), 349–359. https://doi.org/10.1002/biof.1032

Vorhees, C. V., & Williams, M. T. (2006). Morris water maze: procedures for assessing spatial and related forms of learning and memory. *Nature Protocols*, *1*(2), 848–858. https://doi.org/10.1038/nprot.2006.116

Wallace, D. C., & Chalkia, D. (2013). Mitochondrial DNA genetics and the heteroplasmy conundrum in evolution and disease. *Cold Spring Harbor Perspectives in Biology*, *5*(11), a021220. https://doi.org/10.1101/cshperspect.a021220

Wang, X., Su, B., Lee, H. G., Li, X., Perry, G., Smith, M. A., & Zhu, X. (2009). Impaired balance of mitochondrial fission and fusion in Alzheimer's disease. *Journal of Neuroscience*, *29*(28), 9090–9103. https://doi.org/10.1523/jneurosci.1357-09.2009

Weir, H. J. M., Murray, T. K., Kehoe, P. G., Love, S., Verdin, E. M., O'Neill, M. J., Lane, J. D., & Balthasar, N. (2012). CNS SIRT3 expression is altered by reactive oxygen species and in Alzheimer's disease. *PLoS ONE*, *7*(11), e48225. https://doi.org/10.1371/journal.pone.0048225

Wissler Gerdes, E. O., Zhu, Y., Weigand, B. M., Tripathi, U., Burns, T. C., Tchkonia, T., & Kirkland, J. L. (2020). Cellular senescence in aging and age-related diseases: Implications for neurodegenerative diseases. *International Review of Neurobiology*, 203–234. https://doi.org/10.1016/bs.irn.2020.03.019

Wu, Y., Wu, M., He, G., Zhang, X., Li, W., Gao, Y., Li, Z., Wang, Z., & Zhang, C. (2012). Glyceraldehyde-3-phosphate dehydrogenase: A universal internal control for Western blots in prokaryotic and eukaryotic cells. *Analytical Biochemistry*, *423*(1), 15–22. https://doi.org/10.1016/j.ab.2012.01.012

Xu, L. L., Shen, Y., Wang, X., Wei, L. F., Wang, P., Yang, H., Wang, C. F., Xie, Z. H., & Bi, J. Z. (2017). Mitochondrial dynamics changes with age in an APPsw/PS1dE9 mouse model of Alzheimer's disease. *NeuroReport*, *28*(4), 222–228. https://doi.org/10.1097/wnr.0000000000000739

Yan, M. H., Wang, X., & Zhu, X. (2013). Mitochondrial defects and oxidative stress in Alzheimer disease and Parkinson disease. *Free Radical Biology and Medicine*, *62*, 90–101. https://doi.org/10.1016/j.freeradbiomed.2012.11.014

Yang, L., Jiang, Y., Shi, L., Zhong, D., Li, Y., Li, J., & Jin, R. (2020). AMPK: potential therapeutic target for Alzheimer's disease. *Current Protein & Peptide Science*, *21*(1), 66–77. https://doi.org/10.2174/1389203720666190819142746

Yang, W., Zou, Y., Zhang, M., Zhao, N., Tian, Q., Gu, M., Liu, W., Shi, R., Lü, Y., & Yu, W. (2015). Mitochondrial Sirt3 expression is decreased in APP/PS1 double transgenic mouse model of Alzheimer's disease. *Neurochemical Research*, *40*(8), 1576–1582. https://doi.org/10.1007/s11064-015-1630-1

Yoo, S. M., & Jung, Y. K. (2018). A molecular approach to mitophagy and mitochondrial dynamics. *Molecules and cells*, *41*(1), 18–26. https://doi.org/10.14348/molcells.2018.2277

Yu, J. T., Tan, L., & Hardy, J. (2014). Apolipoprotein E in Alzheimer's disease: An update. *Annual Review of Neuroscience*, *37*(1), 79–100. https://doi.org/10.1146/annurev-neuro-071013-014300

Zhao, J., Liu, X., Xia, W., Zhang, Y., & Wang, C. (2020). Targeting amyloidogenic processing of APP in Alzheimer's disease. *Frontiers in Molecular Neuroscience*, *13*. https://doi.org/10.3389/fnmol.2020.00137

Supplementary Data

Table 1 - Summary of the alterations found in SIRT1, SIRT3, SESN2, AMPK, pAMPK, MFN2, LC3, and synaptic markers SNAP-25, syntaxin, synaptophysin and PSD-95 in APP/PS1 with 6 and 9 months old, in cortical synaptosomes and total cortical extracts, and in Aβ1-42-injected mice, in cortical synaptosomes and total cortical extracts, 14 and 20 days after injection. A decrease in the levels of the proteins is represent by (↓), an increase by (↑), no alteration by (=) and if the levels were not assessed a (-) is designated.

	APP/PS1			$A\beta_{1-42}$		
	6 months	**9 months**		**14 days**		**20 days**
	Synaptosomes	Synaptosomes	Total extracts	Synaptosomes	Total extracts	Synaptosomes
SIRT1	=	↓	↓	=	-	=
SIRT3	=	=	=	=	=	=
SESN2	=	=	↓	=	=	=
AMPK	=	=	=	=	-	=
pAMPK	=	↓	=	=	-	=
MFN2	=	=	↓	=	-	↓
LC3-I	↑	=	=	=	=	=
LC3-II	=	-	-	-	-	=
LC3-II/LC3-I	=	-	-	-	-	=
SNAP-25	=	=		↑		=
Syntaxin	↓	=		↑		=
Synaptophysin	=	=		↑		=
PSD-95	↑	=		↑		=